Studies on Synthesis and Structure of Helical Syndiotactic Poly(methyl methacrylate) Complex with Macromolecular Helicity Memory

らせん構造を記憶として保持したシンジオタクチック
ポリメタクリル酸メチル複合体の合成と構造に関する研究

Atsushi Kitaura

北浦　敦志

2011

Studies on Synthesis and Structure of Helical Syndiotactic Poly(methyl methacrylate) Complex with Macromolecular Helicity Memory

らせん構造を記憶として保持したシンジオタクチック ポリメタクリル酸メチル複合体の合成と構造に関する研究

Table of Contents

General Introduction

Selective and specific encapsulation or wrapping of functional guest molecules, in particular, π-conjugated oligomers and polymers, by host molecules through noncovalent bonding interaction has been attracting considerable attention because of possible applications to create diverse supramolecular organic and organic/inorganic hybrid materials for advanced nanotechnology and devices, leading to soluble and processable insulated molecular wires.[1] Helical polymers and oligomers may have potential for versatile hosts when they possess a cavity into which a variety of guest molecules could be encapsulated through an induced fit mechanism (Figure 1).[2]

Polysaccharides are among the most important and abundant natural biopolymers, and some of them, such as amylose, curdlan, and schizophyllan, are known to adopt well-defined helical conformations. For example, amylose, which is essentially a linear polymer of (1→4) linked α-D-glucose units, adopts a left-handed helix with a pitch of 0.8 nm and a diameter of 1.3 nm involving six glucose residues per turn.[2c,3] Amylose and its derivatives can entrap not only small guests, such as iodide,[2a] solvent molecules,[4] and organic molecules,[5] but also polymers[6] and carbon nanotube[7] into the hydrophobic cavities via an induced fit, leading to unique host-guest inclusion complexes (Figure 1). β-1,3-Glucan polysaccharides, such as schizophyllan and curdlan, adopt a right-handed triple-stranded helical structure.[8,9] Shinkai *et al*. recently found that these triple-stranded helical β-1,3-glucan polysaccharides also act as an efficient host for encapsulating or wrapping a variety of guest molecules via an induced-fit including small organic molecules,[10] metal nanoparticles,[11] polymers,[6a,6b,12] and carbon nanotube.[13] The encapsulation or wrapping of guests into hydrophobic cavities is an intriguing feature of these biological helical polysaccharides.

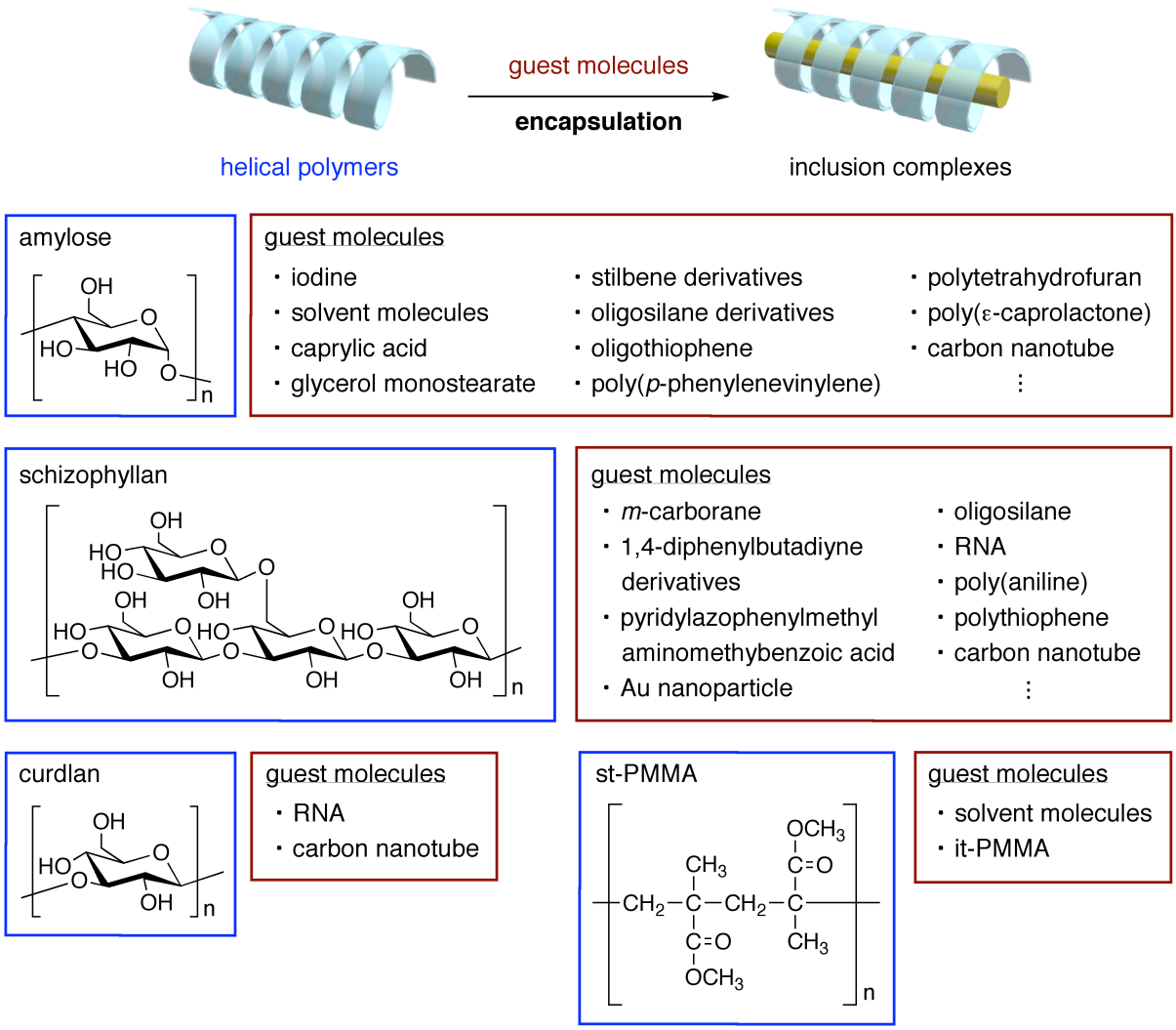

Figure 1. Schematic illustration of the inclusion complex formation composed of helical polymers and guest molecules. The structures of helical polysaccharides and st-PMMA and typical guests included in the polysaccharides and st-PMMA are also shown.

In contrast, very few synthetic helical polymers and oligomers encapsulate specific guest molecules of complementary size and shape into their helical cavities due to a lack of flexibility and adaptability.[14] However, syndiotactic poly(methyl methacrylate) (st-PMMA), a stereoregular commodity plastic, is known to form inclusion complexes with not only organic solvents[15] but also isotactic (it)-PMMA.[16] The latter affords a multiple-stranded complementary supramolecular helical architecture, so-called the stereocomplex, with an it/st

stoichiometry of 1:2.[16,17] X-ray diffraction of well-oriented crystalline st-PMMA samples prepared from a non-crystalline st-PMMA after stretching followed by solvent-induced crystallization with a variety of organic solvents, such as chloroacetone and diethyl ketone, revealed a characteristic reflection of 35.4 Å, indicating that the st-PMMA chains adopt a 74/4 helix with a sufficiently large cavity of about 1 nm, and hence, solvents are encapsulated in the cavity of the inner helix.[15] On the other hand, a triple-stranded helix model has been proposed for the PMMA stereocomplex from the direct observation of a stereocomplex prepared using the Langmuir-Blodgett (LB) technique by high-resolution atomic force microscopy (AFM), which reveals that a double-stranded helix of it-PMMA is included in a single helix of st-PMMA, forming an inclusion complex with a triple-stranded helical structure.[17]

On the basis of these observations, the author anticipated that the helical st-PMMA might serve as a novel host encapsulating functional molecules such as fullerenes of specific sizes into its helical cavity. Fullerenes and their derivatives are a class of attractive carbon-cage molecules with unique chemical, electrochemical, and photophysical properties, thus being applied to many research areas, such as chemistry, physics, and materials science.[18] The development of specific receptors for fullerenes is of great importance for developing fullerene-based architectures with unprecedented properties for further realistic applications to advanced materials.[19] Up to now, a variety of host molecules which can trap fullerenes have been reported (Figure 2).

In 1992, Wennerström *et al*. discovered that γ-cyclodextrin (γ-CyD) (**1**) could extract C_{60} from a mixture of C_{60} and C_{70}.[20] Because the cavity of **1** is too small to completely encapsulate C_{60}, the formation of a 2:1 **1**–C_{60} complex was proposed on the basis of the spectrophotometric and molecular modeling studies. The complex formation was also supported by appearance of the Cotton effects in the achiral C_{60} chromophoric regions induced by the chiral host **1**.[21] The n–π donor–acceptor interactions between the n-orbitals of the sugar O-atoms and the π-system of the fullerene seem to play a key role in the

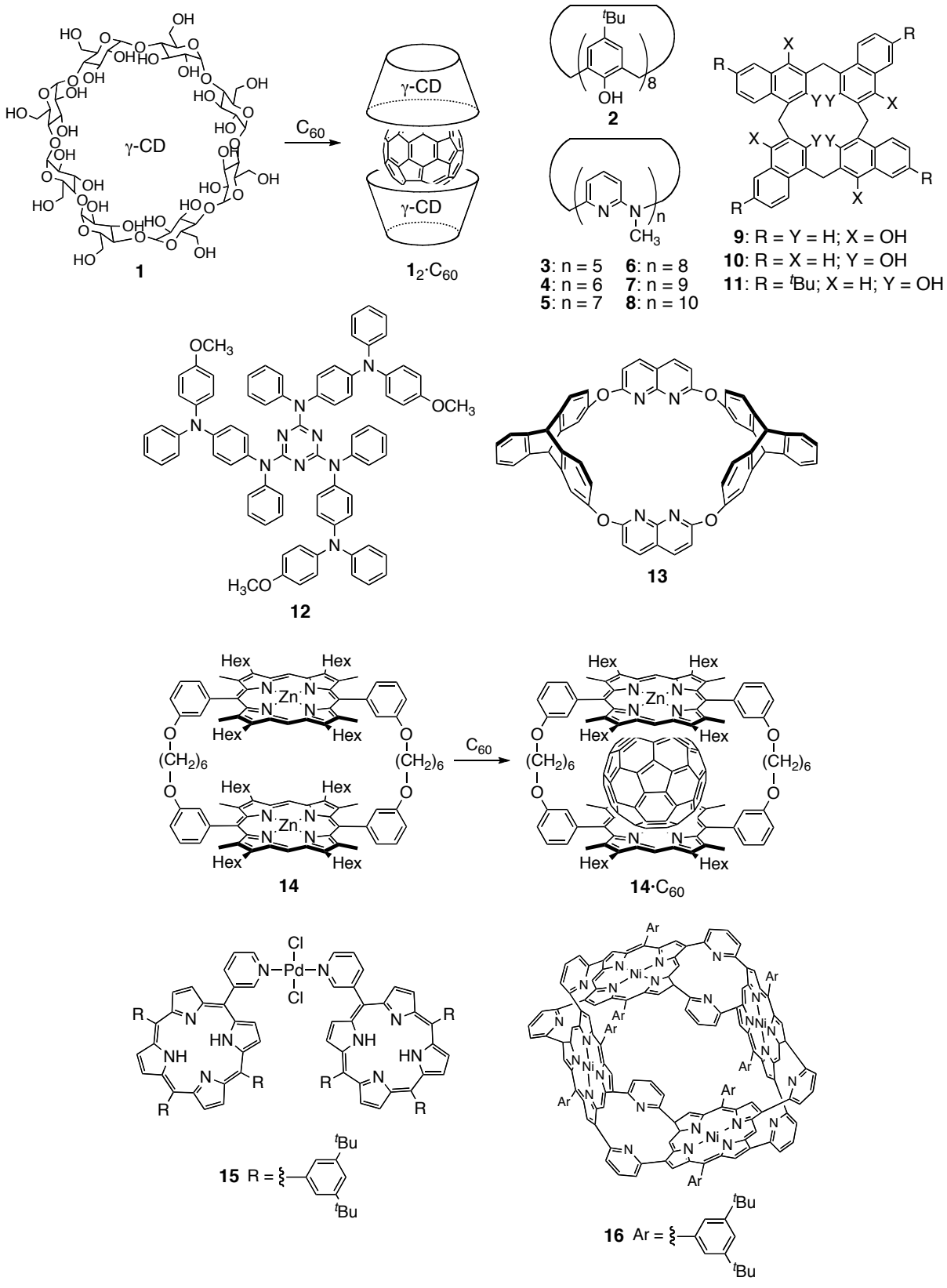

Figure 2. Structures of representative receptors for C_{60}.

complexation.[21-23] A number of studies have been conducted on the complexation between fullerenes and a bowl-shaped macrocycle, calixarenes. In 1994, Atwood and Shinkai *et al*. independently reported that *p-t*Bu-calix[8]arene (**2**) and C_{60} formed a 1:1 complex.[24,25] Analogous azacalix[n]pyridines, heteroatom bridged calixaromatics (**3**–**8**),[26] and calix[4]naphthalenes which possess deeper cavities (**9**–**11**)[27] were also found to form 1:1 complexes with fullerenes. Conformationally flexible substituted triazine (**12**) can adapt their shape to provide a concave binding site showing remarkably strong intermolecular association with fullerenes.[28] A triptycene-derived oxacalixarene (**13**) also possesses the expanded cavity exhibiting a high efficient complexation ability toward fullerenes such as C_{60} and C_{70}.[29]

The porphyrin receptors complexed with fullerenes are known to show unusually short porphyrin/fullerene contacts compared with typical π–π interactions.[30] The interaction between the curved π surface of a fullerene and the planar π surface of a porphyrin has been employed as an effective recognition motif to assemble van der Waals complexes of donor–acceptor chromophores. To date, a number of reports concerning porphyrin receptors for fullerene have been published. Aida *et al*. reported that a face-to-face cyclic dimer of zinc porphyrins (**14**) formed a highly stable 1:1 inclusion complex with C_{60} via the π-electronic donor-accepter interactions, exhibiting a very high binding constant (6.7×10^5 M^{-1}) in benzene.[31] The central metal ions remarkably affected the interaction between metalloporphyrin dimers and fullerenes, and the cyclic dimer **14** bearing rhodium ions exhibited the highest association constant ($\sim 10^8$ M^{-1}) in benzene.[32] Similar cyclic porphyrin dimers with various cavity sizes have been synthesized to create tailor-made hosts for higher fullerenes and a fullerene dimer.[33] Reed, Boyd, and co-workers designed and synthesized a jaw-like porphyrin dimer with a palladium-linker (**15**) which served as an effective host for fullerenes.[34] Furthermore, various unique multiporphyrins, such as foldamer-based,[35] star-shaped,[36] and barrel-shaped receptors (**16**),[37] have been developed for the selective encapsulation of fullerenes.

The development of a practically efficient method for the separation of fullerenes with a specific size, geometry, and, chirality is among the urgent and emerging challenges in advanced materials science due to their attractive applications, such as electronic and optoelectronic materials.[38,39] The supramolecular approach using the designer host molecules as described above has been a powerful method for selectively encapsulating C_{60} and/or C_{70} (Figure 3A) rather than higher fullerenes ($\geq C_{76}$) (Figure 3B).

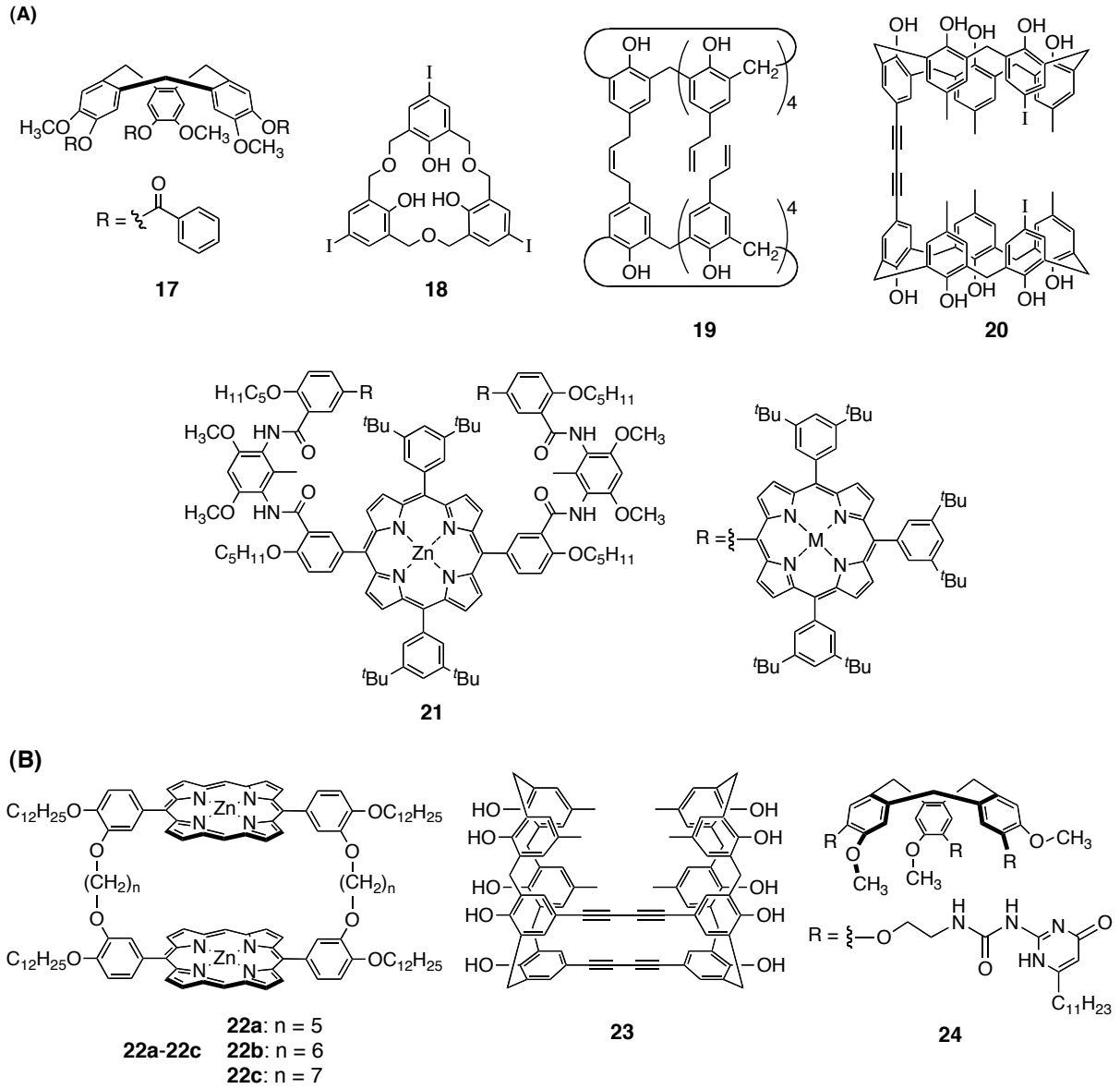

Figure 3. Structures of representative receptors for selective encapsulation of (A) C_{70} or C_{60} and (B) higher fullerenes.

As described previously, γ-CyD (**1**) and calixarene (**2**) can extract C_{60} from a mixture of C_{60} and C_{70} through complexation in a size-selective manner.[20,24,25] A cyclotriveratrylene derivative (**17**) was also utilized for the purification of C_{60} from a toluene solution of fullerite (C_{60} and C_{70} mixture).[40] In contrast, a preferential precipitation of C_{70} over C_{60} was utilized when *p*-triiodohomooxacalix[3]arene (**18**) was used as a host molecule affording the 2:5 **18**–C_{70} complex.[41] The large capacity of **18** for C_{70} may originate from its shallow cavity, intermolecular π–π interactions among the guest molecules, the large van der Waals radii of the heavy halogens, and strong van der Waals interactions between the heavy halogens and the guests. The bridged calix[5]arene dimmers such as **19** and **20** were developed to achieve a dramatic increase in the association constant with fullerenes.[42,43] The dimer **19** showed a unique selectivity with respect to C_{70}/C_{60} opposite to that of **20**. In addition, the porphyrin-containing host (**21**) was known to bind C_{70} even better than C_{60}.[35]

The first selective extraction of higher fullerenes from a fullerene mixture was achieved using cyclodimeric zinc porphyrins **22** with alkylene spacers as the hosts.[44] Although the total content of higher fullerenes in the initial fullerene mixture was only 10 abs %, the higher fullerene content significantly increased to 74 abs % by single extraction with **22a**. After three cycles of the extraction with **22b**, very rare higher fullerenes C_{102}–C_{110} (<0.1 abs %) were enriched up to 82 abs % of total fullerenes. A calix[5]arene dimer with the two 1,3-butadiyne bridges (**23**) possesses syn and anti conformations, and the syn isomer was found to selectively encapsulate higher fullerenes from fullerene mixtures, forming the precipitates of the host-guest complexes.[45] The conformational change of the syn isomer to the anti isomer was accelerated by heating at 100 ˚C, resulting in releasing the encapsulated higher fullerenes. A higher fullerene mixture larger than C_{90} could be obtained after repeating this extraction. A cyclotriveratrylene derivative **24** reversibly forms a dimeric nanoscale capsule, which extracted C_{70} over C_{60} with high selectivity by combining the curvature of cyclotriveratrylene and three high-affinity hydrogen-bonding units.[46] An enriched mixture of higher fullerenes from C_{76} to C_{84} was also extracted from fullerene mixtures by the dimeric spherical host.

The control and fabrication of the molecular ordering of fullerenes has also attracted considerable attention for constructing fullerene-based advanced materials.[18,47] Taking advantage of designer host molecules that can selectively trap fullerenes through inclusion complexation, several supramolecular architectures of fullerenes have been constructed based on the porphyrin and cyclodextrin skeletons along with other organic frameworks (Figure 4). The intermolecular interaction between fullerenes and zinc(II) porphyrins was applied to the first supramolecular assembly system where the zinc(II) porphyrin bearing cholesterol derivatives (**25**) formed a supramolecular organogel in aromatic solvents, such as benzene and toluene in the presence of C_{60}.[48] The spectroscopic studies revealed that the gel was stabilized by the unique 2:1 zinc(II) porphyrin/C_{60} sandwich complex formation. The same group also reported a porphyrin-appended gelator (**26**) in which the hydrogen-bonding sites were programmed so that the resultant assembly can accept C_{60}.[49] The porphyrin derivative **26** formed a one-dimensional multicapsular structure in the presence of C_{60}, while it created a two-dimensional sheet-like structure in the absence of C_{60}. The supramolecular peapods composed of a linear metalloporphyrin nanotube and fullerenes, such as C_{60} and C_{70} were formed by the fullerene-triggered unidirectional supramolecular polymerization of an acyclic zinc porphyrin dimer (**27**) bearing carboxylic acid groups and large dendritic units.[50] A porphyrin nanotube was also constructed by stacking of a cyclic porphyrin dimer (**28**) through unique C–H···N hydrogen bonds and π–π interactions of the pyridyl groups in the crystal.[51] The cyclic porphyrin **28** could encapsulate C_{60} within its cavity, yielding the 1:1 inclusion complex in solution and in the crystal. The X-ray crystal structure analysis of the inclusion complex revealed that fullerenes are linearly arranged in the inner channel of the tubular assembly in crystal. A water-soluble fullerene assembly with a coordinated metal center was prepared through end-to-end intermolecular inclusion complexation of a dimeric cyclodextrin, 6,6'-*o*-phenylenediselenobridged bis(β-CyD) platinum (IV) complex (**29**), with C_{60}.[52] The amino acid naphthalenediimide derivatives (**30** and **31**) self-assembled to form helical nanotubes with a large cavity of about 1.2 nm,[53] and the supramolecular nanotubes

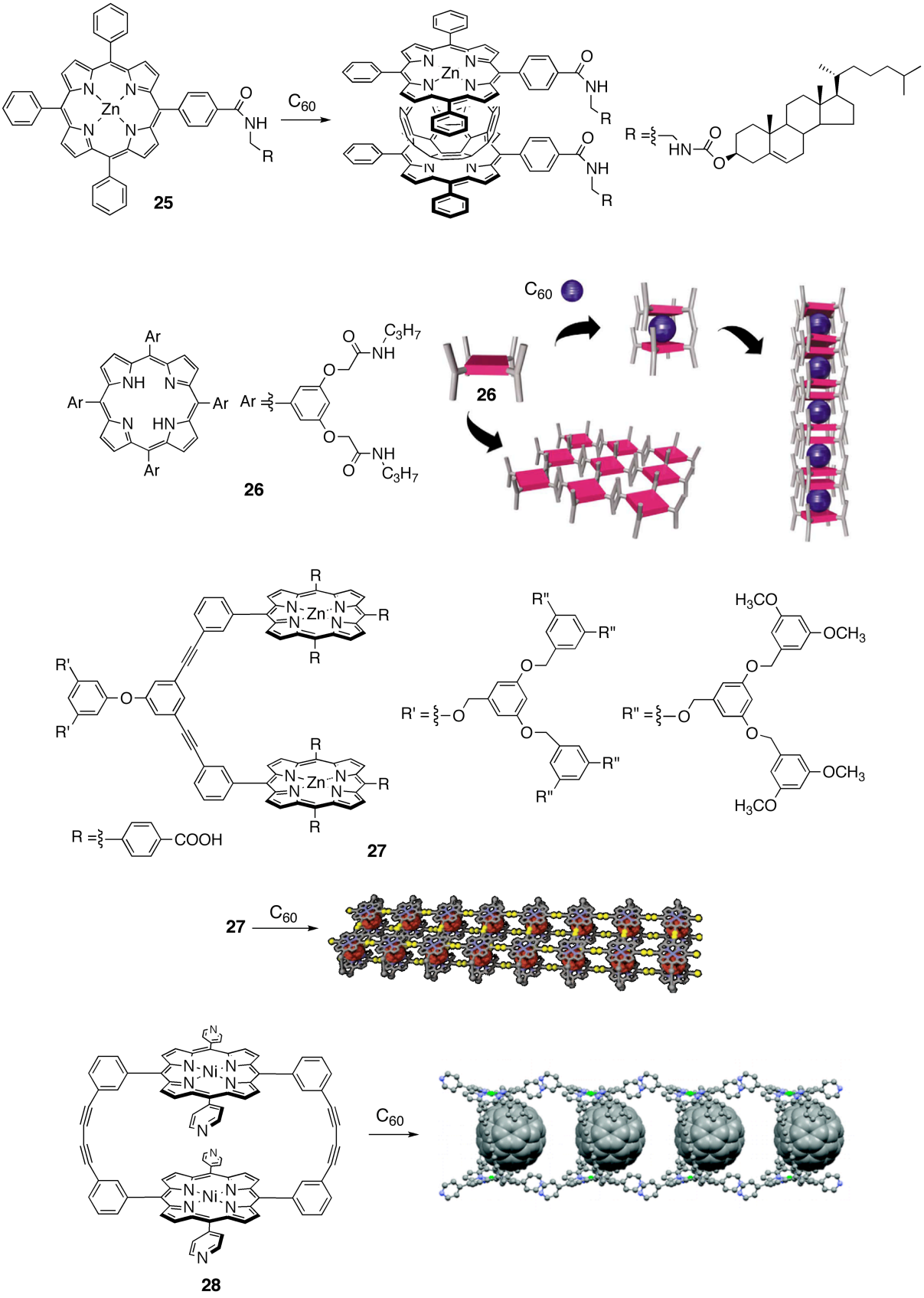

(Figure 4 continued)

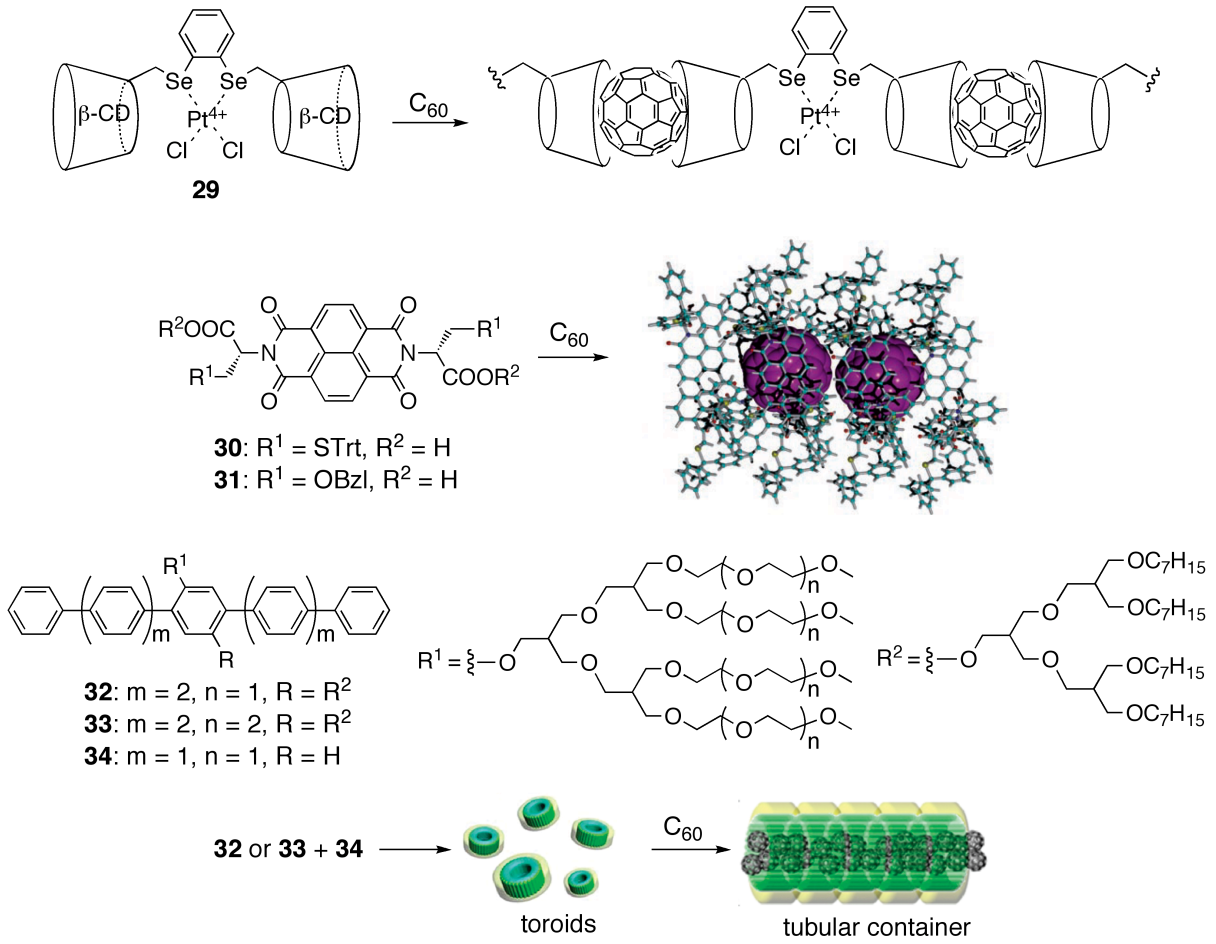

Figure 4. Supramolecular assemblies of various host molecules with fullerenes.

encapsulated C_{60} in the tubular cavity, allowing the formation of a one-dimensional C_{60} array.[54] The inclusion complex showed an induced circular dichroism (ICD) in the absorption region of achiral C_{60}, indicating the chirality of the optically active nanotubes was sensed by C_{60}. Laterally grafted amphiphilic π-conjugated oligomers (**32** or **33** and **34**) self-assembled into a water-soluble toroid with a hydrophobic cavity.[55] The C_{60} was efficiently encapsulated within its internal cavity, stacking on top of each other to form a tubular container.

Higher fullerenes having asymmetrically curved π-electronic surfaces consist of large numbers of isomers including enantiomers, and optically active fullerenes have attracted a great interest due to their unique potential in chiral materials science.[39] Among a large number

of chiral fullerenes, only D_2-symmetric C_{76} (C_{76}-D_2), C_{78}-D_3, and C_{84}-D_2 have been successfully resolved into the enantiomers by kinetic resolution, covalent modification with chiral molecules followed by regeneration, recycling chiral HPLC, and enantioselective extraction with a chiral porphyrin dimer (Figure 5).

In 1993, Hawkins *et al.* reported the kinetic resolution of C_{76} by asymmetric osmylation of racemic C_{76} with OsO_4 and chiral ligands (**35a** or **35b**) derived from a naturally occurring cinchona alkaloids (Figure 5A).[56] The asymmetric Sharpless osmylation gave enantiomerically enriched unreacted C_{76} and a diastereomerically enriched osmate complex (C_{76}(OsO_4**35**). The reduction of the obtained C_{76}(OsO_4**35**) with $SnCl_2$ regenerated C_{76} enriched in one of the enantiomers. This procedure was further applied to the kinetic resolution of C_{78} and C_{84}, affording the enantiomers of C_{78}-D_3 and C_{84}-D_2, respectively.[57] Taking advantage of Bingel and retro-Bingel reaction of fullerenes, Diederich *et al.* successfully prepared enantiomerically pure C_{76} (Figure 5B).[58] Two diastereomeric mono-adducts ((+)- and (–)-C_{76}•**36**) were prepared by Bingel reaction of racemic C_{76} with optically active bis[(*S*)-1-phenylbutyl]-2-bromomalonate (**36**), and the following electrochemical retro-Bingel reaction of each (+)- and (–)-C_{76}•**36** gave the pure C_{76} enantiomers. The Bingel/retro-Bingel approach has been also extended to the separation of three constitutional isomers of C_{84} and the optical resolution of the chiral isomer, D_2-C_{84}.[59]

Judging from the tiny structural differences in the enantiomers and due to a lack of functionality, the direct separation of chiral fullerenes into enantiomers appears to be extremely difficult. However, Okamoto *et al.* succeeded in the direct resolution of racemic C_{76} by high performance liquid chromatography (HPLC) using commercially available amylose tris(3,5-dimethylphenylcarbamate), one of the most popular chiral stationary phases (CSPs) for HPLC (Figure 5C).[60,61] Recently, Aida *et al.* performed one-pot enantioselective extraction of C_{76} using an optically active cyclic host bearing two porphyrin units ((+)- and (–)-**37**) (Figure 5D).[62] The **37** formed an inclusion complex with C_{76} in toluene, showing a typical bathochromic shift in the Soret absorption band, and the association constant K_{assoc} was estimated to be 5.5×10^6 M^{-1}. The enantiomerically enriched C_{76} was released from the

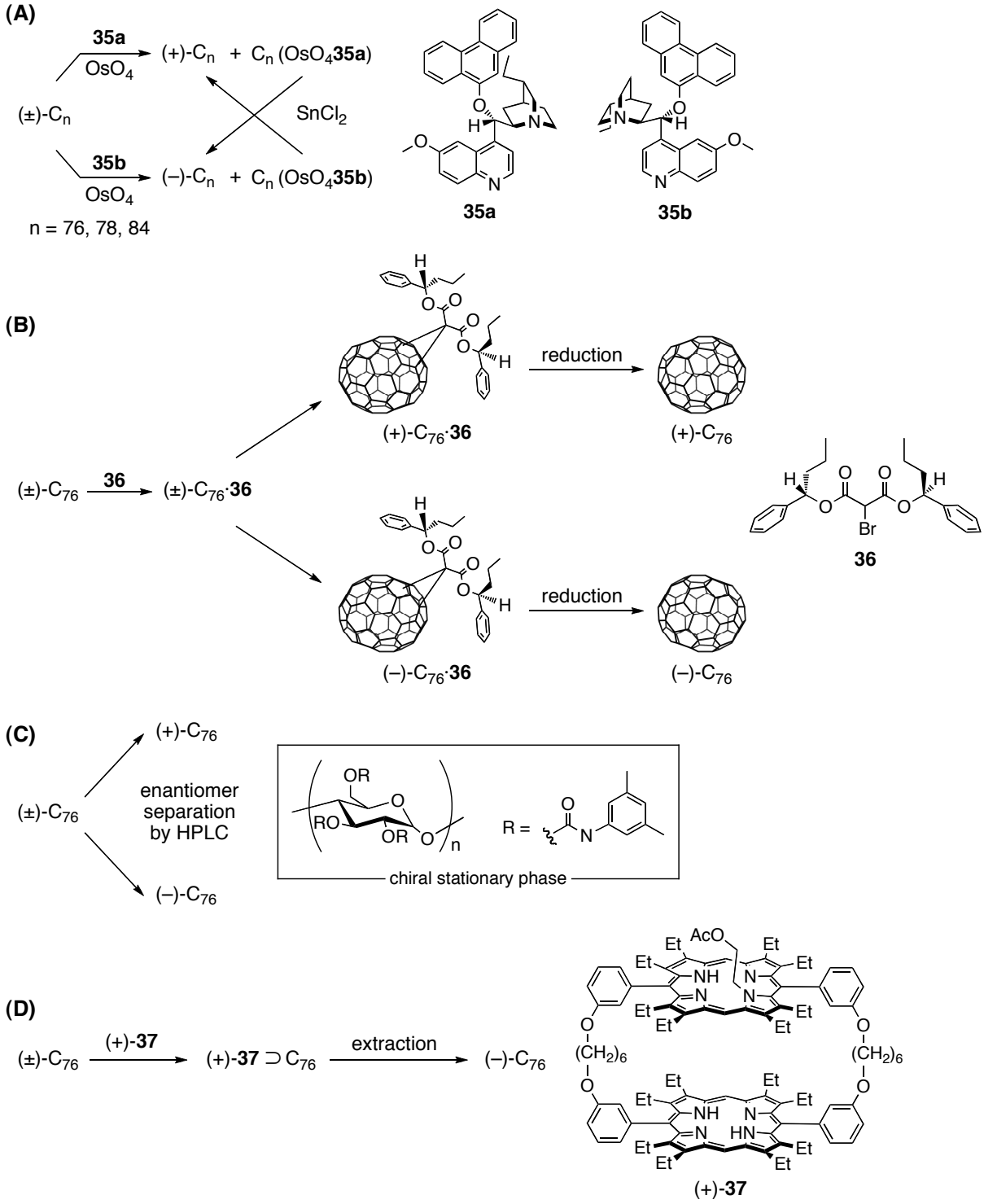

Figure 5. Separation of higher fullerene enantiomers by (A) kinetic resolution using asymmetric osymylation, (B) Bingel—retro-Bingel reaction, (C) chiral HPLC using an amylose-based chiral stationary phase, and (D) chiral cyclic host compound.

inclusion complex by the protonation with silica gel chromatography. The single extraction with (+)-**37** resulted in enrichment of (–)-C_{76} in 7% ee.

On the basis of this information, the author studied the following four areas concerning the synthesis and structure of helical st-PMMA complex with macromolecular helicity memory and its application to separate higher fullerene enantiomers.

(1) Encapsulation of fullerenes in a helical cavity of syndiotactic poly(methyl methacrylate) leading to a robust processable complex with a macromolecular helicity memory
(2) Helix-sense-controlled synthesis of optically active poly(methyl methacrylate) stereocomplex
(3) Helicity induction and memory of syndiotactic poly(methyl methacrylate) assisted by optically active additives and solvents and chiral amplification of helicity
(4) Separation of higher fullerene enantiomers by syndiotactic poly(methyl methacrylate) with a macromolecular helicity memory

These studies will be described in the following four chapters.

In chapter 1, the encapsulation of fullerenes, such as C_{60}, C_{70}, and C_{84}, in the helical cavity of st-PMMA and a preferred-handed helicity induction in st-PMMA using an optically active alcohol are described. st-PMMA has been reported to form a thermoreversible physical gel in aromatic solvent, such as toluene and chlorobenzene, in which the polymer chain adopts a 74/4 helix with a cavity of about 1 nm, and hence, solvents are encapsulated in this cavity of the inner helix. The author anticipated that fullerene molecules might be encapsulated in the helical cavity of st-PMMA to form one-dimensionally regulated fullerene arrays. In the presence of (*S*)- or (*R*)-1-phenylethanol (**38**) as an additive in toluene, st-PMMA

was found to fold into a preferred-handed helix accompanied by gelation, and at the same time, fullerenes, such as C_{60}, C_{70}, and C_{84}, were encapsulated within its helical cavity to form a robust, processable peapod-like complex (Figure 6). Differential scanning calorimetry (DSC) and X-ray diffraction profiles of the st-PMMA/C_{60} films revealed the crystalline structure of the st-PMMA/C_{60} complex, and AFM of a st-PMMA/C_{60} LB film deposited on mica afforded further evidence for the inclusion of C_{60} in the st-PMMA. After removal of optically active **38**, the st-PMMA gel complexed with C_{60} exhibited apparent vibrational CD (VCD) and ICD signals in the PMMA IR regions and in the encapsulated achiral C_{60} chromophore regions, respectively, owing to the helical structure of the st-PMMA with an excess of one handedness whose helicity was "memorized".

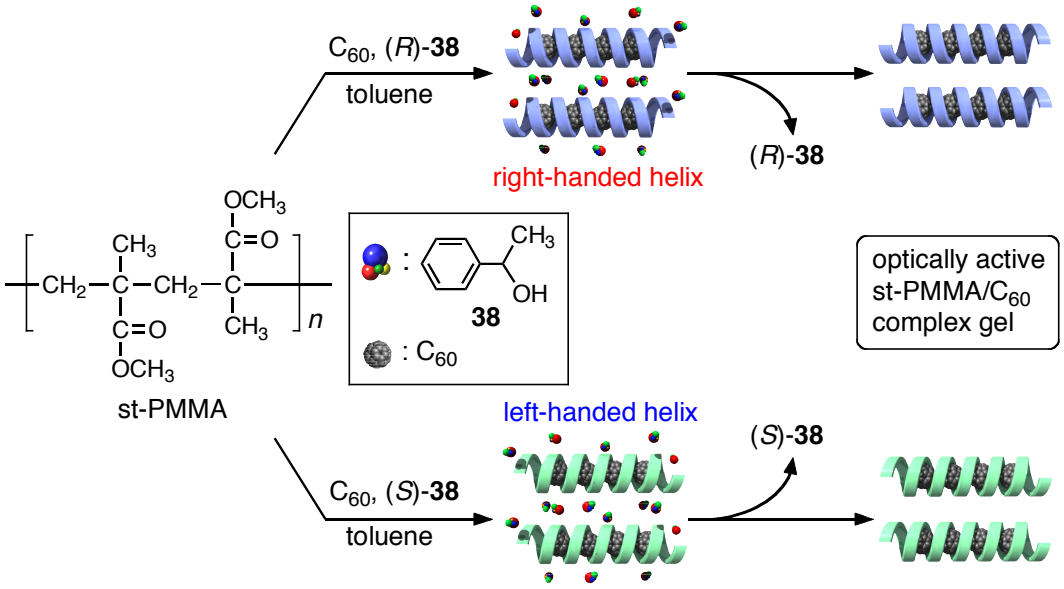

Figure 6. Schematic illustration of right- (top) and left-handed (bottom) helicity induction in the C_{60}-encapsulated st-PMMA in the presence of (*R*)- or (*S*)-**38**.

Chapter 2 deals with the helix-sense-controlled synthesis of the optically active PMMA stereocomplex composed of the complementary it- and st-PMMAs. The author found that the preferred-handed helical st-PMMA/C_{60} complex prepared with optically active **38** could serve as a novel template to encapsulate the complementary it-PMMA chain through replacement

of the encapsulated C_{60} molecules, resulting in the crystalline stereocomplex (Figure 7). The obtained stereocomplex gels exhibited VCDs in the PMMA IR regions, whose VCD patterns significantly changed from those of the optically active st-PMMA/C_{60} gels, in particular, at around the 1260 cm^{-1} regions corresponding to the characteristic absorption band for it-PMMA. These results suggest that the it-PMMA forms a helical conformation with an excess of one-handedness once encapsulated into the helical st-PMMA with a macromolecular helicity memory, which remains intact after the encapsulated fullerenes are replaced by the complementary it-PMMA with the formation of an optically active stereocomplex. The observed VCD spectral patterns of the stereocomplexes fit well to the calculated ones composed of helical it- and st-PMMAs with the same handedness, indicating that it-PMMA recognizes and interacts with the outer st-PMMA helix and folds into a double-stranded helix with the same handedness.

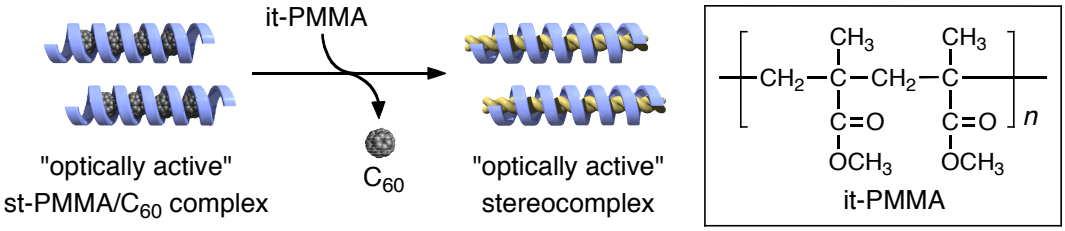

Figure 7. Schematic illustration of right-handed stereocomplex formation.

In chapter 3, the author describes the effects of diverse optically active compounds as chiral additives in toluene or solvents on the gelation abilities and further efficiency of the helicity induction and memory in st-PMMA. A preferred-handed helicity was efficiently induced in st-PMMA with various optically active primary and secondary amines bearing aromatic groups as the gelling solvents and further memorized after removal of the chiral amines and encapsulation of C_{60} while maintaining its gel state (Figure 8). The chiral information of a nonracemic aromatic amine transfers with amplification in the st-PMMA as an excess of a single-handed helix through noncovalent bonding interactions, thus generating a unique “majority rule” effect (nonlinear effect) on a helical system. This amplification of

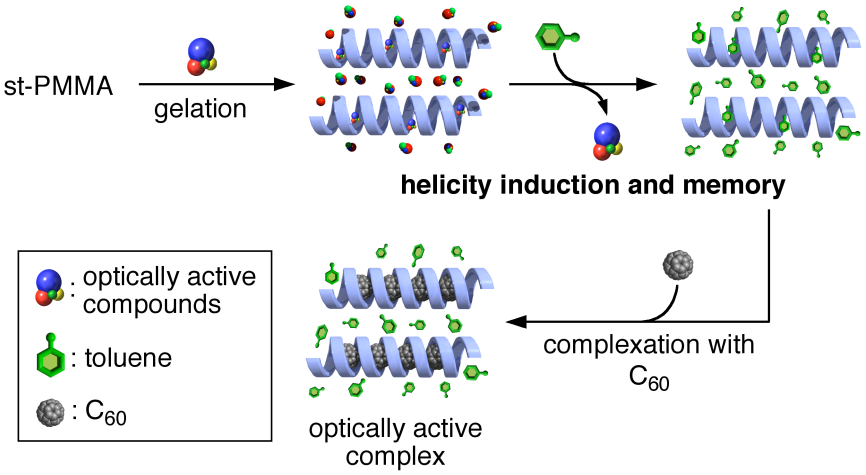

Figure 8. Schematic illustration for the helicity induction and memory in st-PMMA and further encapsulation of C_{60} after complete removal of optically active compounds.

helical chirality suggests that the helical st-PMMA chain may have dynamic characteristics during gelation.

Chapter 4 deals with the optical resolution of higher fullerenes by a preferred-handed helical st-PMMA gel prepared by the same manner described in Chapter 3. A single extraction of fullerene mixtures composed of C_{60}/C_{70}/higher fullerenes (64.0 : 27.2 : 8.8% determined by HPLC analysis) in toluene was carried out using the optically active st-PMMA gel, resulting in the st-PMMA gel complexed with the fullerenes, and the encapsulated fullerenes were then recovered with 1,2-dichlorobenzene (Figure 9). The extraction provided a series of optically active fullerenes (C_{76}, C_{84}, C_{86}, C_{88}, C_{90}, C_{92}, C_{94}, and C_{96}) as supported by

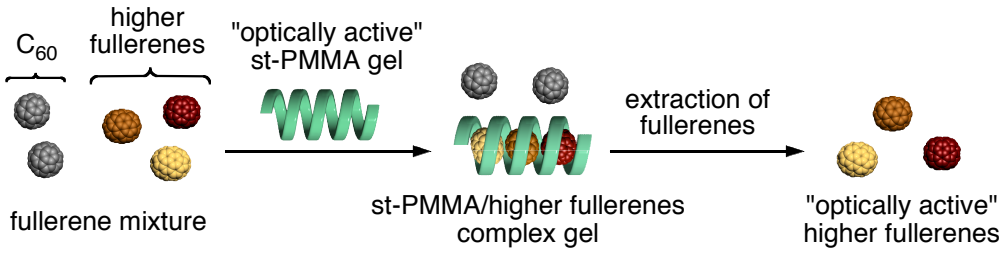

Figure 9. Schematic illustration of the separation of higher fullerene enantiomers by optically active st-PMMA gel.

the CD-detected HPLC chromatograms of the extract, which showed the apparent CDs. A series of optically active fullerenes were then isolated by preparative HPLC, and their CD and absorption spectra were measured, resulting in the characteristic CDs in the long absorption regions. When an opposite enantiomer of the optically active amine was used for the preparation of the preferred-handed helical st-PMMA, the opposite fullerene enantiomers was extracted, as evidenced by the mirror image CDs. The enantiomeric excess (ee) of the isolated C_{76} was estimated to be approximately 4% by comparison with the reported CD intensity of the optically pure C_{76}.

References

(1) (a) Tajima, K.; Aida, T. *Chem. Commun.* **2000**, 2399–2412. (b) Harada, A. *Acc. Chem. Res.* **2001**, *34*, 456–464. (c) Cardin, D. J. *Adv. Mater.* **2002**, *14*, 553–563. (d) Frampton, M. J.; Anderson, H. L. *Angew. Chem., Int. Ed.* **2007**, *46*, 1028–1064. (e) Nakashima, N.; Fujigaya, T. *Chem. Lett.* **2007**, *36*, 692–697. (f) Harada, A.; Osaki, M.; Takashima, Y.; Yamaguchi, H. *Acc. Chem. Res.* **2008**, *41*, 1143–1152. (g) Harada, A.; Hashizume, A.; Yamaguchi, H.; Takashima Y. *Chem. Rev.* **2009**, *109*, 5974–6023.

(2) (a) Immel, S.; Lichtenthaler, F. H. *Starch/Staerke* **2000**, *52*, 1–8. (b) Sakurai, K.; Uezu, K.; Numata, M.; Hasegawa, T.; Li, C.; Kaneko, K.; Shinkai, S. *Chem. Commun.* **2005**, 4383–4398. (c) Numata, M.; Shinkai, S. *Adv. Poly. Sci.* **2008**, *220*, 65–121.

(3) Hinrichs, W.; Büttner, G.; Steifa, M.; Betzel, C.; Zabel, V.; Pfannemüller, B.; Saenger, W. *Sciense* **1987**, *238*, 205–208.

(4) (a) Frenchi, A. D.; Zobel, H. F. *Biopolymers* **1967**, *5*, 457–464. (b) Helbert, W.; Chanzy, H. *Int. J. Biol. Macromol.* **1994**, *16*, 207–213.

(5) (a) Hui, Y.; Russell, C. R.; Whitten, D. G. *J. Am. Chem. Soc.* **1983**, *105*, 1374–1376. (b) Biliaderris, C. G.; Seneviratne, H. D. *Carbohydr. Res.* **1990**, *208*, 199–213. (c) Godet, M. C.; Tran, V, Colonna, P.; Buleno, A.; Pezolet, M. *Int. J. Biol. Macromol.* **1995**, *17*, 405–408. (d) Kim, O.-K.; Choi, L.-S.: Zhang, H.-Y.; He, X.-H.; Shin, Y.-H. *J. Am. Chem. Soc.* **1996**, *118*, 12220–12221. (e) Kato, N.; Sanji, T.; Tanaka, M. *Chem. Lett.* **2009**, *38*, 1192–1193.

(6) (a) Sanji, T.; Kato, N.; Kato, M.; Tanaka, M. *Angew. Chem., Int. Ed.* **2005**, *44*, 7301–7304. (b) Sanji, T.; Kato, N.; Tanaka. M. *Org. Lett.* **2006**, *8*, 235–238. (c) Ikeda, M.; Furusho, Y.; Okoshi, K.; Tanahara, S.; Maeda, K.; Nishino, S.; Mori, T.; Yashima, E. *Angew. Chem., Int. Ed.* **2006**, *45*, 6491–6495. (d) Kida, T.; Minabe, T.; Okabe, S.; Akashi, M. *Chem. Commun.* **2007**, 1559–1561.

(7) (a) Star, A.; Steuerman, D. W.; Heath, J. R.; Stoddart, J. F. *Angew. Chem., Int. Ed.* **2002**, *41*, 2508–2512. (b) Kim, O.-K.; Je. J.; Baldwin, J. W.; Kooi, S.; Pehrsson, P. E.; Buckley, L. J. *J. Am. Chem. Soc.* **2003**, *125*, 4426–4427.

(8) Deslandes, Y.; Marchessault, R. H. *Macromolecules* **1980**, *13*, 1466–1471.

(9) Yanaki, T.; Norisuye, T.; Fujita, H. *Macromolecules* **1980**, *13*, 1462–1466.

(10) (a) Hasegawa, T.; Haraguchi, S.; Numata, M.; Fujisawa, T.; Li, C.; Kaneko, K.; Sakurai, K.; Shinkai, S. *Chem. Lett.* **2005**, *34*, 40–41. (b) Numata, M.; Tamsue, S.; Fujisawa, T.; Haraguchi, S.; Hasegawa, T.; Bae, A.-H.; Li, C.; Sakurai, T.; Shinkai, S. *Org. Lett.* **2006**, *8*, 5533–5536. (c) Numata, M.; Tamesue, S.; Nagasaki, T.; Sakurai, K.; Shinkai, S. *Chem. Lett.* **2007**, *36*, 668–669.

(11) (a) Bae, A.-H.; Numata, M.; Hasegawa, T.; Li, C.; Kaneko, K.; Sakurai, K.; Shinkai, S. *Angew. Chem., Int. Ed.* **2005**, *44*, 2030–2033. (b) Bae, A.-H.; Numata, M.; Yamada, S.; Shinkai, S. *New J. Chem.* **2007**, *31*, 618–622.

(12) (a) Sakurai, K.; Shinkai, S. *J. Am. Chem. Soc.* **2000**, *122*, 4520–4521. (b) Numata, M.; Hasegawa, T.; Fujisawa, T.; Sakurai, K.; Shinkai, S. *Org. Lett.* **2004**, *6*, 4447–4450. (c) Li, C.; Numata, M.; Bae, A.-H. Sakurai, K.; Shinkai, S. *J. Am. Chem. Soc.* **2005**, *127*, 4548–4549. (d) Haraguchi, S.; Hasegawa, T.; Mumata, M.; Fujiki, M.; Uezu, K.; Sakurai, K.; Shinkai, S. *Org. Lett.* **2005**, *7*, 5605–5608.

(13) (a) Numata, M.; Asai, M.; Kaneko, K.; Hasegawa, T.; Fujita, N.; Kitada, Y.; Sakurai, K.; Shinkai, S. *Chem. Lett.* **2004**, *33*, 232–234. (b) Numata, M.; Asai, M.; Kaneko, K.; Bae, A.-H.; Hasegawa, T.; Sakurai, K.; Shinkai, S. *J. Am. Chem. Soc.* **2005**, *127*, 5875–5884.

(14) Ray, C. R.; Moore, J. S. *Adv. Poly. Sci.* **2005**, *177*, 91–149.

(15) (a) Kusuyama, H.; Takase, M.; Higashihata, Y.; Tseng, H.-T.; Chatani, Y.; Tadokoro, H. *Polymer* **1982**, *23*, 1256–1258. (b) Kusuyama, H.; Miyamoto, N.; Chatani, Y.; Tadokoro, H. *Polymer Commun.* **1983**, *24*, 119–122.

(16) (a) Vorenkamp, E. L.; Bosscher, F.; Challa, G. *Polymer* **1979**, *20*, 59–64. (b) Bosscher, F.; Brinke, G. T.; Challa, G. *Macromolecules* **1982**, *15*, 1442–1444. (c) Schomaker, E.; Challa, G. *Macromolecules* **1989**, *22*, 3337–3341.

(17) (a) Kumaki, J.; Kawauchi, T.; Okoshi, K.; Kusanagi, H.; Yashima, E. *Angew. Chem., Int. Ed.* **2007**, *46*, 5348–5351. (b) Kumaki, J.; Kawauchi, T.; Ute, K.; Kitayama, T.;

Yashima, E. *J. Am. Chem. Soc.* **2008**, *130*, 6373–6380. (c) Kumaki, J.; Sakurai, S.-i.; Yashima, E. *Chem. Soc. Rev.* **2009**, 38, 737–746.

(18) (a) Kadish, K. M.; Ruoff, R. S *Fullerenes: Chemistry, Physics, and Technology,* Wiley-Interscience, New York, **2000**. (b) Prato, M. *J. Mater. Chem.* **1997**, *7*, 1097-1109. (c) Chen, Y.; Huang, Z.; Cai, R. F.; Yu, B. C. *Eur. Polym. J.* **1998**, *34*, 137-151. (d) Prato, M.; Maggini, M. *Acc. Chem. Res.* **1998**, *31*, 519-526. (e) Nakamura, E.; Isobe, H. *Acc. Chem. Res.* **2003**, *36*, 807-815. (f) Guldi, D. M.; Zerbetto, F.; Georgakilas, V.; Prato, M. *Acc. Chem. Res.* **2005**, *38*, 38-43.

(19) Kawase, T.; Kurata, H. *Chem. Rev.* **2006**, *106*, 5250-5273.

(20) Andersson, T.; Nilsson, K.; Sundahl, M.; Westman, G.; Wennerström, O. *J. Chem. Soc., Chem. Commun.* **1992**, 604-606.

(21) Yoshida, Z.; Takekuma, H.; Takekuma, S.-i.; Matsubara, Y. *Angew. Chem., Int. Ed. Engl.* **1994**, *33*, 1597-1598.

(22) Consable, E. C. *Angew. Chem., Int. Ed.* **1994**, *33,* 2269–2271.

(23) Diederich, E.; Gómez-López, M. *Chem. Soc. Rev.* **1999**, *28*, 263-277.

(24) Atwood, J. L.; Koutsantonis, G. A.; Raston, C. L. *Nature* **1994**, *368*, 229-231.

(25) Suzuki, T.; Nakashima, K.; Shinkai, S. *Chem. Lett.* **1994**, *23*, 699-702.

(26) (a) Wang, M.-X.; Zhang, X.-H.; Zheng, Q.-Y. *Angew. Chem., Int. Ed.* **2004**, *43*, 838-842. (b) Liu, S.-Q.; Wang, D.-X.; Zheng, Q.-Y.; Wang, M.-X. *Chem. Commun.* **2007**, 3856-3858. (c) Zhang, E.-X.; Wang, D.-X.; Zheng, Q.-Y.; Wang, M.-X. *Org. Lett.* **2008**, *10*, 2565-2568.

(27) Georghiou, P. E.; Mizyed, S.; Chowdhury, S. *Tetrahedron Lett.* **1999**, *40*, 611-614.

(28) Schuster, D. I.; Rosenthal, J.; MacMahon, S.; Jarowski, P. D.; Alabi, C. A.; Guldi, D. M. *Chem. Commun.* **2002**, 2538-2539.

(29) Hu, S.-Z.; Chen, C.-F. *Chem. Commun.* **2010**, *46*, 4199-4201.

(30) (a) Olmstead, M. M.; Costa, D. A.; Maitra, K.; Noll, B. C.; Phillips, L.; Van, P. M.; Balch, A. L. *J. Am. Chem. Soc.* **1999**, *121,* 7090-7097. (b) Boyd, P. D. W.; Hodgson, M. C.; Rickard, C. F. E.; Oliver, A. G.; Chaker, L.; Brothers, P. J.; Bolskar, R. D.; Tham, F.

S.; Reed, C. A. *J. Am. Chem. Soc.* **1999**, *121,* 10487-10495.

(31) Tashiro, K.; Aida, T.; Zheng, J.-Y.; Kinbara, K.; Saigo, K.; Sakamoto, S.; Yamaguchi, K. *J. Am. Chem. Soc.* **1999**, *121*, 9477-9478.

(32) Zheng, J.-Y.; Tashiro, K.; Hirabayashi, Y.; Kinbara, K.; Saigo, K.; Aida, T.; Sakamoto, S.; Yamaguchi, K. *Angew. Chem., Int. Ed.* **2001**, *40*, 1857-1861.

(33) (a) Sato, H.; Tashiro, K.; Shinmori, H.; Osuka, A.; Murata, Y.; Komatsu, K.; Aida, T. *J. Am. Chem. Soc.* **2005**, *127*, 13086-13087. (b) Ouchi, A.; Tashiro, K.; Yamaguchi, K.; Tsuchiya, T.; Akasaka, T.; Aida, T. *Angew. Chem., Int. Ed.* **2006**, *45*, 3542-3546.

(34) (a) Sun, D.; Tham, F. S.; Reed, C. A.; Chaker, L.; Burgess, M.; Boyed, P. E. W. *J. Am. Chem. Soc.* **2000**, *122,* 10704-10705. (b) Sun, D.; Tham, F. S.; Reed, C. A.; Chaker, L.; Boyed, P. E. W. *J. Am. Chem. Soc.* **2002**, *124,* 6604-6612.

(35) Wu, Z.-Q.; Shao, X.-B.; Li, C.; Hou, J.-L.; Wang, K.; Jiang, X.-K.; Li, Z.-T. *J. Am. Chem. Soc.* **2005**, *127*, 17460-17468.

(36) (a) Ayabe, M.; Ikeda, A.; Kubo, Y.; Takeuchi, M.; Shinkai, S. *Angew. Chem., Int. Ed.* **2002**, *41*, 2790-2792. (b) Kubo, Y.; Sugasaki, A.; Ikeda, M.; Sugiyasu, K.; Sonoda, K.; Ikeda, A.; Takeuchi, M.; Shinkai, S. *Org. Lett.* **2002**, *4*, 925-928.

(37) Song, J.; Aratani, N.; Shinokubo, H.; Osuka, A. *J. Am. Chem. Soc.* **2010**, *132*, 16356-16357.

(38) Diederich, F.; Whetten, R. L. *Acc. Chem. Res.* **1992**, *25,* 119–126.

(39) Thilgen, C.; Diederich, F. *Chem. Rev.* **2006**, *106,* 5049–5135.

(40) Matsubara, H.; Shimura, T.; Hasegawa, A.; Semba, M.; Asano, K.; Yamamoto, K. *Chem. Lett.* **1998**, 27, 923-924.

(41) Komatsu, N. *Org. Biomol. Chem.* **2003**, *1*, 204-209.

(42) Wang, J.; Bodige, S. G.; Watson, W. H.; Gutsche, C. D. *J. Org. Chem.* **2000**, *65*, 8260-8263.

(43) Haino, T.; Yanase, M.; Fukazawa, Y. *Angew. Chem., Int. Ed.* **1998**, *37*, 997-998.

(44) Shoji, Y.; Tashiro, K.; Aida, T. *J. Am. Chem. Soc.* **2004**, *126*, 6570-6571.

(45) Haino, T.; Fukunaga, C.; Fukazawa, Y. *Org. Lett.* **2006**, *8*, 3545-3548.

(46) Huerta, E.; Metselaar, G. A.; Fragoso, A.; Santos, E.; Bo, C.; de Mendoza, J. *Angew. Chem., Int. Ed.* **2007**, *46*, 202-205.

(47) (a) Cravino, A.; Sariciftci, N. S. *J. Mater. Chem.* **2002**, *12*, 1931-1943. (b) Fukuzumi, S. *Bull. Chem. Soc. Jpn.* **2006**, *79*, 177-195.

(48) Ishi-i, T.; Iguchi, R.; Snip, E.; Ikeda, M.; Shinkai, S. *Langmuir* **2001**, *17*, 5825-5833.

(49) Shirakawa, M.; Fujita, M.; Shinkai, S. *J. Am. Chem. Soc.* **2003**, *125*, 9902-9903.

(50) Yamaguchi, T.; Ishii, N.; Tashiro, K.; Aida, T. *J. Am. Chem. Soc.* **2003**, *125*, 13934-13935.

(51) Nobukuni, H.; Shimazaki, Y.; Tani, F.; Naruta, Y. *Angew Chem., Int. Ed.* **2007**, *46*, 8975-8978.

(52) Liu, Y.; Wang, H.; Liang, P.; Zhang, H.-Y. *Angew Chem., Int. Ed.* **2004**, *43*, 2690-2694.

(53) Pantos, G. D.; Pengo, P.; Sanders, J. K. M. *Angew Chem., Int. Ed.* **2007**, *46*, 194-197.

(54) Pantos, G. D.; Wietor, J.-L.; Sanders, J. K. M. *Angew Chem., Int. Ed.* **2007**, *46*, 2238-2240.

(55) Lee, E.; Kim, J.-K.; Lee, M. *J. Am. Chem. Soc.* **2009**, *131*, 18242-18243.

(56) Hawkins, J. M.; Meyer, A. *Science* **1993**, *260*, 1918-1920.

(57) Hawkins, J. M.; Nambu, M.; Meyer, A. *J. Am. Chem. Soc.* **1994**, *116*, 7642-7645.

(58) Kessinger, R.; Crassous, J.; Herrmann, A.; Rüttimann, M.; Echegoyen, L.; Diederuch, F. *Angew. Chem., Int. Ed.* **1998**, *37*, 1919-1922.

(59) Crassous, J.; Rivera, J.; Fender, N. S.; Shu, L.; Echegoyen, L.; Thilgen, C.; Herrmann, A.; Diederuch, F. *Angew. Chem., Int. Ed.* **1999**, *38*, 1613-1617.

(60) Yamamoto, C.; Hayashi, T.; Okamoto, Y.; Ohkubo, S.; Kato, T. *Chem. Commun.* **2001**, 925-926.

(61) Ikai, T.; Okamoto, Y. *Chem. Rev.* **2009**, *109*, 6077-6101.

(62) Shoji, Y.; Tashiro, K.; Aida, T. *J. Am. Chem. Soc.* **2010**, *132*, 5928-5929.

Chapter 1

Encapsulation of Fullerenes in a Helical Cavity of Syndiotactic Poly(methyl methacrylate) Leading to a Robust Processable Complex with a Macromolecular Helicity Memory

Abstract: Syndiotactic poly(methyl methacrylate) (st-PMMA), a commonly used plastic, folded into a preferred-handed helix assisted by chiral aromatic alcohols, (*R*)- or (*S*)-1-phenylethanol, and encapsulated fullerenes within its helical cavity to form an optically active peapod-like complex whose helicity was retained after removal of the chiral alcohols.

Introduction

The control and fabrication of the molecular ordering of fullerenes has attracted considerable attention because of their possible applications in advanced materials such as electronic and optoelectronic materials.[1] The supramolecular approach based on the self-assembly of functionalized fullerenes[2] or trapping of fullerenes by host molecules through inclusion[3] has been widely applied to make low-dimensional nanostructures of fullerenes with a rather high polydispersity. The uniform 1D alignment of fullerenes can be attained within carbon nanotubes (CNTs), which encapsulate fullerenes to form so-called fullerene "nanopeapods".[4,5] The unique structural characteristics of fullerene nanopeapods provide intriguing chemical and physical properties,[5] but also make them difficult to synthesize and process. Fullerene-containing polymers may have a great potential for practical purposes owing to their easy processability, high mechanical strength, and availability of the polymers,[6] but there is no clear-cut strategy for controlling the distinct arrays of the fullerenes in such systems. In this chapter, the author reports that st-PMMA, a commodity plastic, encapsulates fullerenes such as C_{60}, C_{70}, and C_{84} within its helical cavity to form a peapod-like crystalline complex that can be readily transformed into a homogeneous film. The author also found that an optically active alcohol induces a preferred-handed helicity in the st-PMMA, whose helical conformation is "memorized"[7] after complete removal of the chiral alcohol and enforced by the inclusion of fullerenes in the st-PMMA helical cavity. st-PMMA has been reported to form a thermoreversible physical gel in aromatic solvents such as toluene, in which the st-PMMA chains adopt a helix of 74 units per 4 turns (74/4 helix) with a sufficiently large cavity of about 1 nm, and hence, solvents are encapsulated in the cavity of the inner helix.[8] The author anticipated that fullerenes of specific sizes might be encapsulated in the helical cavity of the st-PMMA helices to form 1D regulated fullerene arrays (Figure 1-1a).

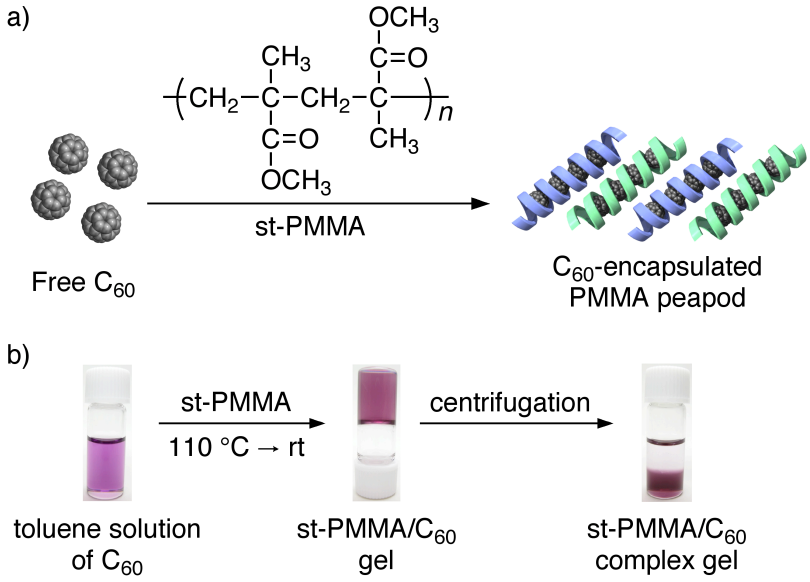

Figure 1-1. (a) Schematic illustration of the encapsulation of C_{60} in the st-PMMA helical cavity upon gelation. Right- (blue) and left-handed (green) helical complexes are equally produced. (b) Photographs of a toluene solution of C_{60} (1 mg/mL, 1 mL; left), st-PMMA/C_{60} gel after the addition of st-PMMA (10 mg) with subsequent heating to 110 °C and then cooling to room temperature (middle), and st-PMMA/C_{60} complex gel after centrifugation at 1700 *g* for 10 min (right).

Results and Discussion

To this end, st-PMMA (10 mg) was dissolved in a toluene solution of C_{60} (1 mg/mL, 1 mL) upon heating at 110 °C. The solution was allowed to cool to room temperature, and it gelled within a few minutes. After centrifugation, the author obtained a purple-colored condensed gel, while the supernatant became pale pink (Figure 1-1b). The electronic absorption spectra of the feed C_{60} solution and the supernatant indicate that 0.91 mg of C_{60} (8.3 wt %) was encapsulated in the st-PMMA cavities. The encapsulated C_{60} content increased with increasing feed C_{60} concentration and reached a maximum amount of 1.3 mg in toluene (Table 1-1). When 1,2-dichlorobenzene (DCB), a better solvent for solubilizing

C_{60}, was used as the cosolvent (50 vol % in toluene), the st-PMMA more efficiently trapped C_{60} (23.5 wt %, 3.1 mg per 10 mg of st-PMMA; Table 1-1; for the effect of the DCB amounts on the encapsulation of C_{60} in toluene, Figure 1-2), and the amount of the st-PMMA helical hollow space that is filled with C_{60} molecules is roughly estimated to be 86% based on a possible helical structure of st-PMMA filled with C_{60} in a 1D close packing manner (Table 1-1).

The author then investigated the thermal stabilities of the st-PMMA and st-PMMA/C_{60} gels by measuring their melting behavior using ^{1}H NMR spectroscopy.[9] A st-PMMA gel started melting at around 40 °C, while the st-PMMA/C_{60} gel maintained its gel structure over 60 °C resulting from encapsulation of the C_{60} molecules within the helical cavity of st-PMMA, thereby acting to reinforce the st-PMMA physical gel (Figure 1-3 and Table 1-1). Differential scanning calorimetry (DSC) and X-ray diffraction (XRD) profiles of the st-PMMA/C_{60} films with different C_{60} contents (11.7 and 23.5 wt %) revealed a

Table 1-1. Encapsulation of C_{60} in st-PMMA Helical Cavity upon Gelation with C_{60}[a]

entry	solvent	C_{60} in feed (mg)	st-PMMA/C_{60} gel	st-PMMA/C_{60} complex gel	
			gel point (°C)[b]	encapsulated C_{60} content (mg)[c]	filling ratio of C_{60} (%)[d]
1	toluene	—	29	—	—
2	toluene	1.0	58	0.91	30
3	toluene	2.0	60	1.3	43
4	toluene-DCB (50 vol%)	11.0	48	3.1	86

[a] The gels were prepared by adding 10 mg of st-PMMA (M_n = 554000, *rr* = 94%) to a toluene solution of C_{60} (1 mL) followed by heating to 110 ºC and cooling to room temperature, and then centrifuged. [b] Estimated based on the changes in the ^{1}H NMR signal intensities of the st-PMMA/C_{60} gel on cooling; see Figure 1-3. [c] Estimated based on the following equation: encapsulated C_{60} content = (C_{60} in feed) x (Abs_0–Abs)/Abs_0, where Abs_0 and Abs represent the absorbance at 336 nm of the feed C_{60} solution and that of the supernatant separated from the st-PMMA/C_{60} complex gel after centrifugation. [d] Estimated based on a possible helical structure of st-PMMA filling with C_{60} in a 1D close packing manner, see Figure 1-8c.

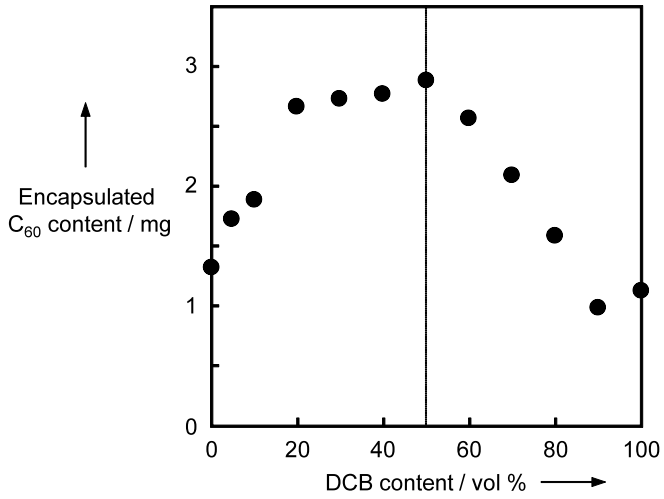

Figure 1-2. Effect of DCB content in toluene on the encapsulation of C_{60} upon gelation of st-PMMA

crystalline structure of the st-PMMA/C_{60} complex (Figure 1-4) that is essentially different from that of the st-PMMA film. The st-PMMA/C_{60} film containing 23.5 wt % of C_{60} maintained the crystal structure after evaporation of the solvents and exhibited a birefringence as observed by polarizing optical microscopy (Figure 1-4k), whereas the st-PMMA film showed no birefringence (Figure 1-4j). The author notes that it-PMMA cannot encapsulate C_{60} molecules at all, and the C_{60} precipitated upon evaporating the solvent from an it-PMMA/C_{60} mixture in toluene in spite of the low C_{60} content (4.8 wt %; Figure 1-5). The st-PMMA film showed only a heat capacity change at the glass-transition temperature (T_g = 126.7 °C) as observed for typical amorphous st-PMMAs (Figure 1-4a), indicating that a helical conformation induced in the st-PMMA chains in a gel formed in aromatic solvents is disrupted once the solvents are completely removed by evaporation, as supported by the broad XRD pattern (Figure 1-4e). In sharp contrast, the st-PMMA/C_{60} film containing 11.7 wt % of C_{60} revealed an additional endothermic peak at 224.9 °C corresponding to the melting temperature (T_m) of the st-PMMA/C_{60} complex (Figure 1-4b). Increasing the C_{60}

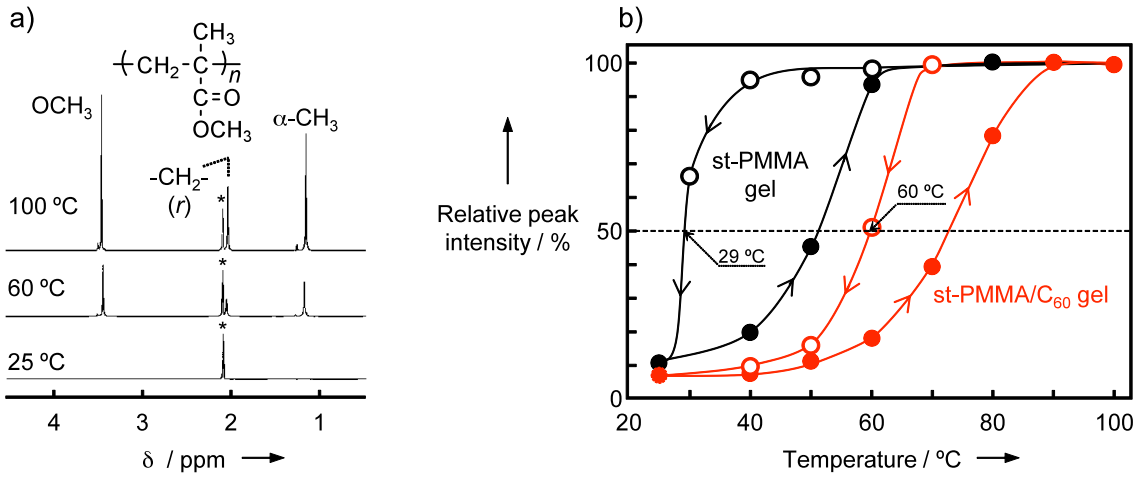

Figure 1-3. Thermal stability of the st-PMMA and st-PMMA/C_{60} gels. (a) ^{1}H NMR spectra (500 MHz) of st-PMMA in the presence of C_{60} in toluene-d_8 at 100 (solution), 60 and 25 ºC (gel). st-PMMA, 10 mg/mL; C_{60}, 2 mg/mL. The asterisk denotes the resonances from the solvent. (b) Changes in the relative peak intensity of the methoxy proton resonances of st-PMMA in the presence (○, cooling; ●, heating) and absence (○, cooling; ●, heating) of C_{60} in toluene-d_8. The peak intensity at 110 ºC was used as the base value (100 %).

content (23.5 wt %) brought about an increase in the crystallinity, and the melting peak increased, accompanied by the near disappearance of the T_g peak (Figure 1-4c). As a consequence, the st-PMMA helical hollow spaces may be filled with 23.5 wt % C_{60} molecules, which agrees approximately with the estimated filling ratio (86%; Table 1-1). Further strong evidence for the crystalline structure of the st-PMMA/C_{60} complex observed is its characteristic XRD pattern, which is completely different from those of the st-PMMA (Figure 1-4e) and C_{60} films (Figure 1-4i); the st-PMMA/C_{60} complex has an apparent d spacing of 1.67 nm (Figures 1-4f and g). Further heating of the st-PMMA/C_{60} film (23.5 wt %) at 280 °C, which is higher than T_m, gave rise to an irreversible release of the encapsulated C_{60} molecules, resulting in amorphous st-PMMA and C_{60} aggregates as supported by the DSC and XRD profiles (Figures 1-4d and h, respectively).

In the same way, C_{70} and C_{84} molecules can be encapsulated in the st-PMMA hollow

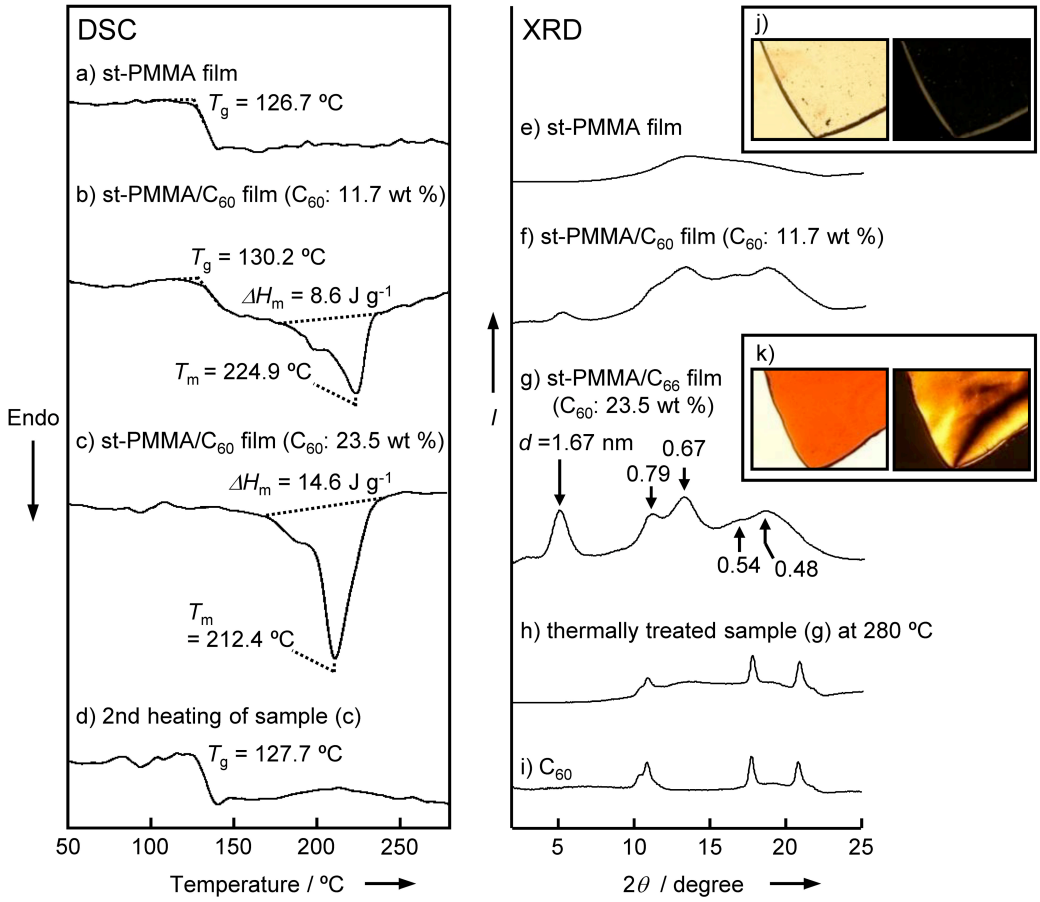

Figure 1-4. DSC thermograms of (a) st-PMMA film and (b, c) st-PMMA/C_{60} complex films containing (b) 11.7 and (c) 23.5 wt % C_{60}. These films were prepared by evaporating the solvents from the st-PMMA and st-PMMA/C_{60} complex gels in toluene or a toluene/DCB mixture (50 vol %), thus producing homogeneous films without any phase separation even at a high C_{60} content. The measurements were conducted after cooling the samples at 0 °C, followed by heating to 280 °C (10 °C/min) under nitrogen. (d) The sample (c) was then cooled to 0 °C (10 °C/min), and then heated again (10 °C/min). The arrow to the left of the DSC data indicates the endothermic direction. XRD profiles of (e) st-PMMA film, (f) st-PMMA/C_{60} complex film (11.7 wt % C_{60}), st-PMMA/C_{60} complex film (23.5 wt % C_{60}) (g) before and (h) after thermal treatment at 280 °C for 3 min, and (i) bulk C_{60}. Polarized (right) and nonpolarized (left) optical micrographs of (j) st-PMMA and (k) st-PMMA/C_{60} complex (23.5 wt % C_{60}) films. Dimensions of micrographs in (j) and (k): 1 x 1.3 mm^2.

spaces to form crystalline condensed gels and films (Figures 1-6 and 1-7, respectively). Interestingly, the *d*-spacing value observed by XRD increased with an increase in the size of the encapsulated fullerenes, from 1.67 (C_{60}) to 1.92 (C_{70}) and 2.04 nm (C_{84}), indicating that the st-PMMA helical cavity likely expands upon encapsulation of the larger fullerenes, and this change may be accompanied by a change in the helical pitch of the st-PMMA.

Atomic force microscopy (AFM) of a st-PMMA/C_{60} Langmuir–Blodgett (LB) film deposited on mica afforded further evidence for the inclusion of C_{60} in the st-PMMA. The mixed monolayer of st-PMMA and C_{60}, spread on a water surface, formed a crystalline rodlike structure with a lamellar alignment upon compression (Figure 1-8a) whose surface pressure–area (π–A) isotherm was different from those of st-PMMA and C_{60} alone (Figure 1-9). The AFM image revealed helix-bundle structures, which are further resolved into individual stripe-patterned chains with a chain–chain lateral spacing of (1.9 ± 0.1) nm and a helical pitch of 0.9 ± 0.1 nm. Transmission electron microscopy (TEM) of the LB film suggests a 1D alignment of C_{60} molecules (with an average intermolecular distance of about 1 nm), which may be encapsulated within the undetectable st-PMMA helices during irradiation with 120-keV electrons (Figures 1-8b and 1-10). In the TEM observations, low doses and

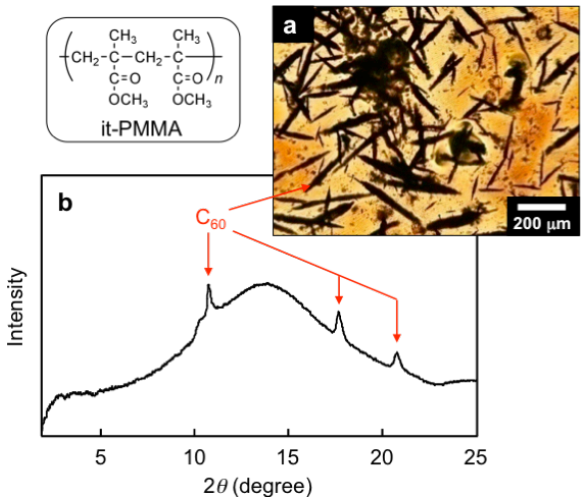

Figure 1-5. (a) Optical micrograph and (b) XRD profile of an it-PMMA/C_{60} film (4.8 wt % of C_{60}).

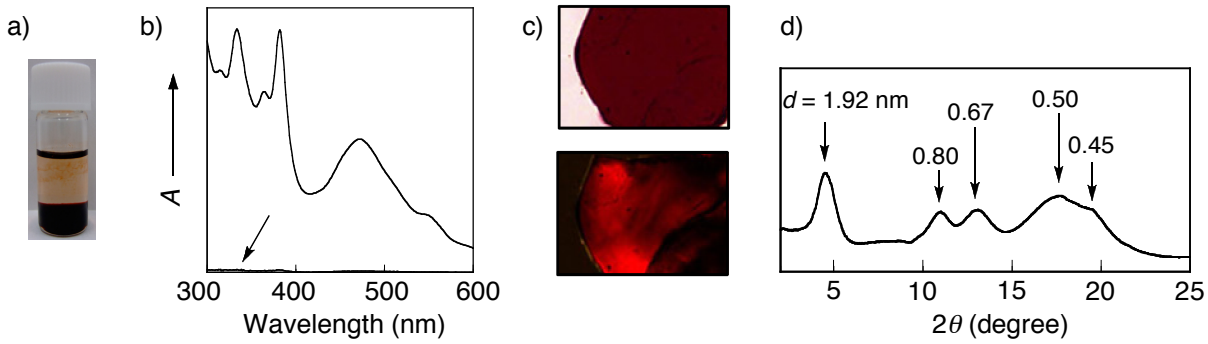

Figure 1-6. (a) Photograph of a st-PMMA/C_{70} complex gel in toluene after centrifugation. (b) Absorption spectra of the feed solution of C_{70} (top) and the supernatant separated from the st-PMMA/C_{70} complex gel after centrifugation (bottom). (c) Polarized (bottom) and non-polarized (top) optical micrographs of a st-PMMA/C_{70} complex film (20.6 wt % of C_{70}). The film was prepared by evaporating the solvent of the corresponding gel. Scale, 150 x 250 μm. (d) XRD profile of the st-PMMA/C_{70} complex film (20.6 wt % of C_{70}).

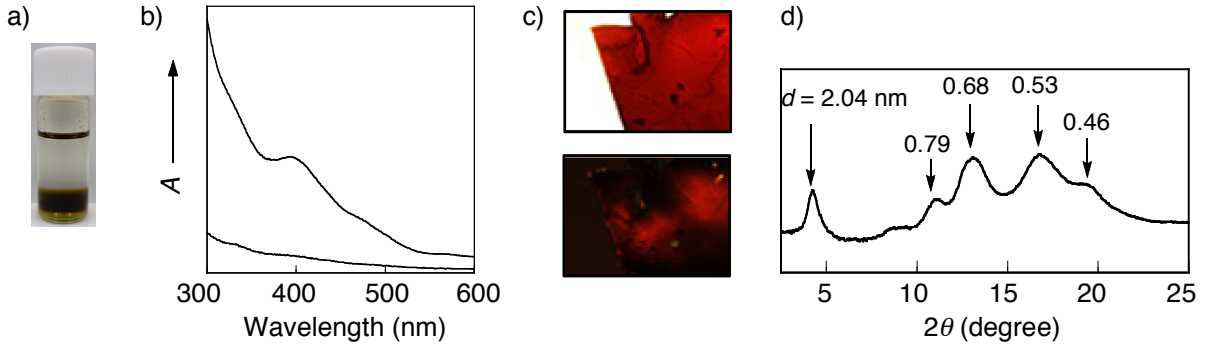

Figure 1-7. (a) Photograph of a st-PMMA/C_{84} complex gel in toluene and DCB (50 vol %) after centrifugation. (b) Absorption spectra of the feed solution of C_{84} (top) and the supernatant separated from the st-PMMA/C_{84} complex gel after centrifugation (bottom). (c) Polarized (bottom) and non-polarized (top) optical micrographs of a st-PMMA/C_{84} complex film (4.7 wt % of C_{84}). The film was prepared by evaporating the solvent of the corresponding gel. Scale, 550 x 750 μm. (d) XRD profile of the st-PMMA/C_{84} complex film (4.7 wt % of C_{84}).

short exposure times were carefully applied to minimize any electron beam damage, but the st-PMMA chains were damaged, resulting in release of the encapsulated C_{60} molecules from the st-PMMA nanotubes, and a uniform and long 1D array of C_{60} molecules, as expected from the AFM image (Figure 1-8a), could not be observed (Figure 1-10 shows more details of the TEM observations.). Figure 1-8c shows a possible structure of the st-PMMA/C_{60} complex calculated on the basis of the reported helical structure of st-PMMA[8,10] (Figure 1-11 and Table 1-2) in which the C_{60} molecules are encapsulated to form a regular 1D array with an intermolecular distance of 1.0 nm. The helical pitch and lateral spacing of the st-PMMA including the C_{60} molecules, estimated by AFM, are in good agreement with those of the proposed model. Molecular dynamics (MD) simulations revealed that the included C_{60} molecules remain within the helical cavity of the st-PMMA at 400 K for 200 ps, which supports its thermal stability.

The author also found that a preferred-handed helical st-PMMA can be formed by an optically active aromatic alcohol,[11] (*R*)- or (*S*)-1-phenylethanol (**1**), when used as the gelling medium during the st-PMMA/C_{60} gel formation (Figure 1-12a). Surprisingly, the induced form of the helix is retained after the optically active **1** is completely removed. The optically active st-PMMA/C_{60} complex gel was prepared in a similar way in toluene-d_8 with (*R*)-**1** (20 vol %) and subsequent complete removal of the (*R*)-**1** by repeatedly washing the gel with toluene-d_8, and then isolated by centrifugation (Table 1-3). The gelation of st-PMMA (10 mg/mL) slowly took place in 10 vol % **1** in toluene after 3 h, but the solution did not turn into a gel in 20 vol % **1**. In contrast, the gelation kinetics were accelerated in the presence of C_{60}, and the st-PMMA/C_{60} solution formed a gel in 10 and 20 vol % **1** after 10 min and 15 h, respectively (Table 1-3). The gel without any trace amount of (*R*)-**1** exhibited a vibrational circular dichroism (VCD) in the PMMA IR regions owing to the helical structure of the st-PMMA with an excess of one handedness whose helicity is further "memorized" after removal of the (*R*)-**1** (Figure 1-12b). When (*S*)-**1** was used instead, st-PMMA with the opposite helicity was formed, as evidenced by the mirror-image VCD. The IR and VCD

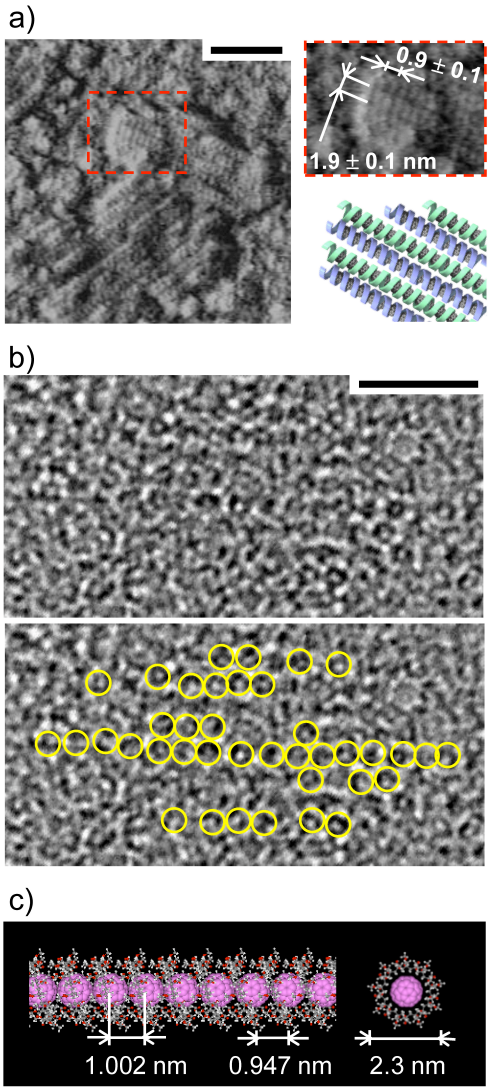

Figure 1-8. (a) Left: Tapping-mode AFM phase image of an LB film of the st-PMMA/C_{60} complex deposited on mica; scale bar: 10 nm. Right: Magnified image of the area indicated by the dotted square (top) and schematic representation of a possible bundle structure of the helical st-PMMA/C_{60} complex (bottom). (b) High-resolution TEM image of an LB film of the st-PMMA/C_{60} complex (top) and 1D alignment of the C_{60} molecules (bottom), indicated by the yellow circles (diameter: 1 nm);[11] scale bar: 5 nm. (c) Energy-minimized structure of the st-PMMA/C_{60} complex: side view (left) and top view (right). A computational study was performed at the B3LYP/6-31(d) level under periodic boundary conditions.

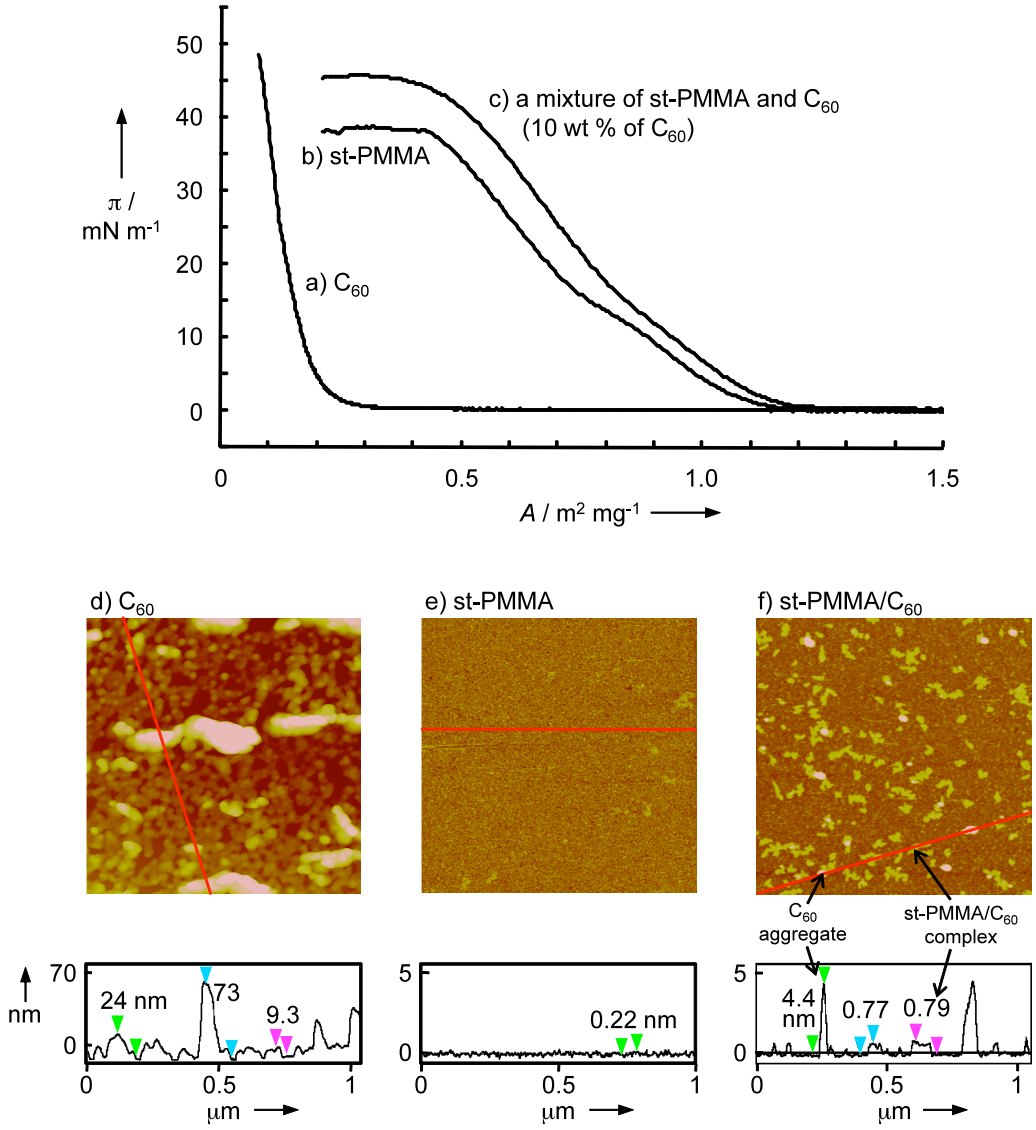

Figure 1-9. *π–A* isotherms of (a) C_{60}, (b) st-PMMA and (c) st-PMMA and C_{60} mixture (10 wt % of C_{60}) on water. Each benzene solution having a concentration of *ca.* 7 x 10^{-6} g/mL was spread on a water surface at 25 ºC in an LB trough with the area of 60 x 15 cm^2, compressed at the rate of 45 cm^2/min and deposited at 10 mN/m onto a freshly cleaved mica by pulling them out of the water at the rate of 4.2 mm/min while compressing the monolayer at that pressure (the vertical dipping method). Tapping mode AFM height images of deposited (d) C_{60}, (e) st-PMMA and (f) the mixture of st-PMMA and C_{60} on mica. Scale, 1 x 1 μm. The height profiles measured along the red lines in the images are also shown (bottom).

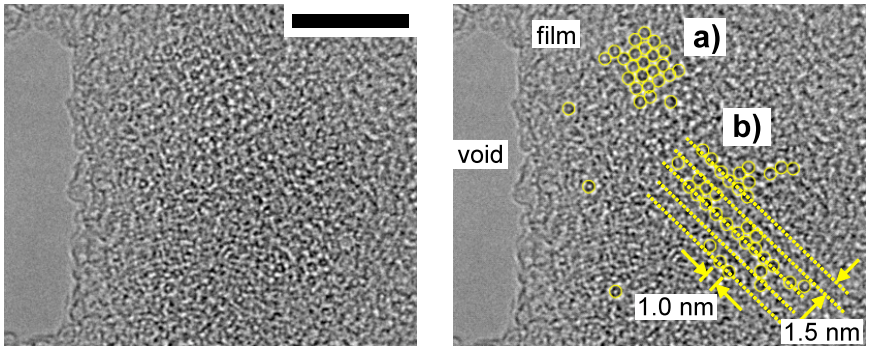

Figure 1-10. TEM image of an LB film of the st-PMMA/C_{60} complex (left) and 1D alignment of C_{60} molecules indicated by the yellow circles (1 nm ϕ) (right). Bar, 10 nm. The region (a) may correspond to a structure derived from the 2D hexagonally close-packed C_{60} molecules, probably released from the st-PMMA nanotubes because the hexagonally close-packed arrangement of C_{60} is significantly different from a center cubic structure observed for the C_{60} crystals.[28] For an expanded TEM image, see Figure 1-8b.

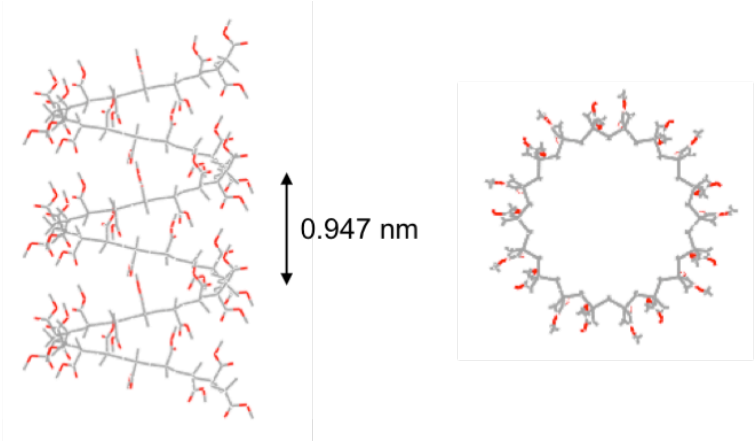

Figure 1-11. A stick model of the 18/1 st-PMMA helix used for the construction of the C_{60}-encapsulated st-PMMA model (Figure 1-8c) optimized by using *ab initio* quantum chemical calculations at the HF/STO-3G level and further at the B3LYP/6-31G(d) level, see Table 1-2. Side view (left) and top view (right).

Table 1-2. Internal Coordinates of the Optimized 18_1 st-PMMA Helix by Using *Ab Initio* Quantum Chemical Calculations at the HF/STO-3G Level and Further at the B3LYP/6-31G(d) Level

bond length	(nm)
trans-isomer	
C2b^{-1}-C1a	0.1571
C1a-C2a	0.1569
C1a-C3a	0.1537
C1a-C5a	0.1536
C3a-O1a	0.1350
C3a-O2a	0.1214
O1a-C4a	0.1441
C-H	0.109-0.110
cis-isomer	
C2a-C1b	0.1572
C1b-C2b	0.1573
C1b-C3b	0.1537
C1b-C5b	0.1537
C3b-O1b	0.1348
C3b-O2b	0.1217
O1b-C4b	0.1438
C-H	0.109-0.110

bond angle	(degree)
trans-isomer	
C2b^{-1}-C1a-C2a	103.3
C1a-C2a-C1b	122.4
C2b^{-1}-C1a-C3a	109.8
C2b^{-1}-C1a-C5a	112.3
C3a-C1a-C5a	109.0
C1a-C3a-O1a	111.8
C1a-C3a-O2a	125.3
O1a-C3a-O2a	122.9
C3a-O1a-C4a	116.0
H-C-H	106.9-111.2
cis-isomer	
C2a-C1b-C2b	103.1
C1b-C2b-C1a^{+1}	123.3
C2a-C1b-C3b	107.5
C2a-C1b-C5b	112.6
C3b-C1b-C5b	112.9
C1b-C3b-O1b	113.6
C1b-C3b-O2b	123.7
O1b-C3b-O2b	122.6
C3b-O1b-C4b	115.9
H-C-H	106.9-111.2

torsion angle	(degree)
trans-isomer	
C1b^{-1}-C2b^{-1}-C1a-C2a	179.05
C2b^{-1}-C1a^{-1}-C2a-C1b	-175.20
C1b^{-1}-C2b^{-1}-C1a-C3a	-63.67
C1b^{-1}-C2b^{-1}-C1a-C5a	57.85
C2b^{-1}-C1a-C3a-O1a	-57.89
C2b^{-1}-C1a-C3a-O2a	121.65
C5a-C1a-C3a-O1a	178.63
C1a-C3a-O1a-C4a	178.16
C3a-O1a-C4a-H	~ staggered
C3a-C1a-C5a-H	~ staggered
cis-isomer	
C1a-C2a-C1b-C2b	-170.72
C2a-C1b-C2b-C1a^{+1}	176.14
C1a-C2a-C1b-C3b	75.63
C1a-C2a-C1b-C5b	-49.26
C2a-C1b-C3b-O1b	-126.38
C2a-C1b-C3b-O2b	53.67
C5b-C1b-C3b-O1b	-1.65
C1b-C3b-O1b-C4b	-179.99
C3b-O1b-C4b-H	~ staggered
C3b-C1b-C5b-H	~ staggered

Numbering of Atoms

a-MMA unit (*trans*-isomer) b-MMA unit (*cis*-isomer)

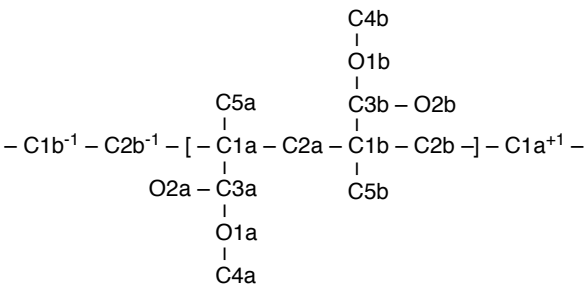

spectra for the right- and left-handed helical 18/1 st-PMMAs were them calculated at the B3LYP/6-31G(d) level (Figure 1-12c and Table 1-4). The calculated spectra fit well to the observed spectra, suggesting that the st-PMMA helix induced by (*R*)-**1** is likely right handed.

Owing to a preferred-handed helical structure of the st-PMMA nanotube, the author also observed an induced electronic CD (ECD) in the encapsulated C_{60} chromophore regions, although C_{60} itself is achiral (Figures 1-12b and 1-13).[12,13] A weak but apparent bisignate ECD band at 656 nm also supports the encapsulation of the C_{60} molecules within the tubular cavity of the helical st-PMMA. The fact that the broad absorption band at around 450 nm only appears in the st-PMMA/C_{60} complex gel (Figure 1-14) supports the stacking interactions between neighboring C_{60} molecules,[15,16] which may lead to a color change of the complex gel (Figure 1-1b). The encapsulation of C_{60} in the helical st-PMMA nanotube is essential for the

Table 1-3. Gelation of st-PMMA in Toluene and (*R*)-**1** in the Presence and Absence of C_{60}[a]

entry		(*R*)-**1** in feed (% v/v)	C_{60} in feed (mg)	gelation time (min)	encapsulated C_{60} content (mg)	filling ratio of C_{60} (%)[b]
1	st-PMMA	0	–	3	–	–
2		10	–	180	–	–
3		20	–	no gelation	–	–
4	st-PMMA/C_{60}	0	1.0	1	0.91	30
5		10	0.9	10	0.79	27
6		20	0.8	900	0.64	22
7		30	0.7	no gelation	–	–

[a] The gels were prepared by adding 10 mg of st-PMMA (M_n = 554000, *rr* = 94%) to a toluene solution of C_{60} (1 mL) with (*R*)-**1** followed by heating to 110 ºC and cooling to room temperature, and then centrifuged. [b] Estimated based on a possible helical structure of st-PMMA filling with C_{60} in a 1D close packing manner, see Figure 1-8c.

induced ECD since a solution of st-PMMA and C_{60} in toluene with 30 vol % (*R*)-**1** does not turn into a gel and exhibits no ECD at all. The optically active st-PMMA/C_{60} complex gel and film are thermally stable up to their melting temperatures. In the absence of C_{60}, a similar optically active st-PMMA gel can be prepared with (*R*)- or (*S*)-**1** in toluene. The induced st-

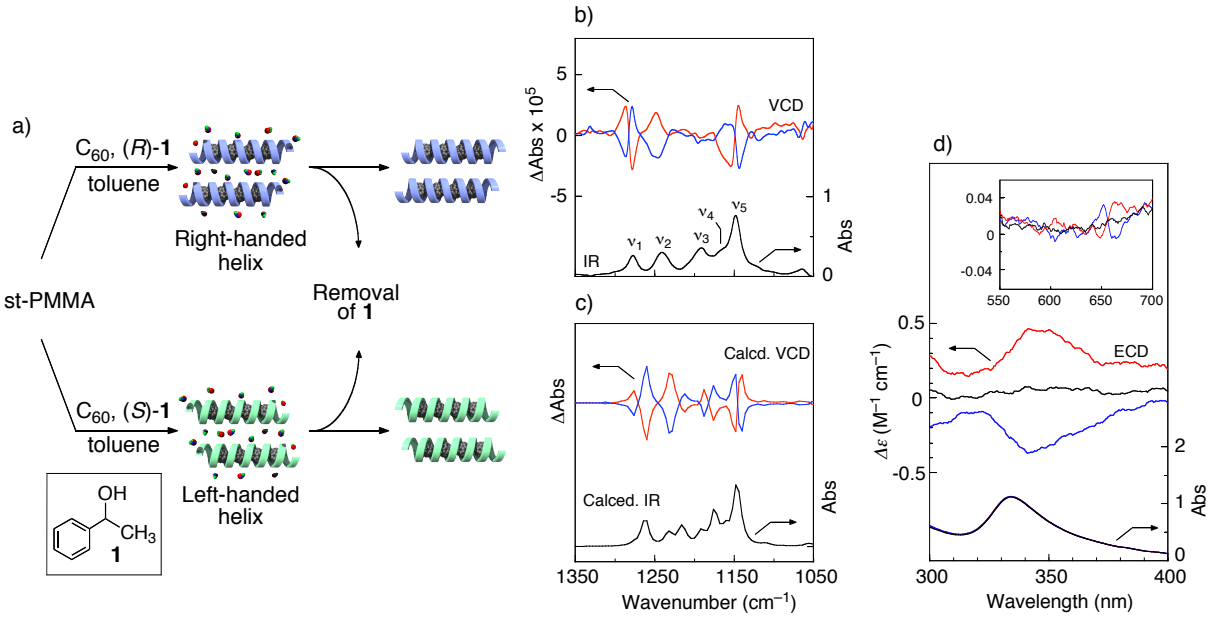

Figure 1-12. Optically active C_{60}-encapsulated st-PMMA with macromolecular helicity memory. (a) Schematic illustration of right- (top) and left-handed (bottom) helicity induction in the C_{60}-encapsulated st-PMMA in the presence of (*R*)- or (*S*)-**1**. (b) Observed VCD (top) and IR (bottom) spectra of isolated st-PMMA/C_{60} complex gels (3.1 wt % C_{60}) in toluene-d_8 prepared by (*R*)-**1** (red lines) and (*S*)-**1** (blue lines), measured after the complete removal of **1**. The assignments of the experimental and calculated IR and VCD bands (ν_1–ν_5) are in Table 1-4. The x axis is the same as in (c). (c) Calculated VCD (top) and IR (bottom) spectra of right- (red line) and left-handed (blue line) helical st-PMMAs. (d) Observed ECD (top) and absorption (bottom) spectra of isolated st-PMMA/C_{60} complex gels in toluene prepared by racemic **1** (black lines), (*R*)-**1** (red lines), and (*S*)-**1** (blue lines). The inset shows the corresponding ECD spectra in the long-wavelength regions (Figure 1-13). The contribution of the linear dichroism caused by the macroscopic anisotropy was negligible.

PMMA helix also remains after complete removal of the optically active **1**, and this helical st-PMMA can serve as a template for the further inclusion of C_{60} molecules, resulting in a st-PMMA/C_{60} complex gel, thus showing virtually the same VCD and ECD spectra as shown in Figures 1-12 and 1-15.

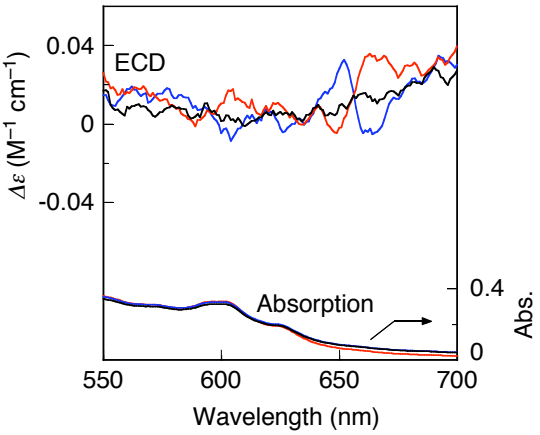

Figure 1-13. Observed ECD (top) and absorption (bottom) spectra of isolated st-PMMA/C_{60} complex gels in toluene prepared by (*RS*)-**1** (black lines), (*R*)-**1** (red lines), and (*S*)-**1** (blue lines).

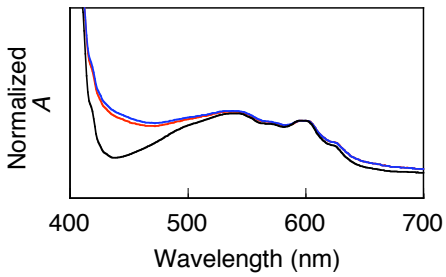

Figure 1-14. Absorption spectra of a toluene solution of C_{60} (1 mg/mL) (black line) and isolated st-PMMA/C_{60} complex gels in toluene containing 8.3 (red line) and 23.7 (blue line) wt % of C_{60}. The st-PMMA/C_{60} gels were washed with toluene to remove the unencapsulated C_{60} molecules before the measurements.

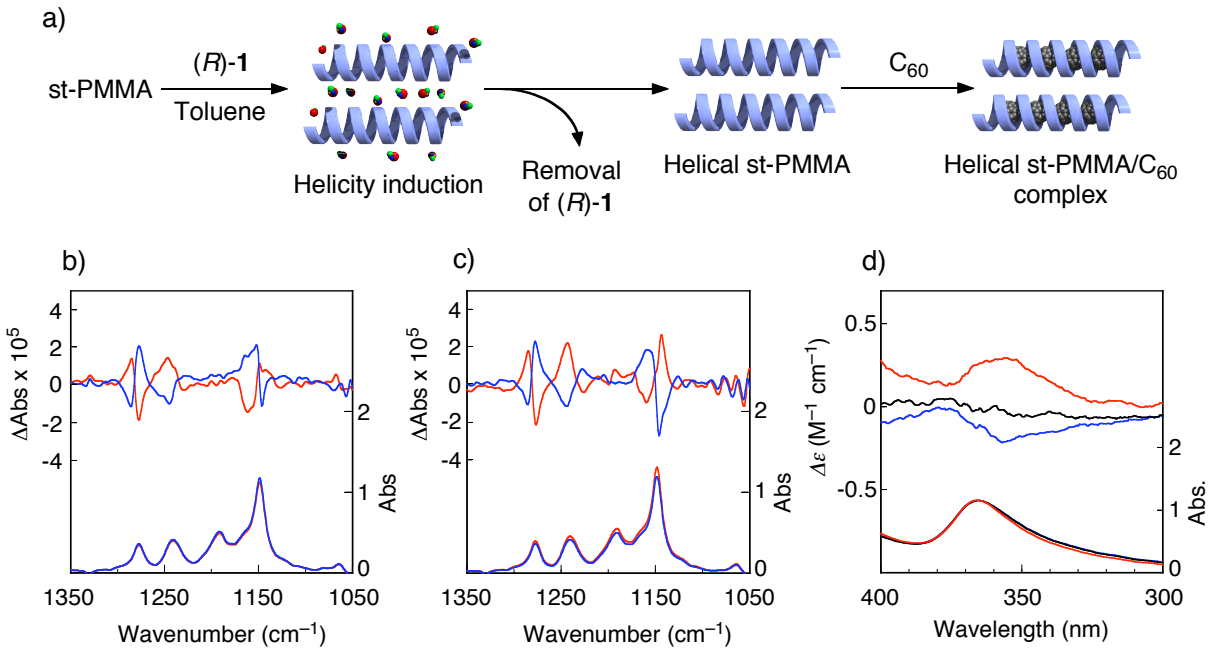

Figure 1-15. Synthesis of optically active helical st-PMMA and encapsulation of C_{60} within its helical cavity with macromolecular helicity memory. (a) Schematic illustration of right-handed helicity induction in st-PMMA in the presence of (*R*)-**1**. The induced helicity is memorized after (*R*)-**1** is completely removed and further encapsulation of C_{60} molecules. (b) Observed VCD and IR spectra of isolated st-PMMA gels in toluene-d_8 prepared by (*R*)-**1** (red lines) and (*S*)-**1** (blue lines). (c) Observed VCD and IR spectra of st-PMMA/C_{60} complex gels in toluene-d_8 obtained after the addition of C_{60} to the isolated st-PMMA gels prepared by (*R*)-**1** (red lines) and (*S*)-**1** (blue lines). (d) ECD and absorption spectra of st-PMMA/C_{60} complex gels in toluene-d_8 obtained after the addition of C_{60} to the isolated st-PMMA gels prepared by (*RS*)-**1** (black lines), (*R*)-**1** (red lines), and (*S*)-**1** (blue lines).

Table 1-4. Observed and Calculated Frequencies and Peak Assignments for the IR and VCD Spectra of the Optically Active st-PMMA/C_{60} Complex

band	IR^{obsd} frequency (cm^{-1})	IR^{calcd} frequency (cm^{-1})	VCD^{obsd} frequency (cm^{-1})	VCD^{calcd} frequency (cm^{-1})	assignment[a]
ν_1	1278	1264	1286 (ν_{1p})[b]	1276 (ν_{1p})[b]	out-of-phase ν_a(C-C-O) + $\rho(CH_2)$
			1279 (ν_{1v})[b]	1260 (ν_{1v})[b]	in-phase ν_a(C-C-O) + $\rho(CH_2)$
ν_2	1241	1232	1249 (ν_{2p})[b]	1233 (ν_{2p})[b]	ν_a(C-C-O) + $\tau(CH_2)$
		1216			
ν_3	1192	1192	—	1186 (ν_{3p})[b]	out-of-phase ν_a(C-O-C) + $\tau(CH_2)$
		1176	—	1176 (ν_{3v})[b]	
ν_4	1172	1160	Shoulder	—	ν_a(C-O-C) + $\rho(CH_3)$
ν_5	1148	1148	1154 (ν_{5v})[b]	1148 (ν_{5v})[b]	in-phase ν_a(C-O-C) + $\rho(CH_2)$
			1145 (ν_{5p})[b]	1141 (ν_{5p})[b]	out-of-phase ν_a(C-O-C) + $\rho(CH_2)$

[a] st-PMMA is assumed to have a 18/1 helix. Abbriviations, ν_a: anti-symmetric stretching, ρ: rocking, τ: twisting. [b] Bisignate VCD band. The band assignments for the right-handed helix are shown.

Conclusions

The results reported here show that st-PMMA can encapsulate fullerenes to mimic to some extent the behavior of CNTs. Unlike the latter, the fullerene-encapsulated st-PMMA is easy to prepare, inexpensive, and processable. Moreover, its helical sense can be controlled to produce an optically active supramolecular peapod. These unique supramolecular helical complexes offer potentially useful chiral materials as well as optoelectronic materials.

Experimental Section

Materials. The st-PMMA was synthesized by the syndiotactic-specific polymerization of MMA in toluene at –95 ºC using a typical Ziegler-type catalyst derived from $Al(C_2H_5)_3$ and $TiCl_4$.[14] The it-PMMA was prepared by the isotactic-specific anionic living polymerization of MMA in toluene at –78 ºC with *tert*-C_4H_9MgBr.[15] The number-average molecular weights (M_n), molecular weight distributions (M_w/M_n), and tacticities (*mm*:*mr*:*rr*) were as follows: st-PMMA: M_n = 544000, M_w/M_n = 1.29, and *mm*:*mr*:*rr* = 0:6:94; it-PMMA: M_n = 21800, M_w/M_n = 1.12, and *mm*:*mr*:*rr* = 97:3:0. The M_n and M_w/M_n values were measured by size exclusion chromatography in $CHCl_3$ using PMMA standards (Shodex, Tokyo, Japan) for the calibration. The tacticities were determined from the ^{1}H NMR signals due to the α-methyl protons.

Benzene, toluene, and 1,2-dichlorobenzene (DCB) (extra-pure grade) were purchased from Wako Chemicals (Osaka, Japan). (*R*)-, (*S*)-, and (*RS*)-1-phenylethanol (**1**) were obtained from Azmax (Chiba, Japan) and were used as received. [60]Fullerene (C_{60}) (99.5 %) was obtained from Tokyo Kasei (TCI, Tokyo, Japan) and [70]fullerene (C_{70}) (99 %) and [84]fullerene (C_{84}) (98 %) were from Aldrich. They were used without further purification. Water purified by a Milli-Q system was used as the subphase for the Langmuir-Blodgett (LB) investigations.

Instruments. Nuclear magnetic resonance (NMR) spectra were recorded on a Varian Unity Inova 500 spectrometer (500 MHz for ^{1}H and 125 MHz for ^{13}C) in $CDCl_3$ or toluene-d_8. Infrared (IR) spectra were recorded using a JASCO (Hachioji, Japan) Fourier Transform IR-620 spectrophotometer. Absorption and circular dichroism (CD) spectra were measured in a 0.1- or 0.2-mm quartz cell on a JASCO V-570 spectrophotometer and a JASCO J-820 spectropolarimeter, respectively. Vibrational CD (VCD) spectra were measured in a 0.15-mm BaF_2 cell with a JASCO JV-2001 spectrometer. The concentration was *ca.* 30 mg/mL in toluene-d_8. All spectra were collected for ca. 4–5 h at a resolution of 4 cm^{-1}.

Differential scanning calorimetry (DSC) measurements were performed on a SEIKO (Chiba, Japan) EXSTAR 6000 under a nitrogen atmosphere. The samples were sealed in

aluminum pans. The glass transition temperature (T_g) was defined as the intersection of the initial baseline and the sloping portion of the curves. The melting temperature (T_m) and heat of melting (ΔH_m) were determined from the minimum of the endothermic peak and by the peak area, respectively.

X-ray measurements were carried out using a Rigaku RINT RAPID-R X-ray diffractometer with a rotating-anode generator with graphite monochromated Cu Kα radiation (0.15418 nm) focused through a 0.3 mm pinhole collimator, which was supplied at 45 kV and 60 mA current, equipped with a flat imaging plate having a specimen-to-plate distance of 120.0 mm.

Polarizing optical microscopic observations were carried out with a Nikon (Tokyo, Japan) E600POL polarizing optical microscope equipped with a DS-5M CCD camera (Nikon) connected with a DS-L1 control unit (Nikon). The molecular modeling was performed on the program system MS Modeling software (version 3.1, Accelrys Inc., San Diego, CA). The molecular orbital (MO) and molecular dynamics (MD) calculations were conducted using Gaussian 03 (Gaussian, Inc., Pittsburgh, PA)[16] and WinMASPHYC Pro. (version 2.0, Fujitsu Co. Ltd., Tokyo, Japan) softwares, respectively.

The LB trough system (FSD-300AS, USI, Japan) was used for LB film preparations. Atomic force microscopy (AFM) observations were done using a Nanoscope IIIa microscope (Veeco Instruments, Santa Barbara, CA) in air at ambient temperature with standard silicon cantilevers (NCH, NanoWorld, Neuchâtel, Switzerland) in the tapping mode. The settings of the AFM observations were as follows: the free amplitude of the oscillation of 1.0 V, the set-point amplitude of 0.84 V, and the scan rate of 2.0 Hz. The Nanoscope image processing software was used for the image analysis.

The transmission electron microscopy (TEM) measurements were conducted using a JEM- 2100F transmission electron microscope (JEOL, Akishima, Japan) equipped with an MSC 600HP CCD camera (Gatan, Pleasanton, CA) operating at 120 kV.

Preparation of st-PMMA Gel and Film. Ten mg of st-PMMA was dissolved in toluene (1 mL) at 110 ºC. After the solution was cooled to room temperature (ca. 20 ºC), the solution gelled within 3 min. The st-PMMA film was obtained by evaporating the solvent under reduced pressure at room temperature for 12 h followed by drying under vacuum at 160 ºC for 1 h. The residual solvent content was estimated to be <0.3 wt % by ^{1}H NMR analysis.

Preparation of st-PMMA/C_{60} and st-PMMA/C_{70} Complex Gels and Films. A typical experimental procedure is described below. Ten mg of st-PMMA was dissolved in a toluene solution of C_{60} (2 mg/mL, 1 mL) at 110 ºC. After the solution was cooled to room temperature (*ca*. 20 ºC), the solution gelled within 1 min. The obtained soft gel was centrifuged at 1700 *g* for 10 min and the supernatant containing unencapsulated C_{60} molecules was removed from the gel by decantation. The condensed gel was then washed with toluene and the solvent was removed by decantation after centrifugation. This procedure was repeated several times. The encapsulated C_{60} content was estimated using the following equation: encapsulated C_{60} content (mg) = (C_{60} in feed (mg)) x (Abs_0 – Abs)/(Abs_0), where Abs_0 and Abs represent the absorbance at 336 nm of the feed C_{60} solution and that of the supernatant separated from the st-PMMA/C_{60} gel after centrifugation (Table 1-1). The st-PMMA/C_{60} complex film was obtained by evaporating the solvent in the condensed gel under reduced pressure at room temperature for 12 h followed by drying under vacuum at 160 ºC for 1 h. The residual solvent content was estimated to be <0.3 wt % by ^{1}H NMR analysis. In the same way, st-PMMA/C_{60} complex gels were prepared in toluene or in mixtures of toluene and DCB containing different amounts of st-PMMA and C_{60} (Figure 1-2 and Table 1-1). st- PMMA/C_{70} complex gel and film were also prepared in a similar way (Figure 1-6).

Preparation of st-PMMA/C_{84} Complex Gel and Film. Ten mg of st-PMMA was dissolved in a toluene-DCB (50 vol %) solution of C_{84} (7.1 x 10^{-3} mg/mL, 1 mL) at 110 ºC. After the solution was cooled to room temperature (*ca*. 20 ºC), the solution gelled within 1 min. The obtained soft gel was centrifuged at 1700 *g* for 10 min. After removing the

supernatant, the solution of C_{84} (2 mL) was added to the gel. The mixture was stirred at room temperature for 10 min and then centrifuged at 1700 *g* for 10 min. Because of poor solubility of C_{84}, these procedures were repeated thirty-five times to obtain the st-PMMA/C_{84} complex gel with 4.7 wt % of C_{84} (Figure 1-7). The st-PMMA/C_{84} complex film was obtained by evaporating the solvent in the condensed gel under reduced pressure at room temperature for 12 h followed by drying under vacuum at 160 ºC for 1 h.

Preparation of it-PMMA/C_{60} Film. Ten mg of it-PMMA was dissolved in a toluene solution of C_{60} (2 mg/mL, 0.25 mL) at room temperature, giving a homogeneous solution. The it- PMMA/C_{60} film was obtained by evaporating the solvent under reduced pressure at room temperature for 48 h (Figure 1-5).

Optically Active st-PMMA/C_{60} Complex Gel. A typical experimental procedure is described below. Twenty mg of st-PMMA was dissolved in a toluene-d_8 solution of C_{60} (1.6 mg/mL, 0.5 mL) containing (*R*)-**1** (20 vol %) at 110 ºC. After the solution was cooled to room temperature (*ca*. 20 ºC), the solution gelled within 15 h (Table 1-3). The obtained soft gel was centrifuged at 1700 *g* for 10 min and the supernatant containing unencapsulated C_{60} molecules was removed from the gel by decantation. The condensed gel was then washed with toluene-d_8 to remove the (*R*)-**1**. The residual (*R*)-**1** content was estimated to be <0.002 vol % by ^{1}H NMR analysis. The obtained gel was suspended in a small amount of toluene-d_8, and then subjected to the VCD and ECD measurements (b and d in Figure 1-12). In the same way, st-PMMA/C_{60} complex gels were prepared in a mixture of (*R*)-, (*S*)-, or (*RS*)-**1** and toluene or toluene-d_8 with different volume ratios (Table 1-3). The VCD spectrum of the st-PMMA/C_{60} complex gel prepared with (*RS*)-**1** was subtracted from the VCD spectra with (*R*)- or (*S*)-**1** in toluene-d_8 (Figure 1-12b).

Optically active st-PMMA gels were prepared in a similar way in toluene-d_8 containing 10 vol % of (*R*)- or (*S*)-**1** in the absence of C_{60} and the optically active (*R*)- and (*S*)-**1** were completely removed by washing the gels with toluene-d_8 to measure the VCD spectra (Figure

1-15b). To these gels was then added a toluene-d_8 solution of C_{60} (2 mg/mL, 1 mL) at room temperature. The mixtures were vigorously stirred by a magnetic stirrer and then centrifuged at 1700 *g* for 10 min. The condensed st-PMMA/C_{60} complex gel was washed with toluene-d_8 to remove the unencapsulated C_{60} molecules, and then subjected to the VCD and ECD measurements (c and d in Figure 1-15).

Molecular Modeling of st-PMMA Helix and IR and VCD Calculations. The geometrical parameters of the reported st-PMMA helix[17-20] were referred for the construction of an initial 18/1 st-PMMA (18 units per turn) helix model. The helical pitch was assumed to be 0.92 nm based on the AFM observation results[10] and the side chain conformations for the st- PMMA helix were assumed to take *trans* and *cis* conformations to the α-methyl group, based on the IR analysis by Tretinnikov and Ohta.[22] The detailed procedures for the construction of the initial 18/1 st-PMMA helix model were reported previously.[10]

The initial model was then fully optimized by using *ab initio* quantum chemical calculations at the HF/STO-3G level and further at the B3LYP/6-31G(d) level under the periodic boundary condition in Gaussian 03 program[16] running under Fujitsu PRIMEPOWER HPC2500 in Nagoya University. After the optimization, the helical pitch of 18/1 st-PMMA converged from 0.92 to 0.947 nm; this value fairly agrees with the reported helical pitch for the st-PMMA chain in the st-PMMA–organic molecule complexes determined by X-ray diffraction (0.885 nm)[8] and that for the st-PMMA chain in the it-PMMA–st-PMMA stereocomplex observed by high resolution AFM (0.92 nm).[10] The internal coordinates of the optimized 18/1 helical st-PMMA with the helical pitch of 0.947 nm are shown in Table 1-2 and Figure 1-11.

The IR and VCD spectra for the optimized 18/1 helical st-PMMA were then calculated using the density functional theory (DFT) method at the B3LYP/6-31G(d) level in Gaussian 03 program.[16] The calculated VCD spectra were used to determine the helical senses (right- or left-handed helix) of optically active helical st-PMMAs induced by (*R*)- and (*S*)-**1** by comparison with their experimental VCD spectra.

Because of difficulty in calculating IR and VCD spectra for an entire, large polymer, the IR and VCD for a series of st-PMMA oligomers from tetramer (4mer) to dodecamer (12mer) were calculated; each oligomer was taken from the optimized helical st-PMMA and both the end groups were replaced by methyl groups. We found that the IR and VCD spectra were insensitive to the oligomer length and almost the same when the oligomers were longer than octamer (8mer). The calculated IR and VCD spectra for the right- and left-handed helical st-PMMAs (12mer) are shown in Figure 1-12c using GaussView W 3.0 (Gaussian, Inc., Pittsburgh, PA, USA). These spectra were constructed from calculated dipole and rotational strengths assuming Lorentzian band shape with a half-width at half maximum of 4 cm^{-1}. The calculated frequencies were scaled by a frequency-independent factor of 0.91613.[25] The peakassignments for the main peaks of the IR and VCD spectra based on the calculation results are summarized in Table 1-4, which were fairly in good agreement with the reported ones.[22,26,27]

Molecular Modeling and Molecular Dynamics Simulation of st-PMMA/C_{60} Complex. C_{60} molecules were manually inserted into the optimized 18/1 st-PMMA helix so as to form a st-PMMA/C_{60} inclusion complex as shown in Figure 1-8c, in which the distance between the adjacent encapsulated C_{60} molecules was kept constant at 1.002 nm; this spacing is equal to the distance between the adjacent C_{60} molecules in the crystal.[28] Molecular dynamics (MD) simulations were then performed for the constructed st-PMMA/C_{60} inclusion complex using commercial MD software (Materials Explorer 3.0, Fujitsu, Tokyo, Japan) using an NTV ensemble in order to evaluate the stability of the inclusion complex. The st-PMMA/C_{60} complex was first annealed at 10 K for 100 ps, and then further annealed at 400 K for 200 ps. The inclusion complex was stable and maintained its structure during the MD annealing process.

Sample Preparations for AFM and TEM Measurements and Surface Pressure-Area Isotherm Measurements. A st-PMMA and C_{60} mixture (10 wt % of C_{60}) was spread

from a benzene solution (ca. 7 x 10^{-6} g/mL) on a water surface at 25 ºC in an LB trough with the area of 60 x 15 cm^2, compressed at the rate of 45 cm^2/min and deposited at 10 mN/m onto a freshly cleaved mica by pulling them out of the water at the rate of 4.2 mm/min while compressing the monolayer at that pressure (the vertical dipping method) and subjected to the AFM observations (Figure 1-8a). The surface pressure-area isotherms were measured at a compression rate of 45 cm^2/min using filter paper as a Wilhelmy plate (Figure 1-9). A six layered film was also deposited on a TEM microgrid (Oken Shoji, Tokyo, Japan) by the horizontal lifting method, and subjected to the TEM observations (Figures 1-8b and 1-10).

References

(1) (a) Kadish, K. M.; Ruoff, R. S *Fullerenes: Chemistry, Physics, and Technology,* Wiley-Interscience, New York, **2000**. (b) Prato, M. *J. Mater. Chem.* **1997**, *7*, 1097-1109. (c) Chen, Y.; Huang, Z.; Cai, R. F.; Yu, B. C. *Eur. Polym. J.* **1998**, *34*, 137-151. (d) Prato, M.; Maggini, M. *Acc. Chem. Res.* **1998**, *31*, 519-526. (e) Cravino, A.; Sariciftci, N. S. *J. Mater. Chem.* **2002**, *12*, 1931-1943. (f) Fukuzumi, S. *Bull. Chem. Soc. Jpn.* **2006**, *79*, 177-195.

(2) (a) Nakamura, E.; Isobe, H. *Acc. Chem. Res.* **2003**, *36*, 807-815. (b) Guldi, D. M.; Zerbetto, F.; Georgakilas, V.; Prato, M. *Acc. Chem. Res.* **2005**, *38*, 38-43.

(3) (a) Diederich, F.; López, M. G. *Chem. Soc. Rev.* **1999**, *28*, 263-277. (b) Boyd, P.D.W.; Reed, C. A. *Acc. Chem. Res.* **2005**, *38*, 235-242. (c) Tashiro, K.; Aida, T. *Chem. Soc. Rev.* **2007**, *36*, 189-197.

(4) (a) Smith, B. W.; Monthioux, M.; Luzzi, D. E. Nature **1998**, *396*, 323-324. (b) Hirahara, K.; Suenaga, K.; Bandow, S.; Kato, H.; Okazaki, T.; Shinohara, H.; Iijima, S. *Phys. Rev. Lett.* **2000**, *85*, 5384-5387.

(5) (a) Sloan, J.; Kirkland, A. I.; Hutchison, J. L.; Green, M. L. H. *Chem. Commun.* **2002**, 1319-1332. (b) Vostrowsky, O.; Hirsch, A. *Angew. Chem., Int. Ed.* **2004**, *43*, 2326-2329. (c) Khlobystov, A. N.; Britz, D. A.; Briggs, G. A. D. *Acc. Chem. Res.* **2005**, *38*, 901-909. (d) Kitaura, R.; Shinohara, H. *Chem. Asian J.* **2006**, *1*, 646-655.

(6) (a) Wang, C.; Guo, Z.-X.; Fu, S.; Wu, W.; Zhu, D. *Prog. Polym. Sci.* **2004**, *29*, 1079-1141. (b) Giacalone, F.; Martin, N. *Chem. Rev.* **2006**, *106*, 5136-5190. (c) Ball, Z. T.; Sivula, K.; Fréchet, J. M. J. *Macromolecules* **2006**, *39*, 70-72.

(7) (a) Yashima, E.; Maeda, K.; Okamoto, Y. *Nature* **1999**, *399*, 449-451. (b) Ishikawa, M.; Maeda, K.; Mitsutsuji, Y.; Yashima, E. *J. Am. Chem. Soc.* **2004**, *126*, 732-733. (c) Maeda, K.; Morino, K.; Okamoto, Y.; Sato, T.; Yashima, E. *J. Am. Chem. Soc.* **2004**, *126*, 4329-4342. (d) Miyagawa, T.; Furuko, A.; Maeda, K.; Katagari, H.; Furusho, Y.; Yashima, E. *J. Am. Chem. Soc.* **2005**, *127*, 5018-5019. For supramolecular chiral memory effect, see : (e) Furusho, Y.; Kimura, T.; Mizuno, Y.;

Aida, T. *J. Am. Chem. Soc.* **1997**, *119*, 5267-5268. (f) Mizuno, T.; Takeuchi, M.; Hamachi, I.; Nakashima, K.; Shinkai, S. *J. Chem. Soc. Perkin Trans.* 2 **1998**, 2281-2288. (g) Prins, L. J.; de Jong, F.; Timmerman, P.; Reinhoudt, D. N. *Nature* **2000**, *408*, 181-184. (h) Kubo, Y.; Ohno, T.; Yamanaka, J.; Tokita, T.; Iida, T.; Ishimaru, Y. *J. Am. Chem. Soc.* **2001**, *123*, 12700-12701. (i) Lauceri, R.; Raudino, A.; Scolaro, L. M.; Micali, N.; Purrello, R. *J. Am. Chem. Soc.* **2002**, *124*, 894-895. (j) Onouchi, H.; Miyagawa, T.; Morino, K.; Yashima, E. *Angew. Chem., Int. Ed.* **2006**, *45*, 2381-2384. (k) Miyagawa, T.; Yamamoto, M.; Muraki, R.; Onouchi, H.; Yashima, E. *J. Am. Chem. Soc.* **2007**, *129*, 3676-3682.

(8) (a) Kusuyama, H.; Takase, H.; Higashihara, Y.; Tseng, H.-T.; Chatani, Y.; Tadokoro, H. *Polymer* **1982**, *23*, 1256-1258. (b) Kusuyama, H.; Miyamoto, N.; Chatani, Y.; Tadokoro, H.; *Polymer Commun.* **1983**, *24*, 119-122.

(9) Buyse, K.; Berghmans, H.; Bosco, M.; Paoletti, S. *Macromolecules* **1998**, *31*, 9224-9230.

(10) Kumaki, J.; Kawauchi, T.; Okoshi, K.; Kusanagi, H.; Yashima, E. *Angew. Chem., Int. Ed.* **2007**, *46*, 5348-5351.

(11) Green, M. M.; Khatri, C.; Peterson, N. C. *J. Am. Chem. Soc.* **1993**, *115*, 4941-4942.

(12) Pantos, G. D.; Wietor, J.-L.; Sanders, J. M. K. *Angew. Chem., Int. Ed.* **2007**, *46*, 2238-2240.

(13) Diederich, F.; Effing, J.; Jonas, U.; Jullien, L.; Plesnivy, T.; Ringsdoef, H.; Thilgen, C.; Weinstein, D. *Angew. Chem., Int. Ed. Engl.* **1992**, *31*, 1599-1602.

(14) Abe, H.; Imai, K.; Matsumoto, M. *J. Polym. Sci., Part C* **1968**, *23*, 469–485.

(15) Hatada, K.; Ute, K.; Tanaka, K.; Okamoto, Y.; Kitayama, T. *Polym. J.* **1986**, *18*, 1037–1047.

(16) Frisch, M. J.; Trucks, G. W.; Schlegel, H. B.; Scuseria, G. E.; Robb, M. A.; Cheeseman, J. R.; Montgomery Jr., J. A.; Vreven, T.; Kudin, K. N.; Burant, J. C.; Millam, J. M.; Iyengar, S. S.; Tomasi, J.; Barone, V.; Mennucci, B.; Cossi, M.;

Scalmani, G.; Rega, N.; Petersson, G. A.; Nakatsuji, H.; Hada, M.; Ehara, M.; Toyata, K.; Fukuda, R.; Hasegawa, J.; Ishida, M.; Nakajima, T.; Honda, Y.; Kitao, O.; Nakai, H.; Klene, M.; Li, X.; Knox, J. E.; Hratchian, H. P.; Cross, J. B.; Adamo, C.; Jaramillo, J.; Gomperts, R.; Stratmann, R. E.; Yazyev, O.; Austin, A. J.; Cammi, R.; Pomelli, C.; Ochterski, J. W.; Ayala, P. Y.; Morokuma, K.; Voth, G. A.; Salvador, P.; Dannenberg, J. J.; Zakrzewski, V. G.; Dapprich, S.; Daniels, A. D.; Strain, M. C.; Farkas, O.; Malick, D. K.; Rabuck, A. D.; Raghavachari, K.; Foresman, J. B.; Ortiz, J. V.; Cui, Q.; Baboul, A. G.; Clifford, S.; Cioslowski, J.; Stefanov, B. B.; Liu, G.; Liashenko, A.; Piskorz, P.; Komaromi, I.; Martin, R. L.; Fox, D. J.; Keith, T.; Al-Laham, M. A.; Peng, C. Y.; Nanayakkara, A.; Challacombe, M.; Gill, P. M. W.; Johnson, B.; Chen, W.; Wong, M. W.; Gonzalez, C.; Pople, J. A. *Gaussian 03* Gaussian Inc., Pittsburgh, **2003**.

(17) Schomaker, E.; Challa, G. *Macromolecules* **1989**, *22*, 3337–3341.

(18) Tadokoro, H.; Tai, K.; Yokoyama, M.; Kobayashi, M. *J. Polym. Sci. Polym. Phys. Ed.* **1973**, *11*, 825–840.

(19) Vacattello, M.; Flory, P. J. *Macromolecules* **1986**, *19*, 405–415.

(20) Sundararajan, P. R. *Macromolecules* **1986**, *19*, 415–421.

(21) Kumaki, J.; Kawauchi, T.; Okoshi, K.; Kusanagi, H.; Yashima, E. *Angew. Chem., Int. Ed.* **2007**, *46*, 5348–5351.

(22) Tretinnikov, O. N.; Ohta, K. *Macromolecules* **2002**, *35*, 7343–7353.

(23) Kusuyama, H.; Takase, M.; Higashihata, Y.; Tseng, H.-T.; Chatani, Y.; Tadokoro, H. *Polymer* **1982**, *23*, 1256–1258.

(24) Kusuyama, H.; Miyamoto, N.; Chatani, Y.; Tadokoro, H. *Polymer* **1983**, *24*, 119–122.

(25) Foresman, J. B.; Frisch, Æ. in *Exploring Chemistry with Electronic Structure Methods 2nd edn* Gaussian Inc., Pittsburgh, **1996**.

(26) Dybal, J.; Krimm, S. *Macromolecules* **1990**, *23*, 1301–1308.

(27) Brinkhuis, R. H. G.; Schouten, A. J. *Macromolecules* **1991**, *24*, 1496–1504.

(28) Fischer, J. E.; Heiney, P. A.; Smith, A. B. *Acc. Chem. Res.* **1992**, *25*, 112–118.

Chapter 2

Helix-Sense-Controlled Synthesis of Optically Active Poly(methyl methacrylate) Stereocomplex

Abstract: Optically active poly(methyl methacrylate) (PMMA) stereocomplexes were prepared through the helix-sense-controlled supramolecular inclusion of an isotactic (it) PMMA within the helical cavity of an optically active, fullerene-encapsulated syndiotactic (st) PMMA with a macromolecular helicity memory. The observed and calculated vibrational circular dichroism spectra revealed that the it-PMMA replaced the encapsulated fullerenes to fold into a double-stranded helix with the same handedness as that of the st-PMMA single helix through the formation of a topological triple-stranded helix.

Introduction

The stereocomplex of poly(methyl methacrylate) (PMMA) is a unique polymer-based supramolecule composed of complementary isotactic (it)- and syndiotactic (st)-PMMAs with an it/st stoichiometry of 1:2 that exhibits a definite melting point in specific solvents or in solids.[1] Since the discovery of the PMMA stereocomplex,[2] the molecular basis of the structure and the mechanism of complex formation have been a long-standing question in polymer chemistry.[1] In 1989 Schomaker and Challa proposed a double-stranded helical structure composed of a 9_1 it-PMMA helix (nine repeating MMA units per turn) surrounded by an 18_1 st-PMMA helix with a monomer ratio of 1:2.[3] Recently, Yashima *et al.* proposed a triple-stranded helix model from the direct observation of a stereocomplex prepared using the Langmuir-Blodgett (LB) technique by high-resolution atomic force microscopy (AFM), which reveals that a double-stranded helix of it-PMMA is included in a single helix of st-PMMA, forming an inclusion complex with a triple-stranded helical structure.[4] "Molecular sorting" experiment results using uniform it- and st-PMMAs with different molecular weights support the triple-stranded helix model.[5]

More recently, Yashima *et al.* found that st-PMMA folded into a preferred-handed helical conformation assisted by chiral alcohols and encapsulated [60]fullerene (C_{60}) within its helical cavity to form an optically active supramolecular peapod-like complex gel (st-PMMA/C_{60}), whose helicity was retained after complete removal of the chiral alcohols.[6] Based on these results, the author anticipated that the preferred-handed helical st-PMMA/C_{60} complex could serve as the template to further encapsulate the complementary it-PMMA through replacement of the encapsulated C_{60} molecules, resulting in a practically versatile stereocomplex with optical activity (Figure 2-1A). The PMMA stereocomplex has been applied to advanced materials in many fields, such as ultrathin films,[7] microcellular foams,[8] dialyzers,[9] thermoplastic elastomers,[10] and ion gels.[11] It is also a versatile structural motif for template polymerization[12] and self-assembled nanomaterials.[13] However, an optically active stereocomplex has not yet been synthesized.[14]

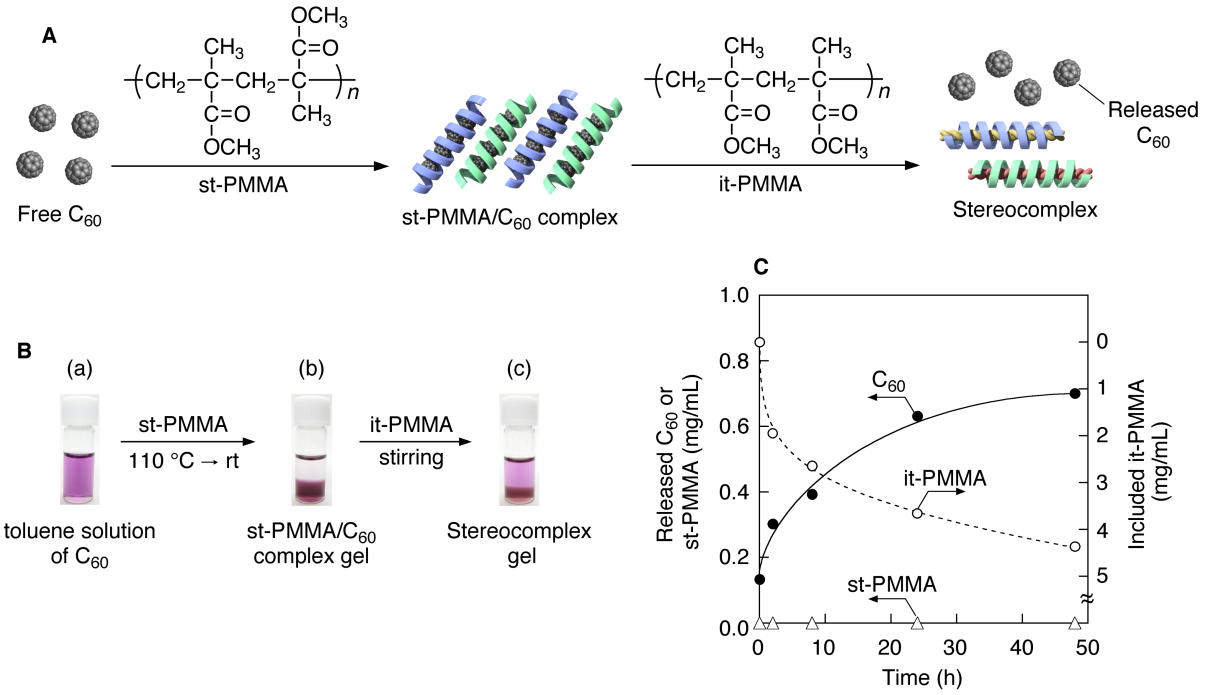

Figure 2-1. (A) Schematic illustration of the encapsulation of C_{60} in the st-PMMA helical cavity upon gelation and the release of the C_{60} through stereocomplex formation with it-PMMA (orange and yellow). The right- (blue) and left-handed (green) helical st-PMMA complexes are equally produced. (B) Photographs of a toluene solution of C_{60} (1 mg/mL, 1 mL) (a), st-PMMA/C_{60} gel (8.3 wt % of C_{60}) after the addition of st-PMMA (10 mg) followed by heating to 110 ºC and then cooling to room temperature (b), and stereocomplex gel after the addition of it-PMMA (10 mg) followed by stirring at room temperature for 48 h (c). Samples (b) and (c) were centrifuged at 1700 *g* for 10 min to precipitate the gels. (C) Changes in the concentrations (mg/mL) of released C_{60} and st-PMMA from the st-PMMA/C_{60} complex gel into the supernatant upon complexation with it-PMMA at room temperature. Changes in the concentration (mg/mL) of the included it-PMMA are also shown. The concentrations of C_{60} and it- and st-PMMAs were determined by absorption and ^{1}H NMR measurements of the supernatants, respectively.

Results and Discussion

To this end, the author first investigated if it-PMMA could replace the encapsulated C_{60} molecules within the st-PMMA cavity to form a stereocomplex. An optically inactive st-PMMA/C_{60} complex gel (0.91 mg of C_{60} (8.3 wt %) was encapsulated in 10 mg st-PMMA) was prepared in toluene according to a previously reported method (b in Figure 2-1B and Figure 2-2A).[6] To this was added it-PMMA (10 mg), and the changes in the concentrations of C_{60} and st-PMMA released from the st-PMMA/C_{60} complex gel and that of it-PMMA included in the st-PMMA gel from the supernatant were followed by measuring the absorption and ^{1}H NMR spectra of the supernatant at appropriate time intervals after centrifugation (Figures 2-1B, 2-1C, and, 2-2B).

The encapsulated C_{60} molecules were gradually replaced by it-PMMA and the supernatant changed to a purple color (c in Figure 2-1B). After 48 h, *ca.* 80% of the C_{60} molecules were released to form the stereocomplex gel (Figure 2-1C). The film derived from the gel showed a characteristic differential scanning calorimetry (DSC) profile that is virtually the same as that of the bulk stereocomplex prepared from the it- and st-PMMAs in acetonitrile (Figure 2-2C). These results clearly indicate that a stereocomplex certainly forms upon the addition of it-PMMA to the st-PMMA/C_{60} complex gel. This finding provides the first direct experimental evidence for the molecular basis of the PMMA stereocomplex formation mechanism; that is, a double-stranded helix of it-PMMA is included in a preformed single helix of st-PMMA, thus producing a supramolecular inclusion complex with a triple-stranded helical structure.[4,5]

Next, the author used an optically active st-PMMA/C_{60} complex gel induced by (*R*)- or (*S*)-1-phenylethanol (**1**),[6] which will produce an optically active stereocomplex after replacement of the encapsulated C_{60} by it-PMMA (Figure 2-3). The optically active st-PMMA/C_{60} complex gel was prepared in the same manner as previously reported in toluene-d_8 in the presence of (*R*)- or (*S*)-**1** (20 vol %) followed by complete removal of the (*R*)- or (*S*)-**1**, and then isolated by centrifugation.[6] The it-PMMA was added to the optically active st-PMMA/C_{60} gel under vigorous stirring at room temperature. After 48 h, the resulting

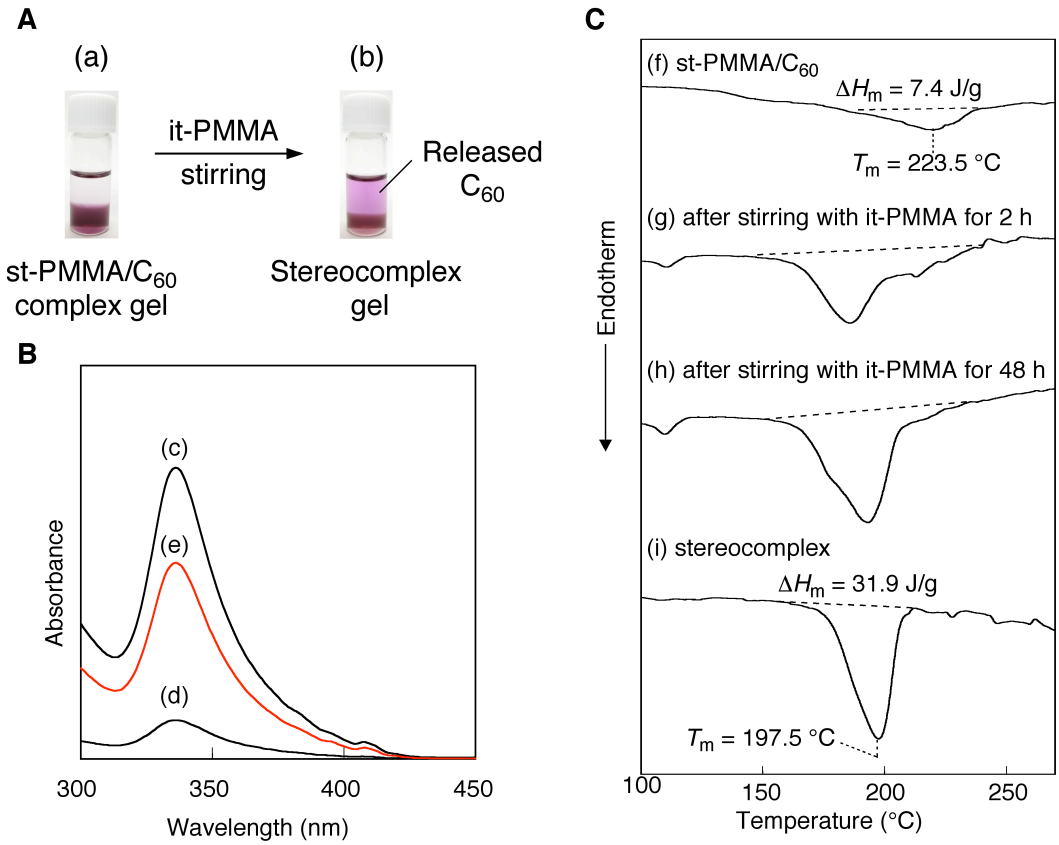

Figure 2-2. (A) Photographs of a st-PMMA/C_{60} complex gel (10 mg of st-PMMA containing 8.3 wt % of C_{60}) in toluene before (a) and after (b) the addition of it-PMMA (10 mg) followed by stirring at room temperature for 48 h and then centrifugation at 1700 *g* for 10 min. See also Figure 2-1B. (B) Absorption spectra of toluene solutions of the feed C_{60} (1 mg/mL) (c), the supernatant isolated from the st-PMMA/C_{60} complex gel after centrifugation (d), and the supernatant after complexation of the st-PMMA/C_{60} complex gel with it-PMMA for 48 h followed by centrifugation (e). (C) DSC thermograms of the st-PMMA/C_{60} complex film (8.3 wt % of C_{60}) (f), films of st-PMMA/C_{60} complexes obtained after mixing with it-PMMA for 2 (g) and 48 h (h), and stereocomplex film (i). The films were obtained by evaporating the solvent of the corresponding gels after centrifugation. The stereocomplex film was prepared by mixing st-PMMA (10 mg) and it-PMMA (5 mg) in toluene (1 mL) at 110 ºC followed by cooling to room temperature, and then evaporating the solvent. The measurements were conducted after cooling the samples at 0 ºC, followed by heating to 280 ºC at 10 ºC/min under nitrogen.

stereocomplex was isolated by centrifugation and its vibrational circular dichroism (VCD) and IR spectra (Figure 2-4C) were measured. For comparison, the VCD and IR spectra of the optically active st-PMMA/C_{60} gel prepared with (*R*)- or (*S*)-**1** and the IR spectrum of it-PMMA are shown in Figures 2-4A and 2-4B, respectively. The stereocomplex gels exhibited mirror-image VCDs in the PMMA IR regions, whose VCD patterns significantly changed from those of the optically active st-PMMA/C_{60} gels, in particular, at around the 1260 cm^{-1} (ν_6) regions corresponding to the characteristic absorption band for it-PMMA (Table 2-1). These results suggest that the it-PMMA forms a helical conformation with an excess one-handedness once encapsulated into the helical st-PMMA with a macromolecular helicity memory, which remains intact after the encapsulated fullerenes are further replaced by the complementary it-PMMA with the formation of an optically active stereocomplex.

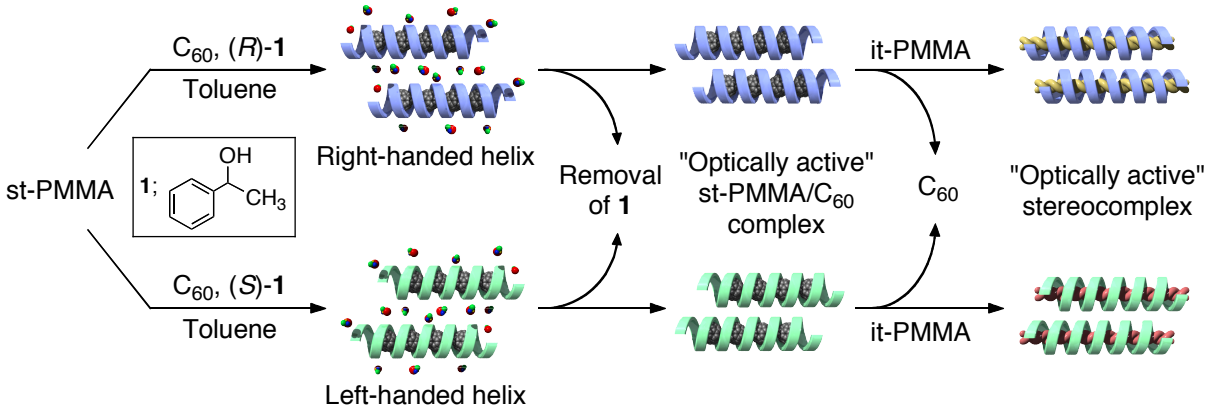

Figure 2-3. Schematic illustration of right- (top) and left- (bottom) handed stereocomplex formation with a triple-stranded helical structure. Right- and left-handed single helices are induced in the st-PMMA/C_{60} complex in the presence of (*R*)- or (*S*)-**1** (left). The induced helicity is memorized after **1** is completely removed (middle). The encapsulated C_{60} molecules are further replaced by it-PMMA along with the formation of an optically active stereocomplex (right).

Inclusion of an it-PMMA helix into an outer st-PMMA helix may produce a pair of diastereomeric helical assemblies composed of the same or opposite handed it- and st-PMMAs helices. The author then calculated the IR and VCD spectra for all the possible combinations of the triple-stranded helical stereocomplexes[4,5] on the basis of the right- and left-handed single helical 18_1 st-PMMAs and double helical 9_1 it-PMMAs at the B3LYP/6-31G(d) level (Figures 2-4D and 2-5C). The experimental VCD spectral patterns of the stereocomplexes fit well to the calculated ones composed of helical it- and st- PMMAs with the same handedness (Figures 2-5A–C). Thus, it-PMMA recognizes and interacts with the outer st-PMMA helix and folds into a double-stranded helix with the same handedness as that of the st-PMMA helix through the formation of a topological triple-stranded helix.[4,5]

Additional evidence of a preferred-handed helical structure induced in an it-PMMA encapsulated in the helical st-PMMA cavity with a macromolecular helicity memory was obtained from the experimental and calculated VCD spectra of an optically active stereocomplex prepared from the fully-deuterated helical st-PMMA (st-PMMA-d_8). Figure 2-4E shows the IR and VCD spectra of the optically active st-PMMA-d_8/C_{60} complex. The optically active st-PMMA-d_8/C_{60} complex gel was prepared in a similar way for the synthesis of the optically active st-PMMA/C_{60} complex gel in toluene-d_8 in the presence of (*R*)- or (*S*)-**1** followed by complete removal of the (*R*)- or (*S*)-**1**, and then isolated by centrifugation. Noticeable changes were observed in its IR and VCD spectral patterns caused by deuteration together with a significant decrease in its VCD intensities as compared to those of the st-PMMA/C_{60} complex (Figure 2-4A). The calculated IR and VCD spectra for the right- and left-handed helical st-PMMA-d_8s support the observed changes in their spectral patterns and intensities by deuteration of the st-PMMA (Figure 2-6D).

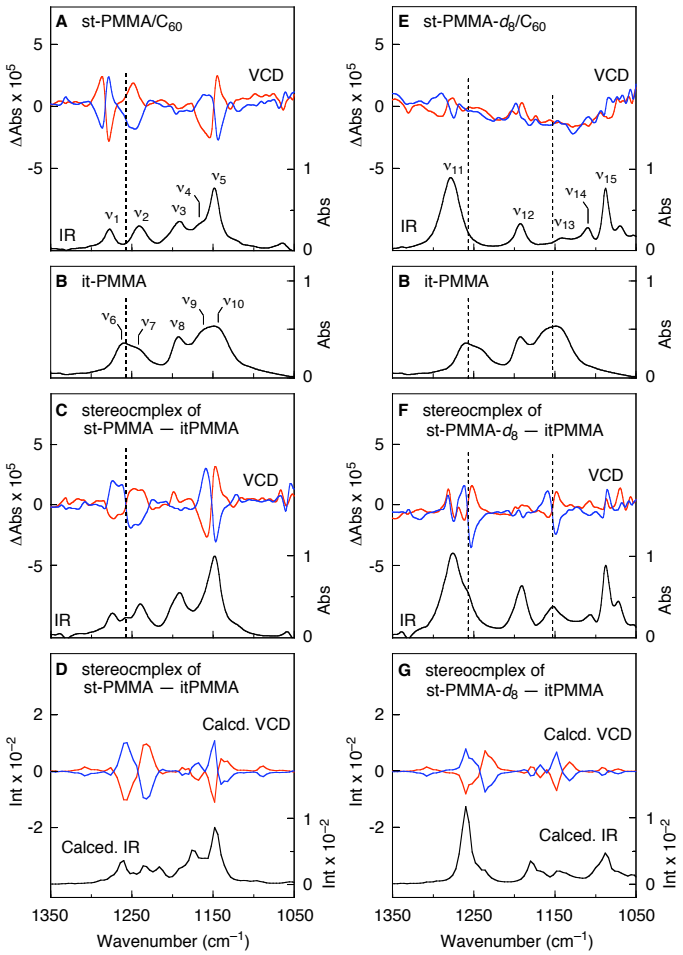

Figure 2-4. (A and E) Observed VCD (top) and IR (bottom) spectra of isolated st-PMMA/C_{60} complex (A) and st-PMMA-d_8/C_{60} complex (E) gels in toluene-d_8 prepared by (*R*)-**1** (red and black lines) and (*S*)-**1** (blue lines), measured after the complete removal of **1**. For the assignments of the experimental and calculated IR and VCD bands (ν_1 – ν_{15}), see Table 2-1. (B) IR spectrum of it-PMMA in toluene-d_8. (C and F) Observed VCD (top) and IR (bottom) spectra of stereocomplex gels obtained from the optically active st-PMMA/C_{60} complex (C) and st-PMMA-d_8/C_{60} complex (F) gels induced by (*R*)-**1** (red and black lines) and (*S*)-**1** (blue lines) upon complexation with it-PMMA (it/st = 1/2, wt/wt). (D and G) Calculated VCD (top) and IR (bottom) spectra of stereocomplexes (it/st = 1/2, wt/wt) composed of the right- (red and black lines) and left- (blue lines) handed it- and st-PMMAs (D), and it-PMMA and st-PMMA-d_8 (G). The contribution of the linear dichroism caused by the macroscopic anisotropy was negligible.

Table 2-1. Observed and Calculated Frequencies and Peak Assignments for the IR and VCD Spectra of the Optically Active st-PMMA/C_{60} and st-PMMA-d_8/C_{60} Complex Induced by (*R*)-**1**, and it-PMMA[a]

polymer	band	IR^{obsd} frequency (cm^{-1})	IR^{calcd} frequency (cm^{-1})	VCD^{obsd} frequency (cm^{-1})	VCD^{calcd} frequency (cm^{-1})	assignment[b]
st-PMMA	ν_1	1278	1264	1286 (ν_{1p})[c]	1276 (ν_{1p})[c]	out-of-phase ν_a(C-C-O) + $\rho(CH_2)$
				1279 (ν_{1v})[c]	1260 (ν_{1v})[c]	in-phase ν_a(C-C-O) + $\rho(CH_2)$
	ν_2	1241	1232	1249 (ν_{2p})[c]	1233 (ν_{2p})[c]	ν_a(C-C-O) + $\tau(CH_2)$
			1216			
	ν_3	1192	1192	—	1186 (ν_{3p})[c]	out-of-phase ν_a(C-O-C) + $\tau(CH_2)$
			1176	—	1176 (ν_{3v})[c]	
	ν_4	1172	1160	shoulder	—	ν_a(C-O-C) + ρ (CH_3)
	ν_5	1148	1148	1154 (ν_{5v})[c]	1148 (ν_{5v})[c]	in-phase ν_a(C-O-C) + $\rho(CH_2)$
				1145 (ν_{5p})[c]	1141 (ν_{5p})[c]	out-of-phase ν_a(C-O-C) + $\rho(CH_2)$
it-PMMA	ν_6	1261	1256	—	1256 (ν_{6p})[c]	in-phase ν_a(C-C-O) + $\rho(CH_2)$
	ν_7	1243	1240	—	1240 (ν_{7v})[c]	out-of-phase ν_a(C-C-O) + $\tau(CH_2)$
			1228	—	1228 (ν_{7v})[c]	
	ν_8	1193	1180	—	1180 (ν_{8v})[c]	ν_a(C-O-C) + $\tau(CH_2)$
	ν_9	1164	1168	—	1168 (ν_{9p})[c]	ν_a(C-O-C) + $\rho(CH_3)$
	ν_{10}	1148	1148	—	1148 (ν_{10p})[c]	in-phase ν_a(C-O-C) + $\rho(CH_3)$
st-PMMA-d_8	ν_{11}	1279	1260	1291 (ν_{11v})[c]	1264 (ν_{11v})[c]	out-of-phase ν_a(C-C-O) + $\rho(CD_2)$
				1276 (ν_{11p})[c]	1256 (ν_{11p})[c]	
	ν_{12}	1193	1180	1199 (ν_{12v})[c]	1181 (ν_{12v})[c]	ν_a(C-C-O) + $\tau(CD_2)$
				1192 (ν_{12p})[c]	1176 (ν_{12p})[c]	
	ν_{13}	1141	1124	1129 (ν_{13p})[c]	1128 (ν_{13p})[c]	out-of-phase ν_a(C-O-C) + $\tau(CD_2)$
	ν_{14}	1110	1100	1110 (ν_{14v})[c]	1105 (ν_{14v})[c]	ν_a(C-O-C) + $\rho(CD_3)$
	ν_{15}	1088	1089	1085 (ν_{15v})[c]	1084 (ν_{15v})[c]	out-of-phase ν_a(C-O-C) + $\rho(CD_3)$

[a] st-PMMA and st-PMMA-d_8, and it-PMMA are assumed to have a 18/1 helix and 9/1 helix, respectively. All spectra were collected for ca. 4-5 h at a resolution of 4 cm^{-1}. [b] Abbriviations, ν_a: anti-symmetric stretching, ρ: rocking, τ: twisting. [c] Bisignate VCD band. The band assignments for the right-handed helix are shown.

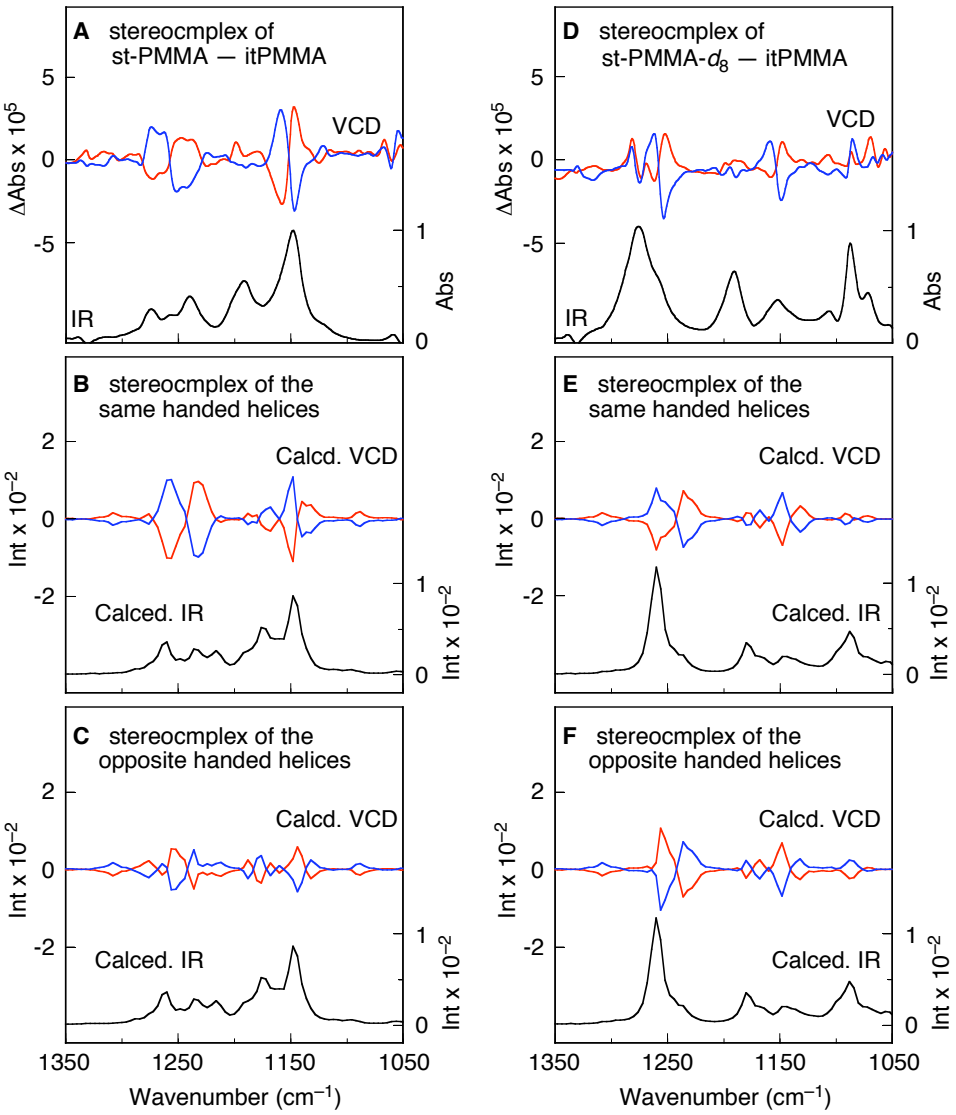

Figure 2-5. (A and D) Observed VCD (top) and IR (bottom) spectra of stereocomplex gels obtained from the optically active st-PMMA/C_{60} (A) and st-PMMA-d_8/C_{60} complexes (D) gels induced by (*R*)-**1** (red and black lines) and (*S*)-**1** (blue lines) upon complexation with it-PMMA (it/st = 1/2, wt/wt). (B and E) Calculated VCD (top) and IR (bottom) spectra of stereocomplexes (it/st = 1/2, wt/wt) composed of the right- (red and black lines) and left- (blue lines) handed it- and st-PMMAs (B), and it-PMMA and st-PMMA-d_8 (E). (C and F) Calculated VCD (top) and IR (bottom) spectra of stereocomplexes (it/st = 1/2, wt/wt) composed of the opposite handed it- and st-PMMAs (C), and it-PMMA and st-PMMA-d_8 (F) helices on the basis of the right- (blue lines) and left- (red and black lines) handed it-PMMAs.

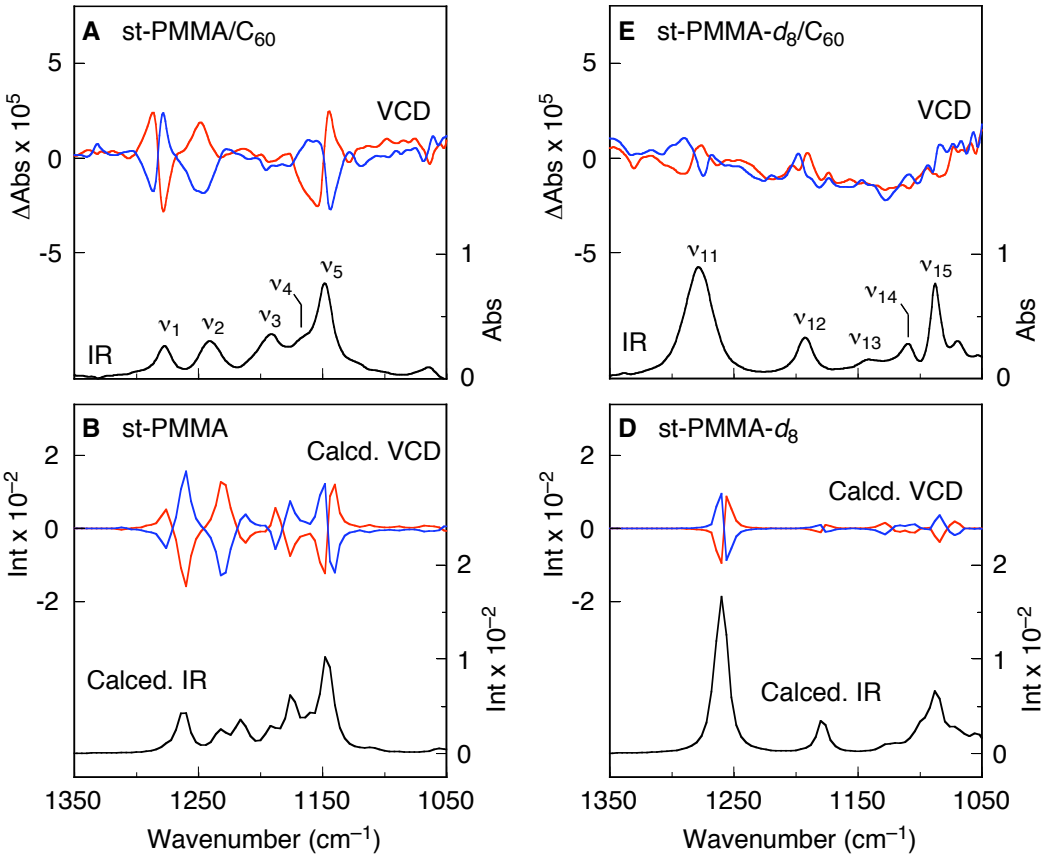

Figure 2-6. (A and C) Observed VCD (top) and IR (bottom) spectra of isolated st-PMMA/C_{60} complex (A) and st-PMMA-d_8/C_{60} complex (C) gels in toluene-d_8 prepared by (*R*)-**1** (red and black lines) and (*S*)-**1** (blue lines). The observed VCD and IR spectra were measured after the complete removal of **1**. (B and D) Calculated VCD (top) and IR (bottom) spectra of right- (red and black lines) and left- (blue lines) handed helical st-PMMAs (B) and st-PMMA-d_8s (D). For the assignments of the experimental and calculated IR and VCD bands ($\nu_1 - \nu_{15}$), see Table 2-1.

A stereocomplex was then prepared from the optically active st-PMMA-d_8/C_{60} complex gel upon the addition of it-PMMA. The resulting it-PMMA–st-PMMA-d_8 stereocomplex exhibited weak, but apparent VCD spectra (Figure 2-4F), whose spectral patterns roughly agree with the calculated VCD spectra of the stereocomplex composed of helical it-PMMA

and st-PMMA-d_8 with the same handedness (Figure 2-4G and Figures 2-5D–F). Because of such an extremely weak VCD of the preferred-handed helical st-PMMA-d_8 as supported by its calculated one, the observed VCD of the it-PMMA–st-PMMA-d_8 stereocomplex likely reflects the VCD derived from the it-PMMA helix induced through encapsulation in the helical st-PMMA-d_8 cavity.

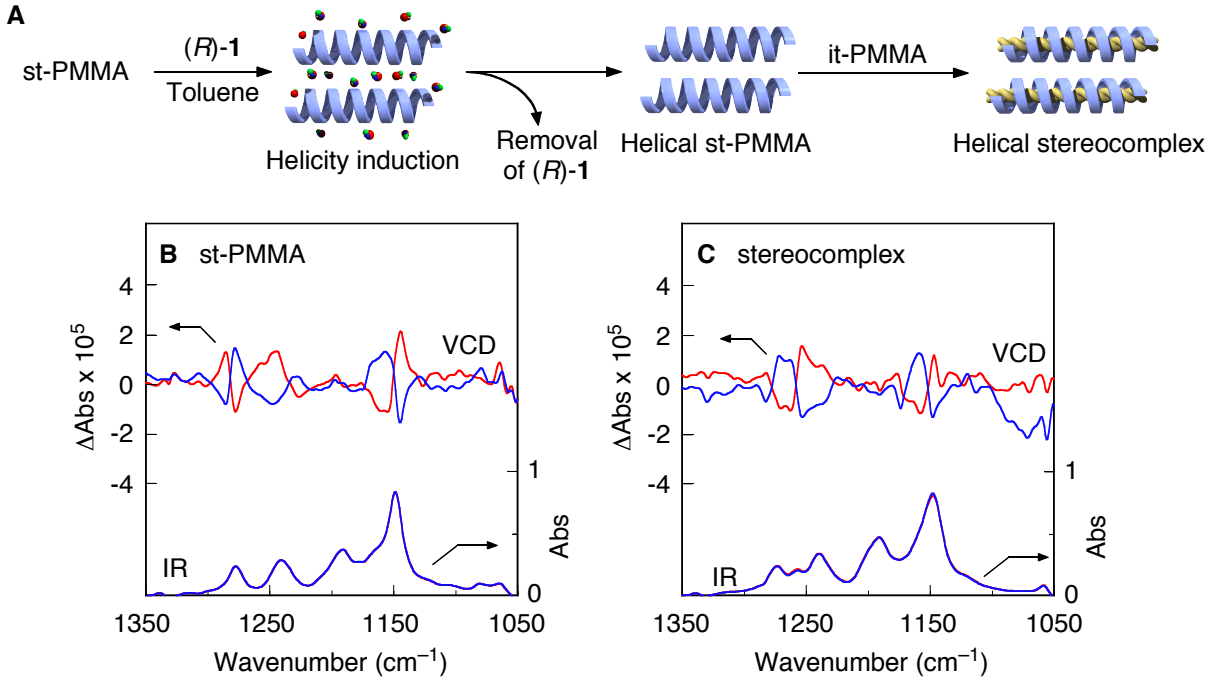

Figure 2-7. (A) Schematic illustration of right-handed helicity induction in st-PMMA (blue) in the presence of (*R*)-**1**. The induced helicity is memorized after (*R*)-**1** is completely removed and further encapsulation of it-PMMA (yellow). (B) Observed VCD and IR spectra of isolated st-PMMA gels in toluene-d_8 prepared by (*R*)-**1** (red lines) and (*S*)-**1** (blue lines). (C) Observed VCD and IR spectra of stereocomplex gels in toluene-d_8 obtained after the addition of it-PMMA to the isolated st-PMMA gels prepared by (*R*)-**1** (red lines) and (*S*)-**1** (blue lines).

As reported previously, a similar optically active st-PMMA gel can be prepared with (*R*)- or (*S*)-**1** in toluene-d_8 in the absence of C_{60}.[6] The induced st-PMMA helix also remains after complete removal of the optically active **1**, and this helical st-PMMA can serve as the template for the further inclusion of it-PMMA, resulting in a stereocomplex gel, thus showing virtually the same VCD spectrum (Figure 2-7). An optically active stereocomplex formation, however, requires the preformed helical st-PMMA with a controlled helical sense since a mixture of toluene-d_8 solutions of it- and st-PMMAs in the presence of (*R*)-**1** (20 vol %) produced a stereocomplex gel with no optical activity.

Conclusions

In summary, the author has, for the first time, synthesized an optically active PMMA stereocomplex through the helix-sense-controlled supramolecular inclusion of an it-PMMA within the helical cavity of the st-PMMA with a macromolecular helicity memory. The author believes that these unique helical st-PMMA and stereocomplex with a controlled helical sense offer potentially useful chiral materials.

Experimental Section

Materials. The st-PMMA and st-PMMA-d_8 were synthesized by the syndiotactic-specific polymerization of MMA and MMA-d_8, respectively, in toluene at –95 ºC using a typical Ziegler-type catalyst derived from $Al(C_2H_5)_3$ and $TiCl_4$.[15] The it-PMMA was prepared by the isotactic-specific anionic living polymerization of MMA in toluene at –78 ºC with *tert*-C_4H_9MgBr.[16] The number-average molecular weights (M_n), molecular weight distributions (M_w/M_n), and tacticities (*mm*:*mr*:*rr*) were as follows: st-PMMA: M_n = 544000, M_w/M_n = 1.29, and *mm*:*mr*:*rr* = 0:6:94; st-PMMA-d_8: M_n = 710000, M_w/M_n = 1.32, and *mm*:*mr*:*rr* = 0:5:95; it-PMMA: M_n = 21800, M_w/M_n = 1.12, and *mm*:*mr*:*rr* = 97:3:0. The M_n and M_w/M_n values were measured by size exclusion chromatography (SEC) in $CHCl_3$ using PMMA standards (Shodex, Tokyo, Japan) for the calibration. The tacticities were determined from the ^{1}H NMR signals due to the α-methyl protons (st- and it-PMMAs) or the ^{13}C NMR signals due to the carbonyl carbon (st-PMMA-d_8).

Toluene (extra-pure grade) and toluene-d_8 (99.6%) were purchased from Wako Chemicals (Osaka, Japan) and were used as received. (*R*)-, (*S*)-, and (*RS*)-1-phenylethanol (**1**) were obtained from Azmax (Chiba, Japan) and were used without further purification. [60]Fullerene (C_{60}) (99.5%) was obtained from Tokyo Kasei (TCI, Tokyo, Japan) and was used as received.

Instruments. NMR spectra were recorded on a Varian Unity Inova 500 spectrometer (500 MHz for ^{1}H and 125 MHz for ^{13}C) in $CDCl_3$. Absorption spectra were measured in a 0.1- or 0.2-mm quartz cell on a JASCO (Hachioji, Japan) V-570 spectrophotometer. IR spectra were recorded using a JASCO Fourier Transform IR-620 spectrophotometer. Vibrational circular dichroism (VCD) spectra were measured in a 0.15-mm BaF_2 cell with a JASCO JV-2001 spectrometer. The concentration was *ca.* 30 mg/mL in toluene-d_8. All spectra were collected for ca. 4–5 h at a resolution of 4 cm^{-1}.

Differential scanning calorimetry (DSC) measurements were performed on a SEIKO (Chiba, Japan) EXSTAR 6000 under a nitrogen atmosphere. The samples were sealed in

aluminum pans. The melting temperature (T_m) and heat of melting (ΔH_m) were determined from the minimum of the endothermic peak and by the peak area, respectively.

The molecular modeling was performed on the program system MS Modeling software (version 3.1, Accelrys Inc., San Diego, CA). The molecular orbital (MO) calculation was conducted using Gaussian 03 program (Gaussian, Inc., Pittsburgh, PA).[17]

Preparation of st-PMMA/C_{60} Complex Gel and Film.[6] Ten mg of st-PMMA was dissolved in a toluene solution of C_{60} (2 mg/mL, 1 mL) at 110 ºC. After the solution was cooled to room temperature (*ca.* 20 ºC), the solution gelled within 1 min. The obtained soft gel was centrifuged at 1700 *g* for 10 min and the supernatant containing unencapsulated C_{60} molecules was removed from the gel by decantation. The condensed gel was then washed with toluene and the solvent was removed by decantation after centrifugation. This procedure was repeated several times. The encapsulated C_{60} content was estimated using the following equation: encapsulated C_{60} content (mg) = (C_{60} in feed (mg)) x (Abs_0 – Abs)/(Abs_0), where Abs_0 and Abs represent the absorbance at 336 nm of the feed C_{60} solution and that of the supernatant separated from the st-PMMA/C_{60} gel after centrifugation (Figure 2-2B). The st-PMMA/C_{60} complex film was obtained by evaporating the solvent in the condensed gel under reduced pressure at room temperature for 12 h followed by drying under vacuum at 160 ºC for 1 h. The residual solvent content was estimated to be <0.3 wt % by ^{1}H NMR analysis. The obtained film was subjected to the DSC measurement (f in Figure 2-2C).

Preparation of Stereocomplex Gel upon Mixing st-PMMA/C_{60} Complex Gel with it-PMMA. A typical experimental procedure is described below. Ten mg of st-PMMA was dissolved in a toluene solution of C_{60} (1 mg/mL, 1 mL) at 110 ºC. After the solution was cooled to room temperature (*ca.* 20 ºC), the solution gelled within 1 min. The obtained soft gel was centrifuged at 1700 *g* for 10 min and to this was added 10 mg of it-PMMA. The mixture was then vigorously stirred by a magnetic stirrer, giving soft gel particles. The changes in the concentrations of C_{60} and st-PMMA released from the st-PMMA/C_{60} complex

gel into the supernatant and that of it-PMMA included into the st-PMMA gel from the supernatant were followed by measuring the absorption and ^{1}H NMR spectra of the supernatant at appropriate time intervals after centrifugation (Figure 2-1C). The obtained stereocomplex gel was then washed with toluene. The stereocomplex film was obtained by evaporating the solvent in the condensed gel under reduced pressure at room temperature for 12 h followed by drying under vacuum at 160 ºC for 1 h, and then subjected to the DSC measurements (g and h in Figure 2-2C).

Preparation of Optically Active st-PMMA/C_{60}[6] and st-PMMA-d_8 Complex Gels. A typical experimental procedure is described below. Twenty mg of st-PMMA was dissolved in a toluene-d_8 solution of C_{60} (1.6 mg/mL, 0.5 mL) containing (*R*)-**1** (20 vol %) at 110 ºC. After the solution was cooled to room temperature (*ca*. 20 ºC), the solution gelled within 15 h. The obtained soft gel was centrifuged at 1700 *g* for 10 min and the supernatant containing unencapsulated C_{60} molecules was removed from the gel by decantation. The condensed gel was then washed with toluene-d_8 to remove the (*R*)-**1**. The residual (*R*)-**1** content was estimated to be <0.002 vol % by ^{1}H NMR analysis. The obtained gel was suspended in a small amount of toluene-d_8, and then subjected to the VCD measurements (Figures 2-4A and 2-6A). In the same way, st-PMMA/C_{60} complex gels were prepared in a mixture of (*S*)- or (*RS*)-**1** (20 vol %) and toluene-d_8. The VCD spectrum of the st-PMMA/C_{60} complex gel prepared with (*RS*)-**1** was subtracted from the VCD spectra with (*R*)- or (*S*)-**1** in toluene-d_8 (Figures 2-4A and 2-6A).

Optically active st-PMMA-d_8/C_{60} gels were prepared in a similar way in toluene-d_8 containing 20 vol % of (*R*)-, (*S*)-, or (*RS*)-**1** and the optically active (*R*)- and (*S*)-**1** were completely removed by washing the gels with toluene-d_8 to measure the VCD spectra (Figures 2-4E and 2-6C).

Preparation of Optically Active Stereocomplex upon Mixing st-PMMA/C_{60} or st-PMMA-d_8/C_{60} Complex Gel with it-PMMA. A typical experimental procedure is described

below. An optically active st-PMMA/C_{60} or st-PMMA-d_8/C_{60} condensed gel (st-PMMA (st-PMMA-d_8): 20 mg) prepared in the same way described above was suspended in toluene-d_8 until the polymer concentration 10 mg/mL and to this was added 20 mg of it-PMMA. The mixture was then vigorously stirred at room temperature for 48 h by a magnetic stirrer, giving soft gel particles. The obtained stereocomplex gel was washed with toluene-d_8 and then subjected to the VCD measurements (Figures 2-4C, 2-4F, 2-5A, and 2-5D).

Preparation of Optically Active Stereocomplex upon Mixing st-PMMA Complex Gel with it-PMMA in the Absence of C_{60}. A typical experimental procedure is described below. Twenty mg of st-PMMA was dissolved in a toluene-d_8 solution (0.5 mL) of (*R*)-**1** (10 vol %) at 110 ºC. After the solution was cooled to room temperature (*ca*. 20 ºC), the solution gelled within 3 h. The obtained soft gel was centrifuged at 1700 *g* for 10 min and the supernatant was removed from the gel by decantation. The condensed gel was then washed with toluene-d_8 to remove the (*R*)-**1**. The obtained gel was suspended in a small amount of toluene-d_8, and then subjected to the VCD measurements (Figure 2-7B). The optically active st-PMMA condensed gel was suspended in toluene-d_8 (10 mg/mL) and to this was added 20 mg of it-PMMA. The mixture was then vigorously stirred at room temperature for 48 h by a magnetic stirrer, giving soft gel particles. The obtained stereocomplex gel was washed with toluene-d_8 and then subjected to the VCD measurements (Figure 2-7C). In the same way, stereocomplex gels were prepared in a mixture of (*S*)- or (*RS*)-**1** in the absence of C_{60}.

Preparation of Stereocomplex in Toluene-d_8 with (*R*)-1. st-PMMA (10 mg) and it-PMMA (5 mg) were dissolved in a toluene-d_8 solution (1 mL) of (*R*)-**1** (20 vol %) by heating at 110 ºC. The solution was allowed to cool to room temperature, which gelled immediately due to the formation of stereocomplex. The obtained stereocomplex gel was washed with toluene-d_8 and then subjected to the VCD measurements.

Molecular Modeling of Double-Stranded Helical it-PMMA and IR and VCD Spectral Calculations. The detailed procedures for the construction of an initial 9_1 (nine units per turn) it-PMMA double-stranded helix model were reported previously.[4] The helical pitch was assumed to be 2.10 nm and the side chain ester group was assumed to take a *trans* conformation to the α-methyl group. The double-stranded 9_1 it-PMMA helical chains were constructed by combining two right-handed helical 9_1 it-PMMA helices in which one of the it-PMMA helices was rotated around the helix axis by 180º.[4]

The initial model of a double-stranded helical it-PMMA nonamer (9mer) was then fully optimized by using *ab initio* quantum chemical calculations at the HF/STO-3G level (774 basis sets) and further at the B3LYP/6-31G(d) level (2178 basis functions) under the periodic boundary condition in Gaussian 03 program[17] running under Fujitsu PRIMEPOWER HPC2500 in Nagoya University. After the optimization, the helical pitch of 9_1 it-PMMA double helix converged from 2.10 to 1.836 nm; this pitch value fairly agrees with the observed fiber identity period for the it-PMMA–st-PMMA stereocomplex determined by X-ray diffraction (1.84 nm).[3] The internal coordinates and the stick model of the optimized 9_1 double helical it-PMMA with the helical pitch of 1.836 nm are shown in Table 2-2 and Figure 2-8, respectively.

The IR and VCD spectra for an optimized 9_1 double helical it-PMMA were then calculated using the density functional theory (DFT) method at the B3LYP/6-31G(d) level in Gaussian 03 program.[17] Because of difficulty in calculating IR and VCD spectra for an entire, large polymer, we calculated the IR and VCD for a series of double helical it-PMMA oligomers from tetramer (4mer) to dodecamer (12mer); each oligomer was taken from the optimized double helical it-PMMA and both the end groups were replaced by methyl groups. we found that the IR and VCD spectra were insensitive to the oligomer length and almost the same when the oligomers were longer than octamer (8mer). Thus, we used the VCD spectrum of dodecamer (12mer) to determine the helical senses of optically active double helical it-PMMAs by comparison with their experimental VCD spectra. These spectra were constructed from calculated dipole and rotational strengths assuming Lorentzian band shape with a half-

width at half maximum of 4 cm^{-1}. The calculated frequencies were scaled by a frequency-independent factor of 0.9613.[18] The peak assignments for the main peaks of the IR and VCD spectra based on the calculation results are summarized in Table 2-1, which were fairly in good agreement with the reported ones.[19–21]

Table 2-2. Internal Coordinates of the Optimized 9_1 it-PMMA Helix by Using *Ab Initio* Quantum Chemical Calculations at the HF/STO-3G Level and Further at the B3LYP/6-31G(d) Level

bond length	nm
C1-C2	0.1580
C2-$C1^{+1}$	0.1578
C1-C3	0.1533
C3-O1	0.1353
C3-O2	0.1213
C1-C4	0.1442
C1-C5	0.1538
C-H	0.109~0.110

bond angle	(degree)
$C1^{-1}$-$C2^{-1}$-C1	126.5
$C2^{-1}$-C1-C2	101.8
$C2^{-1}$-C1-C3	110.6
$C2^{-1}$-C1-C5	112.5
C1-C3-O1	112.2
C1-C3-O2	125.0
C3-O1-C4	115.3
H-C-H	105.0~111.0

torsion angle	degree
$C2^{-1}$-C1-C2-$C1^{+1}$	-166.2
$C1^{-1}$-$C2^{-1}$-C1-C2	-156.3
$C1^{-1}$-$C2^{-1}$-C1-C3	85.6
$C1^{-1}$-$C2^{-1}$-C1-C5	-35.9
$C2^{-1}$-C1-C3-O1	63.5
$C2^{-1}$-C1-C3-O2	-118.3
C1-C3-O1-C4	175.2
C3-O1-C4-H	~staggered
C3-C1-C5-H	~staggered

Numbering of Atoms

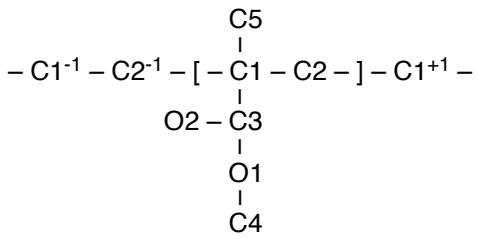

Molecular Modeling of Helical st-PMMA[6] and st-PMMA-d_8 and IR and VCD Spectral Calculations. The detailed procedures for the construction of an initial 18_1 st-PMMA helix model followed by the fully optimization by using *ab initio* quantum chemical calculations at the HF/STO-3G level and further at the B3LYP/6-31G(d) level under the

periodic boundary condition were reported previously.[6] The internal coordinates and the stick model of the optimized 18_1 helical st-PMMA with the helical pitch of 0.947 nm are shown in Table 1-2 and Figure 2-8, respectively.[6] This helical pitch value fairly agrees with the reported helical pitch for the st-PMMA chain in the st-PMMA–organic molecule complexes determined by X-ray diffraction (0.885 nm)[22,23] and that for the st-PMMA chain in the it-PMMA–st-PMMA stereocomplex observed by high resolution AFM (0.92 nm), as reported previsouly.[4] The 18_1 st-PMMA-d_8 helix model was constructed from the optimized st-PMMA by fully deuteration and further *ab initio* quantum chemical calculations were performed at the B3LYP/6-31G(d) level in Gaussian 03 program.[17]

The IR and VCD spectra for the optimized 18_1 helical st-PMMA and st-PMMA-d_8 (12mer) were then calculated using the DFT method at the B3LYP/6-31G(d) level in Gaussian 03 program[17] according to the method previously reported[6] (Figures 2-6B and 2-6D, respectively, and Table 2-1).

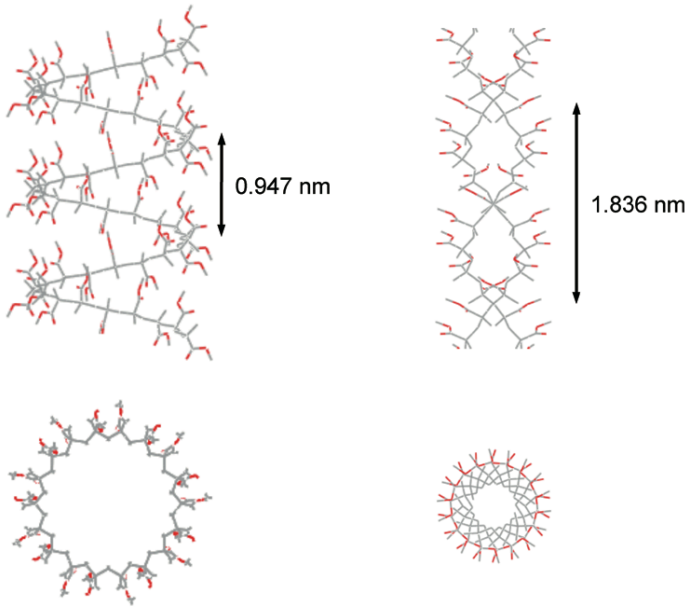

Figure 2-8. Stick models of the 18_1 st-PMMA single helix (left) and 9_1 it-PMMA double-stranded helix (right) used for the IR and VCD calculations. The models were optimized by using *ab initio* quantum chemical calculations at the HF/STO-3G level and further at the B3LYP/6-31G(d) level, see Tables 1-2 and 2-2. Side view (top) and top view (bottom).

Molecular Modeling of Stereocomplex and IR and VCD Calculations. We recently provided convincing evidence for a triple-stranded helix for the stereocomplex by high-resolution AFM, which revealed that a double-stranded helix of it-PMMA is included in a single helix of st-PMMA, thus forming an inclusion complex with a triple-stranded helical structure.[4] Based on these results, we assumed that the IR and VCD spectra of a triple-stranded stereocomplex could be calculated by combining those of a double helix of it-PMMA and a single helix of st-PMMA.

Inclusion of an it-PMMA helix into an outer st-PMMA or st-PMMA-d_8 helix will produce a pair of diastereomeric helical assemblies composed of the same or opposite handed it- and st-PMMAs helices. We then calculated the IR and VCD spectra for all the possible combinations of triple-stranded helical stereocomplexes on the basis of the right- and left-handed single helical 18_1 st-PMMAs or st-PMMA-d_8s and double helical 9_1 it-PMMAs (Figures 2-4D, 2-4G, 2-5B, 2-5C, 2-5E, and 2-5F). The experimental VCD spectral patterns of the stereocomplexes fit well to the calculated ones composed of helical it- and st-PMMAs or helical it- and st-PMMA-d_8s with the same handedness (Figure 2-5).

We also constructed a triple-stranded stereocomplex composed of the optimized double helical 9_1 it-PMMA and single helical 18_1 st-PMMA with the same handedness according to the method previously reported,[6] by manually inserting the it-PMMA double helix into the st-PMMA single helix. The relative positions of the it- and st-PMMA helices were determined in order to avoid any unfavorable van der Waals contacts. However, it was difficult to fully optimize the structure by using *ab initio* quantum chemical calculations because of an entire, large polymer complex.

References

(1) For reviews: (a) Spěváček, J.; Schneider, B. *Adv. Colloid Interface Sci.* **1987**, *27*, 81–150. (b) te Nijenhuis, K. *Adv. Polym. Sci.* **1997**, *130*, 67–81. (c) Hatada, K.; Kitayama, T. *Polym. Int.* **2000**, *49*, 11–47.

(2) (a) Fox, T. G.; Garrett, B. S.; Goode, W. E.; Gratch, S.; Kincaid, J. F.; Spell, A.; Stroupe, J. D. *J. Am. Chem. Soc.* **1958**, *80*, 1768–1769. (b) Watanabe, W. H.; Ryan, C. F.; Fleischer, P. C., Jr.; Garrett, B. S. *J. Phys. Chem.* **1961**, *65*, 896. (c) Liquori, A. M.; Anzuino, G.; Coiro, V. M.; D'Alagni, M.; de Santis, P.; Savino, M. *Nature* **1965**, *206*, 358–362.

(3) Schomaker, E.; Challa, G. *Macromolecules* **1989**, *22*, 3337-3341.

(4) Kumaki, J.; Kawauchi, T.; Okoshi, K.; Kusanagi, H.; Yashima, E. *Angew. Chem., Int. Ed.* **2007**, *46*, 5348–5351.

(5) Kumaki, J.; Kawauchi, T.; Ute, K.; Kitayama, T.; Yashima, E. *J. Am. Chem. Soc.* **2008**, *130*, 6373–6380.

(6) Kawauchi, T.; Kumaki, J.; Kitaura, A.; Okoshi, K.; Kusanagi, H.; Kobayashi, K.; Sugai, T.; Shinohara, H.; Yashima, E. *Angew. Chem., Int. Ed.* **2008**, *47*, 515–519.

(7) Serizawa, T.; Hamada, K.; Kitayama, T.; Fujimoto, N.; Hatada, K.; Akashi, M. *J. Am. Chem. Soc.* **2000**, *122*, 1891–1899.

(8) Mizumoto, T.; Sugimura, N.; Moritani, M.; Sato, Y.; Masuoka, H. *Macromolecules* **2000**, *33*, 6757–6763.

(9) Sugaya, H.; Sakai, Y. *Contrib. Nephrol.* **1998**, *125*, 1–8.

(10) Kennedy, J. P.; Price, J. L.; Koshimura, K. *Macromolecules* **1991**, *24*, 6567–6571.

(11) Kawauchi, T.; Kumaki, J.; Okoshi, K.; Yashima, E. *Macromolecules* **2005**, *38*, 9155–9160.

(12) (a) Serizawa, T.; Hamada, K.; Akashi, M. *Nature* **2004**, *429*, 52–55. (b) Serizawa, T.; Akashi, M. *Polym. J.* **2006**, *38*, 311–328.

(13) Kawauchi, T.; Kumaki, J.; Yashima, E. *J. Am. Chem. Soc.* **2006**, *128*, 10560–10567.

(14) Wulff, G.; Petzoldt, J. *Angew. Chem., Int. Ed. Engl.* **1991**, *30*, 849–850.

(15) Abe, H.; Imai, K.; Matsumoto, M. *J. Polym. Sci., Part C* **1968**, *23*, 469–485.

(16) Hatada, K.; Ute, K.; Tanaka, K.; Okamoto, Y.; Kitayama, T. *Polym. J.* **1986**, *18*, 1037–1047.

(17) Frisch, M. J.; Trucks, G. W.; Schlegel, H. B.; Scuseria, G. E.; Robb, M. A.; Cheeseman, J. R.; Montgomery, J. A., Jr.; Vreven, T.; Kudin, K. N.; Burant, J. C.; Millam, J. M.; Iyengar, S. S.; Tomasi, J.; Barone, V.; Mennucci, B.; Cossi, M.; Scalmani, G.; Rega, N.; Petersson, G. A.; Nakatsuji, H.; Hada, M.; Ehara, M.; Toyata, K.; Fukuda, R.; Hasegawa, J.; Ishida, M.; Nakajima, T.; Honda, Y.; Kitao, O.; Nakai, H.; Klene, M.; Li, X.; Knox, J. E.; Hratchian, H. P.; Cross, J. B.; Adamo, C.; Jaramillo, J.; Gomperts, R.; Stratmann, R. E.; Yazyev, O.; Austin, A. J.; Cammi, R.; Pomelli, C.; Ochterski, J. W.; Ayala, P. Y.; Morokuma, K.; Voth, G. A.; Salvador, P.; Dannenberg, J. J.; Zakrzewski, V. G.; Dapprich, S.; Daniels, A. D.; Strain, M. C.; Farkas, O.; Malick, D. K.; Rabuck, A. D.; Raghavachari, K.; Foresman, J. B.; Ortiz, J. V.; Cui, Q.; Baboul, A. G.; Clifford, S.; Cioslowski, J.; Stefanov, B. B.; Liu, G.; Liashenko, A.; Piskorz, P.; Komaromi, I.; Martin, R. L.; Fox, D. J.; Keith, T.; Al-Laham, M. A.; Peng, C. Y.; Nanayakkara, A.; Challacombe, M.; Gill, P. M. W.; Johnson, B.; Chen, W.; Wong, M. W.; Gonzalez, C.; Pople, J. A. *Gaussian 03*; Gaussian, Inc.: Pittsburgh, PA, 2003.

(18) Foresman, J. B.; Frisch, Æ. In *Exploring Chemistry with Electronic Structure Methods 2nd ed.*; Gaussian Inc.: Pittsburgh, 1996.

(19) Tretinnikov, O. N.; Ohta, K. *Macromolecules* **2002**, *35*, 7343–7353.

(20) Dybal, J.; Krimm, S. *Macromolecules* **1990**, *23*, 1301–1308.

(21) Brinkhuis, R. H. G.; Schouten, A. J. *Macromolecules* **1991**, *24*, 1496–1504.

(22) Kusuyama, H.; Takase, M.; Higashihata, Y.; Tseng, H.; Chatani, Y.; Tadokoro, H. *Polymer* **1982**, *23*, 1256–1258.

(23) Kusuyama, H.; Miyamoto, N.; Chatani, Y.; Tadokoro, H. *Polymer Commun.* **1983**, *24*, 119–122.

Chapter 3

Helicity Induction and Memory of Syndiotactic Poly(methyl methacrylate) Assisted by Optically Active Additives and Solvent and Chiral Amplification of Helicity

Abstract: Syndiotactic poly(methyl methacrylate) (st-PMMA) was found to fold into a preferred-handed helix with amplification of helicity assisted by chiral additives and solvents and further encapsulated fullerenes within its helical cavity whose helicity was memorized after removal of the chiral molecules.

Introduction

Syndiotactic poly(methyl methacrylate) (st-PMMA), a stereoregular commodity polymer, forms a thermoreversible gel in aromatic solvents, such as toluene and chlorobenzene, in which the st-PMMA possesses a 74/4 helical conformation with a large cavity of about 1 nm and the solvent molecules are encapsulated in the cavity of the st-PMMA interior.[1,2] Taking advantage of this unique helix formation of the st-PMMA with a specific cavity in the gel state, Yashima *et al*. recently succeeded in encapsulation of fullerenes in the cavity of st-PMMA, resulting in a robust, processable and peapod-like complex.[3] In addition, preferred-handed helical structures in st-PMMA and its complex with fullerenes could be induced in the presence of an optically active alcohol (**1**)[3] and amine (**6**)[4] as an additive and solvent, respectively, as evidenced by an electronic circular dichroism (ECD) induced in the encapsulated C_{60} chromophore regions and vibrational CD (VCD) in the PMMA IR regions. Furthermore, the induced st-PMMA helix was retained ("memorized")[5-7] after complete removal of the chiral molecules (Figure 3-1)[3] and could recognize the size and chirality of higher fullerenes through an induced-fit mechanism to selectively extract enantiomers of the higher fullerenes.[4]

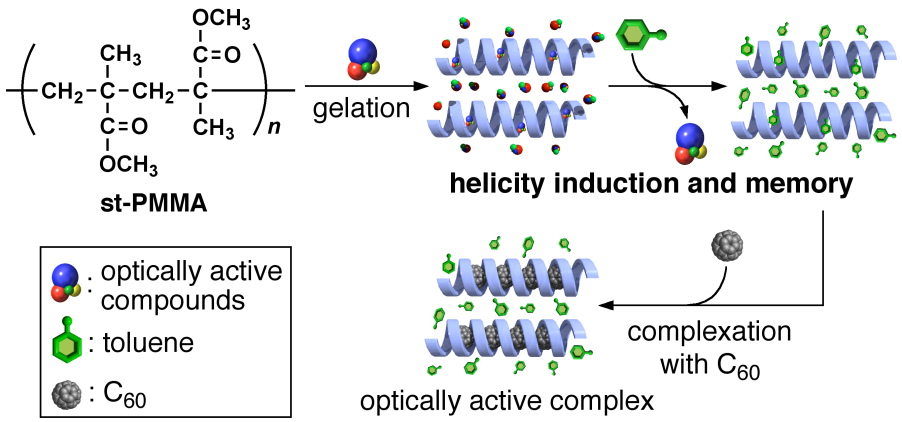

Figure 3-1. Schematic illustration for the helicity induction and memory in st-PMMA and further encapsulation of C_{60} after complete removal of optically active compounds.

In this study, the author investigated the effects of diverse optically active compounds (**1**–**12**) (Chart 3-1) as chiral additives in toluene or solvents on the gelation abilities and further efficiency of the helicity induction and memory in st-PMMA. During the course of our studies, the author found that the chiral information of a nonracemic aromatic amine transfers with amplification in the st-PMMA as an excess of a single-handed helix through noncovalent bonding interactions, thus generating a unique "majority rule" effect (nonlinear effect)[7-9] on a helical system.

Chart 3-1

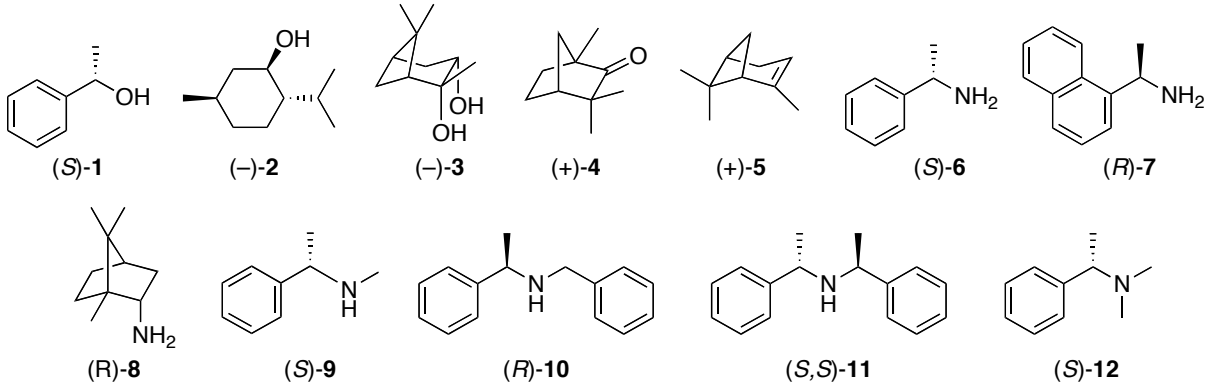

Results and Discussion

First, the helicity induction abilities of aromatic and aliphatic optically active alcohols (**1**–**3**) and amines (**6**–**12**), and aliphatic (**5**) and carbonyl (**4**) compounds toward st-PMMA were systematically investigated in toluene (Tables 3-1 and 3-2). The st-PMMA gel and its inclusion complex with C_{60} were prepared according to previously reported methods with a slight modification.[3,4,10] St-PMMA (4 mg) was dissolved in toluene (0.1 mL) containing **1**–**12** (2 equiv with respect to the monomer units of st-PMMA) upon heating at 110 ˚C. Cooling to room temperature, the gelation rapidly took place within 4 min except for the solutions with **1**

Table 3-1. Gelation and Helicity Induction of st-PMMA in Various Solvents with or without Chiral Additives[a]

entry	solvent	additive[b]	gelation time[c]	$\Delta\varepsilon_{346}$ /M^{-1} cm^{-1} [d]
1[e]	toluene	—	3 min	—
2	toluene	(*S*)-**1**	3 h	–0.3
3	toluene	(*S*)-**6**	4 min	0.2
4	toluene	(*R*)-**7**	4 min	–0.4
5	(*S*)-**1**	—	—[f]	—
6	(+)-**4**	—	1 min	—[g]
7	(+)-**5**	—	—[h]	—
8	(*S*)-**6**	—	15 h	1.3
9	(*R*)-**6**	—	15 h	–1.5
10	(*R*)-**7**	—	1 h	–1.4
11	(*S*)-**9**	—	1.5 h	1.0
12	(*R*)-**10**	—	2 min	–0.8
13	(*S*,*S*)-**11**	—	4 min	1.3
14	(*S*)-**12**	—	1 min	—[g]

[a] The concentration of st-PMMA was 40 mg/mL. [b] The molar ratio of additives to the monomer unit of st-PMMA was 2. [c] The gelation time was estimated by the inverse flow method. [d] Measured after removal of chiral compounds followed by encapsulation of C_{60}. [e] Cited from ref 3. [f] No gelation after 24 h. [g] Apparent CD (>0.2 M^{-1} cm^{-1}) was not observed. [h] st-PMMA was insoluble.

(3 h) and **3** (10 min) (Table 3-2). The author note that a toluene solution of st-PMMA gelled within 3 min without any additives (Table 3-1). After complete removal of the chiral additives from the st-PMMA gels and further encapsulation of C_{60} molecules within its helical cavity in

toluene, the ECD spectra of the st-PMMA/C_{60} complex gels were measured. Among the diverse optically active additives (**1**–**12**), the chiral aromatic alcohol (**1**) and amines (**6** and **7**) successfully induced and memorized a preferred-handed helicity in st-PMMA, thus producing the optically active st-PMMA/C_{60} complex gels, which exhibited weak but apparent ECDs in the encapsulated C_{60} chromophore regions at around 346 nm (entries 2–4 in Tables 3-1 and 3-2). The author presumes that a helical sense excess of st-PMMA induced and memorized by the chiral additives and the ECD intensity at the C_{60} chromophore regions encapsulated in the

Table 3-2. Gelation and Helicity induction of st-PMMA in Toluene with Chiral Additives

entry	additive[b]	gelation time[c]	$\Delta\varepsilon_{346}$ /M^{-1} cm^{-1} [d]
1	(*S*)-**1**	3 h	–0.3
2	(–)-**2**	3 min	—[e]
3	(–)-**3**	10 min	—[e]
4	(+)-**4**	2 min	—[e]
5	(+)-**5**	0.3 min	—[e]
6	(*S*)-**6**	4 min	0.2
7	(*R*)-**7**	4 min	–0.4
8	(*R*)-**8**	1 min	—[e]
9	(*S*)-**9**	3 min	—[e]
10	(*R*)-**10**	2 min	—[e]
11	(*S,S*)-**11**	3 min	—[e]
12	(*S*)-**12**	2 min	—[e]

[a] The concentration of st-PMMA was 40 mg/mL. [b] The molar ratio of additives to the monomer unit of st-PMMA was 2. [c] The gelation time was estimated by the inverse flow method. [d] Measured after removal of chiral additives followed by encapsulation of C_{60}. [e] Apparent CD (>0.2 M^{-1} cm^{-1}) was not observed.

helical cavity of st-PMMA may be correlated to each other, and hence, the ECD intensity most likely reflects the helical sense excess of st-PMMA, thereby, the helix-inducing ability of the chiral additives.

With these results in mind, the author next investigated if optically active liquids (**1**, **4**–**7**, and **9**–**12**) could be used as a solvent to dissolve and then gelate the st-PMMA with a greater helical sense excess (entries 5–14 in Table 3-1). St-PMMA was not soluble in **5** and a solution of st-PMMA in **1** did not gel, but other chiral liquids (**4** and aromatic amines (**6**, **7**, and **9**–**12**)) dissolved the st-PMMA and then gelled. Interestingly, solutions of st-PMMA in **4** and **10**–**12** rapidly gelled within 1–4 min like that in toluene. The st-PMMA gels were then repeatedly washed with toluene to remove the chiral solvents, and subsequently, C_{60} molecules were encapsulated in the st-PMMA cavity to make the st-PMMA/C_{60} complex gels and their ECD and VCD spectra were measured.

Figure 3-2 shows the typical absorption, VCD, and ECD spectra of the st-PMMA/C_{60} complex gels in toluene assisted by (*S*)- and (*R*)-**6** or racemic **6**. The st-PMMA/C_{60} complex gels, which contained no trace amount of **6**, showed mirror-imaged VCDs in the PMMA IR regions due to the preferred-handed helicity (a) and also ECDs in the encapsulated C_{60} chromophore regions (b). The VCD intensities of the st-PMMA/C_{60} complex gels at around 1150 and 1280 cm^{-1} were approximately three times larger than those prepared with (*S*)- and (*R*)-**1** (20 vol %),[3] indicating the remarkable increase in the helical sense excess of the st-PMMA induced by (*S*)- and (*R*)-**6**. Based on the calculated IR and VCD spectra for the right- and left-handed helical 18/1 st-PMMAs at the B3LYP/6-31G(d) level, the st-PMMA induced by (*R*)-**6** likely possesses a left-handed helix.[3]

The ECD measurement results of the st-PMMA/C_{60} complexes assisted by optically active liquids are summarized in Table 3-1, which revealed that the use of optically active solvents (entries 8–13), in particular, the aromatic optically active primary (**6** and **7**) and secondary amines (**9**–**11**) more efficiently induced an excess one-handedness in the st-PMMA backbone, thus showing intense ECDs in the C_{60} chromophore regions as compared with

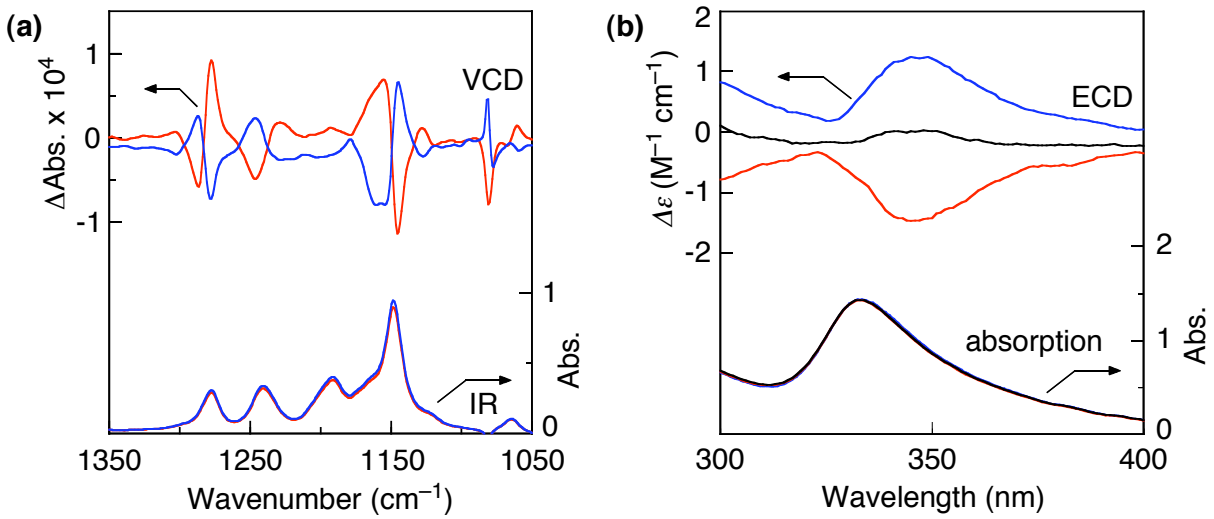

Figure 3-2. (a) VCD (top) and IR (bottom) spectra of isolated st-PMMA/C_{60} complex gels in toluene prepared by the complexation with C_{60} after the gelation of st-PMMA with (*R*)-**6** (red lines) and (*S*)-**6** (blue lines). (b) ECD (top) and absorption (bottom) spectra of isolated st-PMMA/C_{60} complex gels in toluene prepared by the complexation with C_{60} after the gelation of st-PMMA with racemic **6** (black lines), (*R*)-**6** (red lines), and (*S*)-**6** (blue lines). The racemic and (*R*)- and (*S*)-**6** were completely removed before the complexation with C_{60}.

those induced by chiral additives (entries 2–4). On the other hand, the tertiary amine (*S*)-**12** as well as the aliphatic (+)-**4** showed no preference in the helical sense bias in st-PMMA, thus no ECD (entries 6 and 14). These results suggest that the NH protons as well as the aromatic groups may play an important role in the helicity induction in st-PMMA, probably through intermolecular hydrogen bonding interactions between the pendant ester groups of st-PMMA and the NH residues of the amines. Therefore, the aromatic primary and secondary chiral amines (**6**, **7**, **9**–**11**) exhibited the same chiral bias for the helicity induction in st-PMMA, thus showing the ECDs with the same Cotton effect sign when their absolute configurations are the same. In contrast, the Cotton effect sign of the st-PMMA/C_{60} complex induced by (*S*)-**6** was opposite to that induced by (*S*)-**1** (entries 2 and 3 or 8), indicating an opposite chiral bias

for the helicity induction in st-PMMA. As for the helicity induction and gelation abilities assisted by chiral compounds, there is almost no clear relationship between them.

The helix formation of st-PMMA in the chiral amine **6** gel showed a unique positive nonlinear relationship between the enantiomeric excess (ee) of **6** and the observed ECD intensities of the corresponding st-PMMA/C_{60} complexes; the ECD intensities of the gels in the encapsulated C_{60} chromophore regions were out of the proportion to the ee values of **6** (Figure 3-3). This is a typical example of chiral amplification ("majority rule" effect[7-9]) often observed in dynamic helical polymers[7,11] and self-assembled helical systems.[12-14] Although the convex deviation from the linearity was not so impressive, this positive nonlinear relationship is of particular interesting to understand the mechanistic insight into the helix formation of st-PMMA followed by gelation in specific solvents. The st-PMMA backbone may possess a dynamic nature in its helical conformation during the gelation process in the optically active **6**. Because the st-PMMA backbone may become static in the gel state, an excess of one-handed

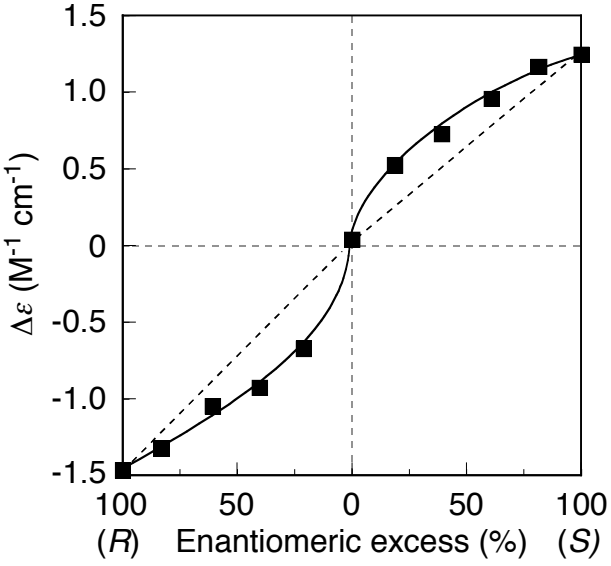

Figure 3-3. Changes in the ECD intensity at around 350 nm of st-PMMA/C_{60} complex gels versus the % ee of **6** during the gelation of st-PMMA. ECD spectra were measured after removal of **6** followed by encapsulation of C_{60}.

helical conformation with chiral amplification may be induced in st-PMMA before the noncovalent network formation generated by helix bundles as a cross-linker, resulting in the gelation. Therefore, once gelation takes place, the induced st-PMMA helix with a helicity memory is stabilized by helix-bundles and maintains before melting of the gel.

Conclusion

In summary, the author has found that the preferred-handed helicity was efficiently induced in st-PMMA with various optically active primary and secondary amines bearing aromatic groups as the gelling solvents, and further memorized after removal of the chiral amines while maintaining its gel state. An excess of one-handed helix was also induced with nonracemic amines during the gelation, resulting in the amplification of helical chirality, suggesting that the helical st-PMMA chain may have a dynamic characteristic during the gelation process. These findings will contribute to the development of readily available, unique chiral and optoelectronic materials with a controlled helical sense and specific chiral cavity, in which a variety of functional molecules will be encapsulated.

Experimental Section

Materials. The st-PMMA was synthesized by the syndiotactic-specific polymerization of MMA in toluene at –95 ºC using a typical Ziegler-type catalyst derived from $Al(C_2H_5)_3$ and $TiCl_4$.[15] The number-average molecular weight (M_n), molecular weight distribution (M_w/M_n), and tacticity (*mm*:*mr*:*rr*) were as follows: M_n = 573000, M_w/M_n = 1.42, and *mm*:*mr*:*rr* = 1:5:94. The M_n and M_w/M_n values were measured by size exclusion chromatography (SEC) in $CHCl_3$ using polystyrene standards for the calibration. The tacticity was determined from the ^1H NMR signals due to the α-methyl protons.

[60]Fullerene (C_{60}) was purchased from Frontier Carbon (Tokyo, Japan). (–)-Menthol ((–)-**2**), (1*R*,2*R*,3*S*,5*R*)-(–)-pinanediol ((–)-**3**), (+)-α-pinene ((+)-**5**), (*R*)-(+)-bornylamine ((*R*)-**8**), (*S*)-(–)-*N*,α-dimethylbenzylamine ((*S*)-**9**) and (–)-bis[(*S*)-1-phenylethyl]amine ((*S,S*)-**11**) were purchased from Aldrich (Milwaukee, WI). (*S*)-1-Phenylethanol ((*S*)-**1**) and (*R*)-(+)-*N*-benzyl-α-methylbenzylamine ((*R*)-**10**) were obtained from Azmax (Chiba, Japan) and Fluka (Buchs, Switzerland), respectively. (+)-Fenchone ((–)-**4**) and (*S*)-(–)-*N*,*N*-dimethyl-1-phenylethylamine ((*S*)-**12**) were purchased from Tokyo Kasei (TCI, Tokyo, Japan). (*R*)- and (*S*)-1-Phenylethylamine (**6**) and (*R*)-1-(1-naphthyl)ethylamine (**7**) were kindly supplied from Yamakawa Chemical (Tokyo, Japan).

Instruments. NMR spectra were recorded on a Varian UNITY INOVA 500AS spectrometer operating at 500 MHz for ^1H in $CDCl_3$. Absorption spectra were measured in a 0.2- or 1 mm quartz cell on a JASCO (Hachioji, Japan) V-550 or V-570 spectrophotometer and electronic circular dichroism (ECD) spectra were measured on a JASCO J-820 spectropolarimeter. Vibrational CD (VCD) spectra were measured in a 0.15-mm BaF_2 cell with a JASCO JV-2001 spectrometer. The concentration was *ca*. 30 mg/mL in toluene. All spectra were collected for *ca*. 4–5 h at a resolution of 4 cm^{-1}.

Preparation of Optically Active st-PMMA Gels in Toluene with Chiral Additives and Complexation with C_{60}. A st-PMMA/C_{60} complex gel was prepared according to a previously reported method with a slight modification.[3] A typical experimental procedure is described below. A 4 mg of st-PMMA was dissolved in toluene (0.1 mL) containing (*S*)-**1** (2 equiv with respect to the monomer units of st-PMMA) at 110 ºC. After the solution was cooled to room temperature, the solution gelled within 3 h. The obtained soft gel was collected by centrifugation at 1700 *g* for 10 min and the supernatant was removed by decantation. The condensed gel was then washed with toluene to remove (*S*)-**1**. This procedure was repeated several times. The gel was then suspended in a toluene solution of C_{60} (1 mg/mL, 0.2 mL). The mixture was vigorously stirred at room temperature by a magnetic stirrer, thus producing soft gel particles. The obtained st-PMMA/C_{60} complex gel was collected by centrifugation at 1700 *g* for 10 min and the supernatant containing the unencapsulated fullerenes was removed by decantation. The condensed gel was then washed with toluene and the solvent was removed by decantation after centrifugation. This procedure was repeated several times. The obtained gel was suspended in a small amount of toluene, and then subjected to the ECD measurement.

Preparation of Optically Active st-PMMA Gels in Chiral Solvents and Complexation with C_{60}. A typical experimental procedure is described below. A 4 mg of st-PMMA was dissolved in (*S*)-**6** (0.1 mL) at 110 °C. After the solution was cooled to room temperature, the solution gelled within 15 h. The obtained soft gel was collected by centrifugation at 1700 *g* for 10 min and the supernatant was removed by decantation. The condensed gel was then washed with toluene to remove (*S*)-**6**. This procedure was repeated several times. The gel was then suspended in a toluene solution of C_{60} (1 mg/mL, 0.2 mL). The mixture was vigorously stirred at room temperature by a magnetic stirrer, thus producing soft gel particles. The obtained st-PMMA/C_{60} complex gel was collected by centrifugation at 1700 *g* for 10 min and the supernatant containing the unencapsulated fullerenes was removed

by decantation. The condensed gel was then washed with toluene and the solvent was removed by decantation after centrifugation. This procedure was repeated several times. The obtained gel was suspended in a small amount of toluene, and then subjected to the ECD and VCD measurements.

References

(1) Kusuyama, H.; Yakase, M.; Higashihata, Y.; Tseng, H.-T.; Chatani, Y.; Tadokoro, H. *Polymer* **1982**, *23*, 1256–1258.

(2) Kusuyama, H.; Miyamoto, N.; Chatani, Y.; Tadokoro, H. *Polymer Commun.* **1983**, *24*, 119–122.

(3) Kawauchi, T.; Kumaki, J.; Kitaura, A.; Okoshi, K.; Kusanagi, H.; Kobayashi, K.; Sugai, T.; Shinohara, H.; Yashima, E. *Angew. Chem., Int. Ed.* **2008**, *47,* 515–519.

(4) Kawauchi, T.; Kitaura, A.; Kawauchi, M.; Takeichi, T.; Kumaki, J.; Iida, H.; Yashima, E. *J. Am. Chem. Soc.* **2010**, *132*, 12191–12193.

(5) Yashima, E.; Maeda, K.; Okamoto, Y. *Nature* **1999**, *399*, 449–451.

(6) Yashima, E.; Maeda, K. *Macromolecules* **2008**, *41*, 3–12.

(7) Yashima, E.; Maeda, K.; Iida, H.; Furusho, Y.; Nagai, K. *Chem. Rev.* **2009**, *109*, 6102–6211.

(8) Green, M. M.; Garetz, B. A.; Munoz, B.; Chang, H. P.; Hoke, S.; Cooks, R. G. *J. Am. Chem. Soc.* **1995**, *117*, 4181–4182.

(9) Green, M. M.; Peterson, N. C.; Sato, T.; Teramoto, A.; Cook, R.; Lifson, S. *Science* **1995**, *268*, 1860–1866.

(10) Kawauchi, T.; Kitaura, A.; Kumaki, J.; Kusanagi, H.; Yashima, E. *J. Am. Chem. Soc.* **2008**, *130*, 11889–11891.

(11) Fujiki, M.; Koe, J. R.; Terao, K.; Sato, T.; Teramoto, A.; Watanabe, J. *Polym. J.* **2003**, *35*, 297–344.

(12) Maeda, K.; Yashima, E. *Top. Curr. Chem.* **2006**, *265*, 47–88.

(13) Palmans, A. R. A.; Meijer, E. W. *Angew. Chem., Int. Ed.* **2007**, *46*, 8948–8968.

(14) Aida, T.; Fukushima, T. *Phil. Trans. R. Soc. A* **2007**, *365*, 1539–1552.

(15) Abe, H.; Imai, K.; Matsumoto, M. *J. Polym. Sci., Part C* **1968**, *23*, 469–485.

Chapter 4

Separation of Higher Fullerene Enantiomers by Syndiotactic Poly(methyl methacrylate) with a Macromolecular Helicity Memory

Abstract: A one-handed helical polymer, syndiotactic poly(methyl methacrylate) (st-PMMA), recognizes the size and chirality of higher fullerenes through an induced-fit mechanism and can selectively extract enantiomers of the higher fullerenes, such as C_{76}, C_{80}, C_{84}, C_{86}, C_{88}, C_{90}, C_{92}, C_{94}, and C_{96}. This discovery will generate a practical and valuable method for selectively extracting the enantiomers of the elusive higher fullerenes and opens the way to developing novel carbon cage materials with optical activities.

Introduction

The development of a practical and efficient method for the separation of higher fullerenes ($\geq C_{76}$) with a specific size, geometry, and in particular, chirality is among the urgent and emerging challenges in advanced materials science due to their attractive applications, such as electronic and optoelectronic materials.[1,2] The iterative chromatographic separation provides a tiny amount of the higher fullerenes, and the supramolecular approach using designer host molecules with a rigid concave cavity or through self-assemblies has been a powerful method for selectively encapsulating C_{60} and/or C_{70} rather than higher fullerenes.[3-12] The cyclic dimers of zinc porphyrins possess an exceptionally high affinity toward the higher fullerenes due to flexible linkers between the metalloporphyrins.[13]

Recently, Yashima *et al.* reported that syndiotactic poly(methyl methacrylate) (st-PMMA), a stereoregular commodity plastic, can encapsulate fullerenes, such as C_{60} and C_{70}, within its helical cavity to form a robust, processable and crystalline complex with optical activity.[14] Preferred-handed helical structures in st-PMMA and its complex with fullerenes could be induced in the presence of an optically active alcohol and amines as an additive and solvent, as evidenced by an electronic circular dichroism (ECD) induced in the encapsulated C_{60} chromophore regions and vibrational CD (VCD) in the PMMA IR regions.[15] In addition, the induced st-PMMA helix could recognize the higher fullerenes through an induced-fit mechanism, and performed selective extraction of the higher fullerenes from carbon soot (a commercially available fullerene mixture) composed of C_{60}/C_{70}/higher fullerenes (64.0:27.2:8.8% determined by high performance liquid chromatography (HPLC) analysis).[16] Remarkably, the higher fullerenes were selectively obtained from the carbon soot and the higher fullerene content significantly increased to 95.4% from 8.8% in the feed by single extraction with st-PMMA.

However, judging from the tiny structural differences in the enantiomers and due to a lack of functionality, the direct separation of chiral fullerenes into enantiomers appears to be extremely difficult, and only D_2-symmetric C_{76} (C_{76}-D_2),[17,18a,19,20] C_{78}-D_3,[17b] and C_{84}-D_2[17b,18b]

were successfully resolved into the enantiomers by recycling chiral HPLC, kinetic resolution, enantioselective extraction with a chiral porphyrin dimer,[20] and the covalent modification with chiral molecules followed by regeneration. The fact that the number of chiral isomers dramatically increases with increasing cage size; for example, 21 of 35 C_{88} isomers are possibly chiral, suggests that there are no feasible methods to resolve the higher fullerenes (>C_{84}) into optical antipodes.

In this chapter, the author shows that an optically active st-PMMA with an excess single-handed helix can be used to enantiomer-selectively extract chiral fullerenes from the fullerene mixture (Figure 4-1).

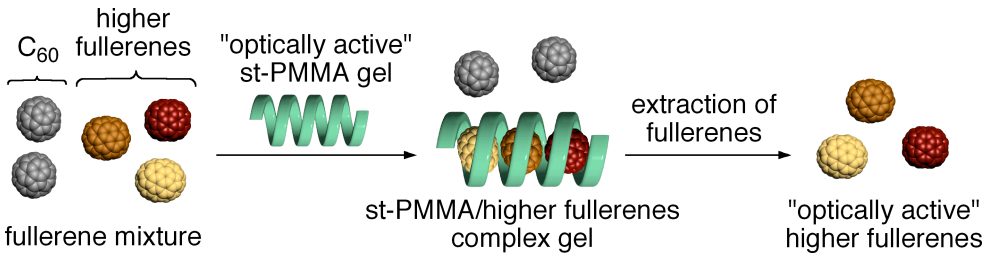

Figure 4-1. Schematic illustration of the separation of higher fullerene enantiomers by optically active st-PMMA gel.

Results and Discussion

The optically active st-PMMA gel was prepared according to the method described in Chapter 3 using (*R*)- or (*S*)-1-phenylethylamine (**1**) as the solvent to induce a preferred-handed helical conformation in st-PMMA followed by complete removal of **1** by repeatedly washing the gel with toluene and then isolated by centrifugation. A single extraction of a large amount of fullerene mixture in toluene (*ca.* 0.3 mg/mL, 800 mL) was

then carried out using a low concentrated optically active st-PMMA gel (0.05 mg/mL), since using lower concentrated st-PMMA appears to encapsulate higher fullerenes more efficiently. The author estimated that approximately 16% of the higher fullerenes, for example, 13% of feed C_{76} and 14% of feed C_{84} in toluene were encapsulated by a single extraction as demonstrated by the HPLC chromatograms of the solution before and after extraction by the optically active st-PMMA (Table 4-1). The extraction provided a series of optically active fullerenes (C_{76}, C_{84}, C_{86}, C_{88}, C_{90}, C_{92}, C_{94}, and C_{96}) as supported by the circular dichroism (CD)-detected HPLC chromatograms of the extract, which showed the apparent CDs (Figures 4-2a and b). Among them, the optically active C_{86}, C_{88}, C_{90}, C_{92}, C_{94}, and C_{96} have never been

Table 4-1. Enantiomer-Selective Extraction of Higher Fullerenes by Optically Active st-PMMA with an Excess Single-Handed Helix

fullerenes	encapsulation ratios of fullerenes (area%)[a]
higher fullerenes (C_{76} ~ C_{96})	16 ± 0.6
C_{76}	13 ± 1.1
C_{78}	17 ± 0.8
C_{80}	27 ± 5.3
C_{82}	11 ± 1.1
C_{84}	14 ± 0.8
C_{86}	10 ± 2.0
C_{88}	25 ± 0.4
C_{90}	20 ± 2.1
C_{92}	36 ± 7.4
C_{94}	30 ± 1.1
C_{96}	28 ± 2.2

[a] The area% was determined by peak integral ratio in HPLC. The values represent an average of three runs.

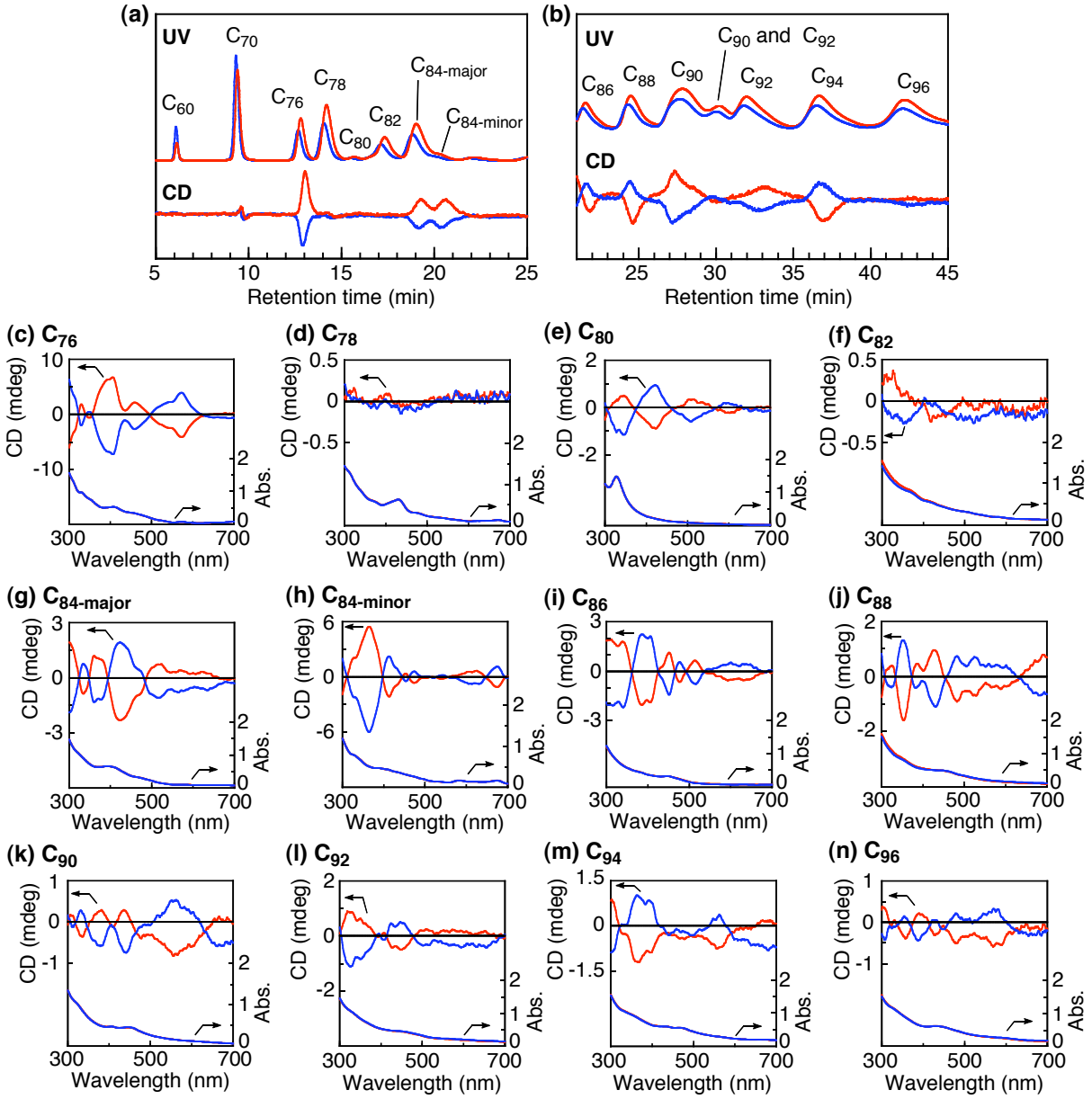

Figure 4-2. (a), (b) UV (356 nm, top) and CD (375 nm, bottom) detected HPLC chromatograms of the extracted fullerenes from carbon soot using optically active helical st-PMMAs prepared with (*R*)-**1** (red lines) and (*S*)-**1** (blue lines). The HPLC measurements were carried out using a COSMOSIL 5PBB column with chlorobenzene as the eluent at the flow rate of 1.0 mL/min. CD (top) and absorption (bottom) spectra of fractionated (c) C_{76}, (d) C_{78}, (e) C_{80}, (f) C_{82}, (g) $C_{84\text{-major}}$, (h) $C_{84\text{-minor}}$, (i) C_{86}, (j) C_{88}, (k) C_{90}, (l) C_{92}, (m) C_{94}, and (n) C_{96} measured in DCB at 25 °C.

isolated. A series of optically active fullerenes were then isolated by preparative HPLC using a COSMOSIL 5PBB column, and their CD and absorption spectra were measured in DCB at 25 ˚C, resulting in the characteristic CDs in the long absorption regions (Figures 4-2c-n). When an opposite enantiomer of 1-phenylethylamine (**1**) was used for the preparation of the preferred-handed helical st-PMMA, the opposite fullerene enantiomers could be extracted, as evidenced by the mirror image CDs. The enantiomeric excess (ee) of the isolated C_{76} was estimated to be approximately 4% by comparison with the reported CD intensity of the optically pure C_{76} in toluene (Figure 4-3).[18a] Two fractions assigned to the C_{84} isomers (C_{84}-major and C_{84}-minor in Figure 4-2a) were also fractionated from the extract, and the CD pattern of the major isomer (C_{84}-major) was in accordance with that reported for the optically pure C_{84}-D_2 (Figures 4-2g and 4-4a),[18b] suggesting that the minor fraction (C_{84}-minor) likely

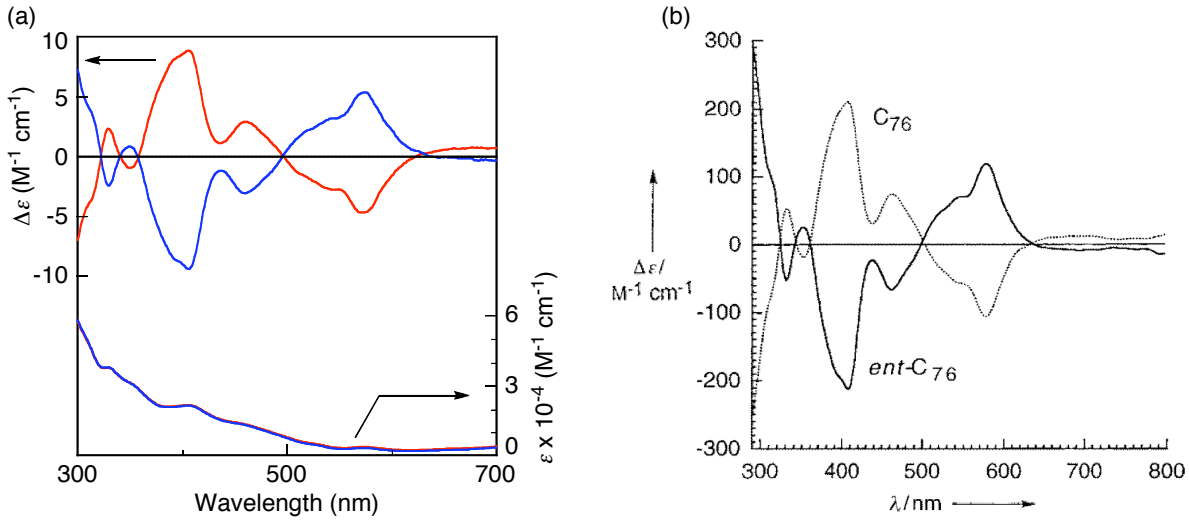

Figure 4-3. (a) CD (top) and absorption (bottom) spectra of fractionated C_{76} measured in toluene at 25 °C after the extraction of fullerenes from carbon soot using optically active helical st-PMMAs prepared with (*R*)-**1** (red lines) and (*S*)-**1** (blue lines). (b) CD spectra of a pair of optically pure C_{76} enantiomers measured in toluene reported by Diederich *et al.*[18a] are also shown for comparison

consists of novel chiral isomers of C_{84} which have never been isolated (Figures 4-2h and 4-4b). Although the ee values of the isolated chiral fullerenes were low, this finding may lead to the development of unique and facile methods to resolve the higher fullerenes.

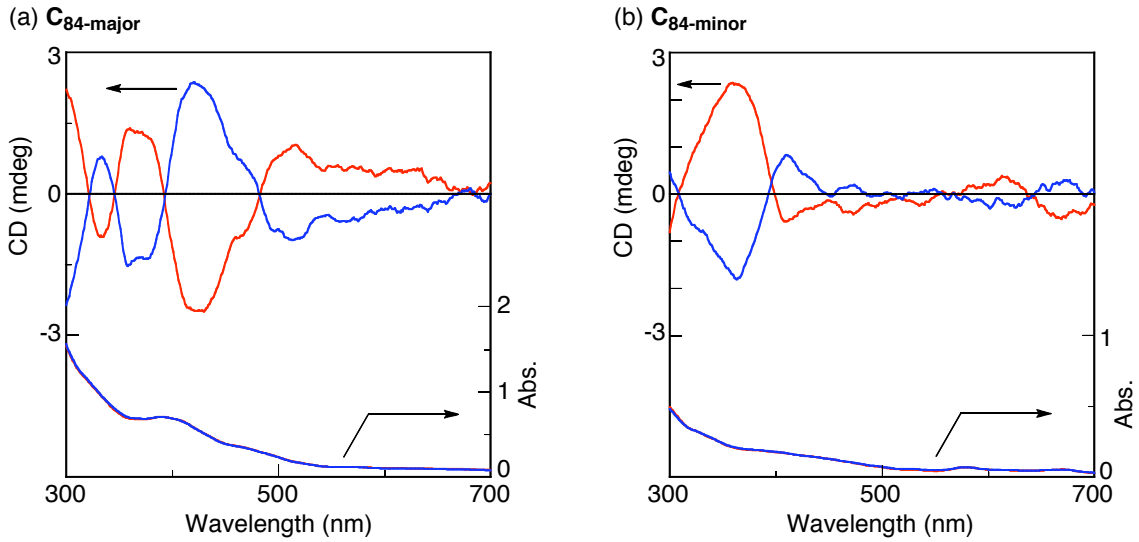

Figure 4-4. CD (top) and absorption (bottom) spectra of fractionated (a) $C_{84\text{-major}}$ and (b) $C_{84\text{-minor}}$ measured in dichloromethane at 25 °C after the extraction of fullerenes from carbon soot using optically active helical st-PMMAs prepared with (*R*)-**1** (red lines) and (*S*)-**1** (blue lines).

Conclusion

In conclusion, this strategy which relies on the inexpensive and readily available helical st-PMMA with a unique induced-fit feature has great potential in the isolation of the higher fullerene enantiomers and, thus, opens the way to developing novel carbon cage materials with optical activities.

Experimental Section

Materials. The st-PMMA was synthesized by the syndiotactic-specific polymerization of MMA in toluene at –95 ºC using a typical Ziegler-type catalyst derived from $Al(C_2H_5)_3$ and $TiCl_4$.[21] The number-average molecular weight (M_n), molecular weight distribution (M_w/M_n), and tacticity (*mm*:*mr*:*rr*) were as follows: M_n = 782000, M_w/M_n = 1.37, and *mm*:*mr*:*rr* = 2:7:91. The M_n and M_w/M_n values were measured by size exclusion chromatography (SEC) in $CHCl_3$ using polystyrene standards for the calibration. The tacticity was determined from the ^1H NMR signals due to the α-methyl protons.

Toluene, chlorobenzene and 1,2-dichlorobenzene (DCB) were purchased from Wako Chemicals (Osaka, Japan) and were used as received. Fullerene mixture (C_{60}: *ca*. 55 wt %, C_{70}: *ca*. 22 wt %, higher fullerenes: *ca*. 23 wt %) was purchased from Frontier Carbon Co. (Fukuoka, Japan). (*R*)- and (*S*)-1-Phenylethylamine (**1**) were kindly supplied from Yamakawa Chemical (Tokyo, Japan).

Instruments. The absorption spectra were measured in a 0.1-, 0.2- or 2 mm quartz cell on a JASCO (Hachioji, Japan) V-570 spectrophotometer and circular dichroism (CD) spectra were measured in a 2 mm quartz cell on a J-820 spectropolarimeter. HPLC was performed with a JASCO PU-2080 or PU-2086 liquid chromatograph (Hachioji, Japan) equipped with UV–visible (JASCO UV-2070) and CD (JASCO CD-2095) detectors. A Nacalai Tesque (Kyoto, Japan) COSMOSIL 5PBB (4.6 mm x 250 mm or 10 mm x 250 mm) column was connected, and chlorobenzene was used as the eluent.

Resolution of Chiral Fullerenes into Enantiomers with Optically Active st-PMMA. An optically active st-PMMA gel was prepared according to a previously reported method with a slight modification.[14] A 40 mg of st-PMMA was dissolved in (*R*)-1-phenylethylamine ((*R*)-**1**) (1 mL) at 110 ºC. After the solution was cooled to room temperature, the solution gelled within 14 h. The obtained soft gel was collected by centrifugation at 1700 *g* for 10 min

and the supernatant was removed by decantation. The condensed gel was then washed with toluene to remove (*R*)-**1**. The gel was then suspended in a toluene solution of a fullerene mixture (*ca*. 0.3 mg/mL, 800 mL). The mixture was vigorously stirred at room temperature for 24 h by a magnetic stirrer, thus producing soft gel particles. The obtained st-PMMA/higher fullerenes complex gel was collected by centrifugation at 1700 *g* for 10 min and the supernatant containing the unencapsulated fullerenes was removed by decantation. The encapsulation ratios of fullerenes were estimated by the comparison of HPLC chromatograms of the toluene solution before and after the extraction (Table 4-1). The condensed gel was then washed with toluene and the solvent was removed by decantation after centrifugation. This procedure was repeated several times. After drying in vacuo for 30 min, to the gel was added DCB (24 mL) to recover the encapsulated fullerenes from the st-PMMA. In the same way, the resolution of the chiral fullerenes was conducted using the st-PMMA gel prepared in (*S*)-**1**. The extracted fullerenes were subjected to the HPLC analysis after filtration using a membrane filter (pore size 0.45 μm) (Figures 4-2a and b). A series of fullerenes were isolated by preparative HPLC with a 5PBB (10 mm x 250 mm) column using chlorobenzene as the eluent, and the obtained optically active fullerenes were then subjected to CD and absorption measurements (c-n in Figure 4-2 and Figures 4-3 and 4-4). The concentration of the fractionated C_{76} was estimated based on $\varepsilon = 37800\ M^{-1}\ cm^{-1}$ at 330 nm as reported in ref. 22 (Figure 4-3).

References

(1) Diederich, F.; Whetten, R. L. *Acc. Chem. Res.* **1992**, *25,* 119–126.

(2) Thilgen, C.; Diederich, F. *Chem. Rev.* **2006**, *106,* 5049–5135.

(3) Ettl, R.; Chao, I.; Diederich, F.; Whetten, R. L. *Nature* **1991**, *353,* 149–153.

(4) Diederich, F.; Whetten, R. L.; Thilgen, C.; Ettl, R.; Chao, I.; Alvarez, M. M. *Science* **1991**, *254,* 1768–1770.

(5) Kikuchi, K.; Nakahara, N.; Honda, M.; Suzuki, S.; Saito, K.; Shiromaru, H.; Yamauchi, K.; Ikemoto, I.; Kuramochi, T.; Hino, S.; Achiba, Y. *Chem. Lett.* **1991**, *20,* 1607–1610.

(6) Andersson, T.; Nilsson, K.; Sundahl, M.; Westman, G.; Wennerstroem, O. *J. Chem. Soc., Chem. Commun.* **1992**, 604–606.

(7) Atwood, J. L.; Koutsantonis, G. A.; Raston, C. L. *Nature* **1994**, *368,* 229–231.

(8) Suzuki, T.; Nakashima, K.; Shinkai, S. *Chem. Lett.* **1994**, *23,* 699–702.

(9) Komatsu, N. *Org. Biomol. Chem.* **2003**, *1,* 204–209.

(10) Haino, T.; Fukunaga, C.; Fukazawa, Y. *Org. Lett.* **2006**, *8,* 3545–3548.

(11) Huerta, E.; Metselaar, G. A.; Fragoso, A.; Santos, E.; Bo, C.; de Mendoza, J. *Angew. Chem., Int. Ed.* **2007**, *46,* 202–205.

(12) (a) Wietor, J.-L.; Pantos, G. D.; Sanders, J. K. M. *Angew. Chem., Int. Ed.* **2008**, *47,* 2689–2692. (b) Lee, E.; Kim, J.-K.; Lee, M. *J. Am. Chem. Soc.* **2009**, *131,* 18242–18243.

(13) (a) Zheng, J.-K.; Tashiro, K.; Hirabayashi, Y.; Kinbara, K.; Saigo, K.; Aida, T.; Sakamoto, S.; Yamaguchi, K. *Angew. Chem., Int. Ed.* **2001**, *40,* 1857–1861. (b) Shoji, Y.; Tashiro, K.; Aida, T. *J. Am. Chem. Soc.* **2004**, *126,* 6570–6571.

(14) Kawauchi, T.; Kumaki, J.; Kitaura, A.; Okoshi, K.; Kusanagi, H.; Kobayashi, K.; Sugai, T.; Shinohara, H.; Yashima, E. *Angew. Chem., Int. Ed.* **2008**, *47,* 515–519.

(15) Kitaura, A.; Iida, H.; Kawauchi, T.; Yashima, E. *Chem. Lett.* **2011**, *40,* 28–30.

(16) Kawauchi, T.; Kitaura, A.; Kawauchi, M.; Takeichi, T.; Kumaki, J.; Iida, H.; Yashima, E. *J. Am. Chem. Soc.* **2010**, *132*, 12191–12193.

(17) (a) Hawkins, J. M.; Meyer, A. *Science* **1993**, *260,* 1918–1920. (b) Hawkins, J. M.; Nambu, M.; Meyer, A. *J. Am. Chem. Soc.* **1994**, *116,* 7642–7645.

(18) (a) Kessinger, R.; Crassous, J.; Hermann, A.; Rüttimann, M.; Echegoyen, L.; Diederich, F. *Angew. Chem., Int. Ed.* **1998**, *37,* 1919–1922. (b) Crassous, J.; Rivera, J.; Fender, N. S.; Shu, L.; Echegoyen, L.; Thilgen, C.; Herrmann, A.; Diederich, F. *Angew. Chem., Int. Ed.* **1999**, *38,* 1613–1617.

(19) Yamamoto, C.; Hayashi, T.; Okamoto, Y.; Ohkubo, S.; Kato, T. *Chem. Commun.* **2001**, 925–926.

(20) Shoji, Y.; Tashiro, K.; Aida, T. *J. Am. Chem. Soc.* **2010**, *132,* 5928–5929.

(21) Abe, H.; Imai, K.; Matsumoto, M. *J. Polym. Sci., Part C* **1968**, *23*, 469–485.

(22) Bensasson, R. V.; Bienvenue, E.; Janot, J. M.; Land, E. J.; Leach, S.; Seta, P. *Chem. Phys. Lett.* **1998**, *283*, 221-226.

List of Publications

Papers

1) "Encapsulation of Fullerenes in a Helical PMMA Cavity Leading to a Robust Processable Complex with a Macromolecular Helicity Memory"
Takehiro Kawauchi, Jiro Kumaki, Atsushi Kitaura, Kento Okoshi, Hiroshi Kusanagi, Keita Kobayashi, Toshiki Sugai, Hisanori Shinohara, and Eiji Yashima
Angew. Chem., Int. Ed. **2008**, *47*, 515–519.

2) "Helix-Sense-Controlled Synthesis of Optically Active Poly(methyl methacrylate) Stereocomplexes"
Takehiro Kawauchi, Atsushi Kitaura, Jiro Kumaki, Hiroshi Kusanagi, and Eiji Yashima
J. Am. Chem. Soc. **2008**, *130*, 11889–11891.

3) "Helicity Induction and Memory of Syndiotactic Poly(methyl methacrylate) Assisted by Optically Active Additives and Solvents and Chiral Amplification of Helicity"
Atsushi Kitaura, Hiroki Iida, Takehiro Kawauchi, and Eiji Yashima
Chem. Lett. **2011**, *40*, 28–30.

Other Related Papers

1) "Separation of C_{70} over C_{60} and Selective Extraction and Resolution of Higher Fullerenes by Syndiotactic Helical Poly(methyl methacrylate)"
Takehiro Kawauchi, Atsushi Kitaura, Mariko Kawauchi, Tsutomu Takeichi, Jiro Kumaki, Hiroki Iida, and Eiji Yashima
J. Am. Chem. Soc. **2010**, *132*, 12191–12193.

2) "Synthesis of Water-soluble Tris(cyclophane) Hosts and Surface Plasmon Resonance Study on Guest-binding Interaction with Immobilized Guests"
Osamu Hayashida and Atsushi Kitaura
Chem. Lett. **2006**, *35*, 808–809.

Acknowledgment

The present study was carried out at the Department of Molecular Design and Engineering, Graduate School of Engineering, Nagoya University, during 2006–2011.

The author wishes to express his grateful acknowledgment to Professor Eiji Yashima whose encouragement and helpful suggestions have been indispensable to the completion of the present thesis. The author is deeply indebted to Drs. Hiroki Iida, Takehiro Kawauchi, Jiro Kumaki, Hiroshi Kusanagi Katsuhiro Maeda, Yoshio Furusho, Kazuhide Morino, and Toshiaki Kamachi for practical guidance and fruitful discussion.

It is pleasure to express his appreciation to the colleagues of Professor Yashima Laboratory for their encouragement and friendship, especially to Drs. Sousuke Ohsawa, Takashi Hasegawa, and Kanji Nagai, and Messrs. Shinzo Kobayashi, Kazumi Tamura, Kazuhiro Miwa, Motonori Banno, Toshitaka Miyabe, and Hidekazu Yamada.

The author also thanks Mr. Tatsuo Hikage for his help in the X-ray diffraction measurements.

He is very grateful to the Fellowship of the Global COE Program “Establishment of COE for Elucidation and Design of Materials and Molecular Functions” during 2008–2010 and the Japan Society for the Promotion of Science for Young Scientists during 2010–2011.

Finally, he would like to give his special thanks to Professors Takahiro Seki and Shigehiro Yamaguchi for serving on his dissertation committee.

January, 2011

Atsushi Kitaura